CHEMOSTRATIGRAPHY AND PALEOCEANOGRAPHY OF THE MISSISSIPPIAN BARNETT FORMATION, SOUTHERN FORT WORTH BASIN, TEXAS, USA

by

JAMES DANIEL HOELKE

Presented to the Faculty of the Graduate School of

The University of Texas at Arlington in Partial Fulfillment

of the Requirements

for the Degree of

MASTER OF SCIENCE IN GEOLOGY

THE UNIVERSITY OF TEXAS AT ARLINGTON

AUGUST 2011

ACKNOWLEDGEMENTS

First, I would like to thank my advisor, Dr. Harry Rowe, for his patience, time and energy during these past few years. I have learned much from him. This thesis would not have been possible without him. Second, I would like to thank the members of my graduate committee, Dr. Andrew Hunt and Dr. Robert Loucks, for the knowledge and insight you have provided in class and in conversations. I would also like to thank Dr. Christopher Scotese for assistance and advice with paleogeographic maps.

I would also like to thank several members of the Texas Bureau of Economic Geology. I would like to thank especially Dr. Stephen Ruppel for providing core access and material support for this project as well as advice. I would also like to thank James Donnelly, Nathan Ivicic, Kenneth Edwards, and Josh Lambert for core handling assistance.

I want to thank Henry Francis and Andrea Conner at the Kentucky Geological Survey for providing geochemical analyses.

I would also like to thank some members of our geochemistry research group. Niki Hughes provided substantial assistance especially with calibrations and great encouragement. I would also like to thank Jak Kearns, Pukar Mainali, Krystin Robinson, and Robert Nikirk for their help.

I am grateful to the National Science Foundation for grant 0841739, which funded the UIC, Inc. coulometer, permitting the in-house analysis of total inorganic carbon.

Finally, I would like to thank my parents and my brothers for their loving encouragement and support during my studies over the past several years.

July 15, 2011

ABSTRACT

CHEMOSTRATIGRAPHY AND PALEOCEANOGRAPHY OF THE MISSISSIPPIAN BARNETT FORMATION, SOUTHERN FORT WORTH BASIN, TEXAS, USA

James Hoelke, M.S.

The University of Texas at Arlington, 2011

Supervising Professor: Harold Rowe

The Mississippian (Visean-Serpukhovian) Barnett Formation is a lithologic unit composed primarily of laminated siliceous mudstone and calcareous siliceous mudstone. The Barnett Formation was deposited in the Fort Worth Basin, a marine foreland basin that formed as a result of the early Ouachita Orogeny from the collision of Laurasia and Gondwana. In this study we used a variety of geochemical methods to provide a detailed assessment of the chemostratigraphy and paleoceanography of the Barnett Formation in the southern end of the Fort Worth Basin in Texas. Various aspects of the Barnett Formation studied include: degree of basin restriction and deep-water renewal time, redox conditions, organic composition, paleoclimatic indicators, and bulk geochemistry. Eight drill cores along a northeast-southwest transect of the basin in central Texas were evaluated for this study. Each core was scanned at a 1-foot (~0.3m) interval with an X-ray fluorescence (XRF) spectrometer to provide quantitative analysis of major (e.g. Fe, Si, Al) and trace (e.g. Mo, U, V) elements. In addition, total organic carbon (TOC), total inorganic carbon (TIC), percent total nitrogen, and stable isotope ($\delta^{13}C$, $\delta^{15}N$) data were gathered from five of the cores. Percent sulfur data were gathered from three of the cores. The physical paleoceanography of the Barnett Formation reveals that the area of Barnett deposition in the southern Fort Worth Basin was hydrographically restricted. The southern basin

was more restricted than comparable modern anoxic basins during Barnett time. This basin restriction led to deep-water renewal times longer than those of comparable modern anoxic basins and shorter than those for the Barnett Formation of the northern Fort Worth Basin. Deep-water renewal times for the southern basin range from 557-1383 years. The chemical paleoceanography of the Barnett Formation reveals that the Barnett strata were deposited under anoxic to euxinic conditions for essentially the entire depositional timeframe in the mid-late Mississippian. The southernmost end of the transect was deposited initially under anoxic conditions and later under oxic conditions. In addition, high $\delta^{15}N$ values (average 7.76‰) indicate intensified denitrification occurred in the water column. The Barnett strata in the southern Fort Worth Basin is organic rich with total organic carbon (TOC) ranging from 0.07-13.25% with an average TOC of 4%. The organic matter was determined to be primarily of marine origin. The organic matter had $\delta^{13}C_{org}$ values ranged from -24‰ to -32‰ with an average $\delta^{13}C_{org}$ value of -30‰. The carbon-nitrogen ratio values ranged from 1.6 to 92.3 with an average C/N ratio of 21.78. The Barnett Formation was deposited during a second-order eustatic high stand during a warmer, interglacial period based upon stable nitrogen isotope ratios. The bulk geochemistry of the Barnett Formation indicates that it is composed primarily of siliceous mudstone and calcareous siliceous mudstone with significant phosphate and sulfide phases present.

TABLE OF CONTENTS

LIST OF ILLUSTRATIONS

Figure Page

LIST OF TABLES

CHAPTER 1

INTRODUCTION

1.1 Purpose of Study

1.1.1 Study of Mudrocks

Mudrock sedimentology and geochemistry are some of the less-studied areas of geology. It has been noted by several researchers that while mudrocks make up roughly two-thirds of the sedimentary rock record (Blatt, 1980; Potter et al., 1980; Schieber and Zimmerle, 1998; Aplin et al., 1999), scientific studies devoted solely to shales and mudstones constitute a small percentage (1-2%) of sedimentary publications annually (Schieber and Zimmerle, 1998; Aplin et al., 1999). The diverse nature of mudrocks and the valuable scientific information that can be gleaned from them prompts their further geologic study.

Geological studies of mudrocks are important for several reasons. First, they may provide good lithological records of their depositional environments, paleoclimates, and paleoceanography. Mudrocks contain large portions of earth's stratigraphic history, usually in relatively continuous successions (Schieber and Zimmerle, 1998). Marine sedimentary basins, in particular, commonly have excellent lithological records consisting of mudrocks. Second, they serve as important sources of economically vital natural resources. These include serving as source rocks and reservoirs for petroleum deposits (Schieber and Zimmerle, 1998; Aplin et al., 1999) including those found in the Barnett Shale (Hill et al., 2007). In addition, mudrocks serve as sources for building materials and economically important metals (Gustafson and Williams, 1981; Schieber and Zimmerle, 1998). Third, studies of mudrocks are important in sequence stratigraphic studies (Schieber and Zimmerle, 1998). Improved knowledge of mudrocks can help further studies of eustatic and tectonic changes in a sequence stratigraphic framework.

"Black" shales or mudrocks of marine origin such as the Barnett Formation are of particular interest for workers studying mudrocks. Black shales are characterized as being dark gray to black mudstones rich in organic carbon (>1 percent organic carbon), commonly laminated, carbonaceous mudrocks that are poor in bethonic fauna or completely devoid of metazoan organisms (Arthur and Sageman, 1994). Although their primary constituent is mud or clay-size particles, black shales commonly have calcium carbonate ($CaCO_3$), biogenic silica (SiO_2) and other components as major constituents (Arthur and Sageman, 1994; Piper, 1994). Black shales serve as source rocks for petroleum deposits (Arthur and Sageman, 1994; Piper and Calvert, 2009) and contain economically important phosphate deposits (Piper and Calvert, 2009). Like other mudrocks, black shales are also useful indicators of depositional environments that can help elucidate oceanic chemistry and circulation (Arthur and Sageman, 1994; Sageman et al., 2003; Algeo and Lyons, 2006). This last point is of particular importance for this study.

1.2 Previous Work

1.2.1 Geochemical Methods Used in Studies of Mudrocks

Geochemical studies of mudrocks, including those pertaining to paleoceanography, have been conducted for several decades (e.g. Vine and Tourtelot, 1970; Demaison and Moore, 1980; Arthur and Sageman, 1994; Algeo and Lyons, 2006; Rowe et al., 2008). Studies have been focused on various types of geochemical methods include redox-sensitive trace metals, iron-sulfur-organic carbon relationships, iron speciation, and stable isotope methods involving organic carbon and nitrogen (e.g. Dean and Arthur, 1989; Crusius et al., 1996; Rowe et al., 2008). Studies also have been focused on a particular geologic time period and geographic extent include studies of both present-day marine chemistry and those confined to the geologic past (e.g. Morford et al., 2001; Algeo and Maynard, 2004; Rimmer et al., 2004; Brumsack, 2006).

Redox-sensitive trace metals have been utilized for some time in geochemical studies of mudrocks and their relationship to the chemical paleoceanography of the overlying water column. Various trace metals are concentrated in marine sediments under oxic, suboxic, anoxic or euxinic

(sulfidic) conditions in the overlying water column (Calvert and Pedersen, 1993; Piper, 1994; Crusius et al., 1996; Tribovillard et al., 2006) or in the sediment itself (Morford and Emerson, 1999; McManus et al., 2006). Generally these trace metals are assessed as being enriched or depleted relative to their concentration in a reference material in order to determine paleoenvironmental conditions (Tribovillard et al., 2006). In the case of mudrocks, the reference material typically used is average gray shale as defined by Wedepohl (1971, 1991) (Tribovillard et al., 2006). Although various redox-sensitive trace metals have been used, the most commonly accepted trace metals used for paleoredox studies include molybdenum, vanadium, and uranium (Piper, 1994; Crusius et al., 1996; Morford and Emerson, 1999; Rimmer, 2004; Rimmer et al., 2004; McManus et al., 2006; Tribovillard et al., 2006; Algeo and Tribovillard, 2009). Redox-sensitive trace metals have also been used to determine the type of depositional marine environment (Brumsack, 2006; Turgeon and Brumsack, 2006) and as paleoproductivity proxies (Tribovillard et al., 2006; Piper and Calvert, 2009).

Another important application of redox-sensitive trace metals involves studies of basin hydrography. They can be used to determine the occurrence and degree of water-mass restriction and deep-water renewal times. This is accomplished by measuring the slope of the regression line between molybdenum (Mo) and total organic carbon or TOC (Algeo and Lyons, 2006). The regression line slope is used to determine the degree of subpyncnoclinal water mass restriction in the basin. The Mo-TOC relationship is especially useful in analyzing anoxic marine settings (Algeo and Lyons, 2006; Algeo et al, 2007; Algeo and Rowe, 2011). This Mo-TOC relationship can also be used in conjunction with trace-metal covariation to determine the evolution of water masses over time and deep water renewal times (Algeo and Lyons, 2006; Algeo and Maynard, 2008).

Iron-sulphur-carbon relationships have been an important tool used in paleoceanographic studies. Berner and Raiswell (1983) utilized organic carbon and pyrite sulfur ratios to distinguish between normal marine, freshwater, and euxinic environments. Dean and Arthur (1989) utilized

ternary diagrams of iron, sulphur, and organic carbon to determine whether iron, carbon, or sulfur limited the formation of pyrite in marine sediments. Raiswell et al. (1988) pioneered the use of the degree of pyritization (DOP) in marine sediments containing organic carbon as a proxy for the degree of bottom-water oxygenation. Another use of sulphur in paleoceanographic studies involves the presence and size distribution of framboidal pyrite in marine sediments. The size distribution of pyrite framboids has been used as an indicator water-column redox conditions, particularly as an indicator of euxinia in the water column (Wilkin et al, 1996, Wilkin et al, 1997).

Stable isotope ratios of carbon and nitrogen ($\delta^{13}C$, $\delta^{15}N$) and organic carbon/nitrogen ratios (C/N) have also been useful as well in paleoceangraphic studies. Carbon isotopes have been used to determine the provenance of organic matter (Meyers, 1994; Meyers, 1997; Twichell et al., 2002) and to infer paleoproductivity and paleoenvironmental conditions of marine deposits (Meyers, 1994; Meyers, 1997; Meyers et al., 2006). Nitrogen isotopes have also been used to determine organic matter provenance (Meyers, 1997; Meyers et al., 2009A; Meyers et al, 2009B) and have also been used as paleoproductivity and paleoclimatology proxies (Meyers, 1997; Algeo et al., 2008; Meyers et al., 2009B). Ratios of organic carbon to nitrogen have also been important in determining the provenance of organic matter in marine sedimentary deposits (Meyers, 1994; Twichell et al., 2002; Meyers et al., 2006), paleoproductivity (Twichell et al., 2002), and as an indicator of water-column oxygenation (Meyers et al., 2006; Meyers et al., 2009A).

The use of sequence stratigraphy is one of the more important developments in sedimentary geology (Vail et al., 1997; Posamentier and Allen, 1999; Catuneanu et al., 2009). Sequence stratigraphy can be used as an effective tool for correlation on local and regional scales and to determine the chronological order of basin filling and erosional events (Catuneanu et al, 2009). Various methods have been used to determine sequences in the past (e.g. Schieber, 1998; Maynard et al., 2006). More recently, redox-sensitive trace metals have also be used together with other geological methods to delineate sequences in siliciclastic formations

including mudrocks (Ver Straeten et al., 2011). This last method holds promise for determining sequences in black shales which often appear homogenous on the visual scale. This last method also holds promise by providing a geochemical proxy for the grain size of detrital input from sediment sources for sedimentary basins.

1.2.2 Previous Geochemical Studies of the Barnett Formation

Several geochemical studies have been conducted on the Barnett Formation. However, it is important to note that the Barnett Formation has been studied primarily for its organic and petroleum geochemistry, (Hill et al., 2007; Jarvie et al., 2007; Maiz, 2007; Rodriguez and Philp, 2010) but not for its inorganic geochemistry. These previous studies of the geochemistry of the Barnett Formation have been focused on the northern Fort Worth Basin from wells in the Newark East Field and samples from Barnett outcrops near the Llano Uplift (Hill et al., 2007; Jarvie et al., 2007; Maiz, 2007; Rodriguez and Philp, 2010). Loucks and Ruppel (2008) conducted a study of the Barnett outcrops and drill cores in the southern Fort Worth Basin that included sedimentology, mineralogical and organic geochemistry analyses. The few studies of the Barnett's paleoceanography have been conducted with samples from the northern Fort Worth Basin (Rowe et al., 2008) and in the Delaware Basin (Rowe et al., 2009) of West Texas. Hughes et al. (2009) conducted a preliminary study of the Barnett's inorganic geochemistry and paleoceanography on the northern edge of the Llano Uplift. This study aims to build upon these previous geochemical and paleoceanographic studies of the Barnett Formation. In order to have a better understanding of the study area, a more detailed geologic understanding of the Fort Worth Basin and the Barnett Formation is required.

1.3 Geological Information

1.3.1 Geographic Setting of the Fort Worth Basin

The Fort Worth Basin is located in central and north-central Texas (Figure 1). The Fort Worth Basin is delineated by several structural features (Figure 1) including the Muenster Arch

and Red River Arch to the north, the Ouachita fold-and-thrust belt to the east, the Bend Arch to the west, and the Precambrian Llano Uplift to the south (Thompson, 1982; Thompson, 1988). The basin trends approximately northeast to southwest and is asymmetric to the east (Thompson, 1988). It is approximately 200 miles (~322km) long and ranges in width from more than 100 miles (~161 km) on the north end to less than 10 miles (~16km) on the south end of the basin (Thompson, 1982; Thompson, 1988). The basin deepens toward the northeast end and shallows toward the west and southwest (Loucks and Ruppel, 2007; Pollastro et al., 2007).

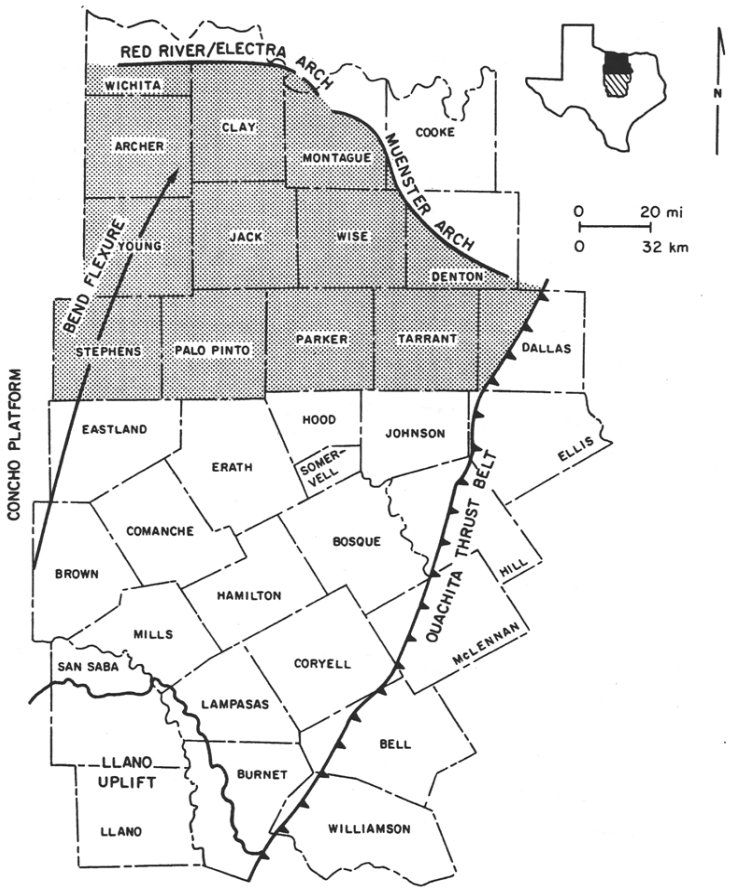

Figure 1. Structural boundaries of the Fort Worth Basin (Thompson,1982).

1.3.2 Structural Geology and Tectonics of the Fort Worth Basin

The Fort Worth Basin is a marine foreland basin that formed by the collision between the Laurussia and Gondwana paleocontinents during the early Ouachita Orogeny (Walper, 1982; Thompson, 1988). The basin was originally part of the greater Oklahoma Basin during pre-Pennsylvanian time (Thompson, 1988). During the mid-late Mississippian, the Fort Worth Basin was located on the southern side of Laurussian paleocontinent (Gutschick and Sandberg, 1983; Blakely, 2005; Scotese, 2010). Reconstructions by Scotese (2010) and Blakely (2005) show the paleogeography at approximately the onset of Barnett deposition (Figure 2) and end of Barnett deposition (Figure 3), respectively. The Fort Worth Basin was bordered on the west by the Llano Uplift and the Chappell carbonate shelf and on the east by the Caballos Arkansas island arc during deposition of the Barnett Formation (Loucks and Ruppel, 2007). The Barnett Formation itself was deposited on a marine shelf on the southern margin of Laurussia initially and then in the still forming Fort Worth Basin (Henry, 1982).

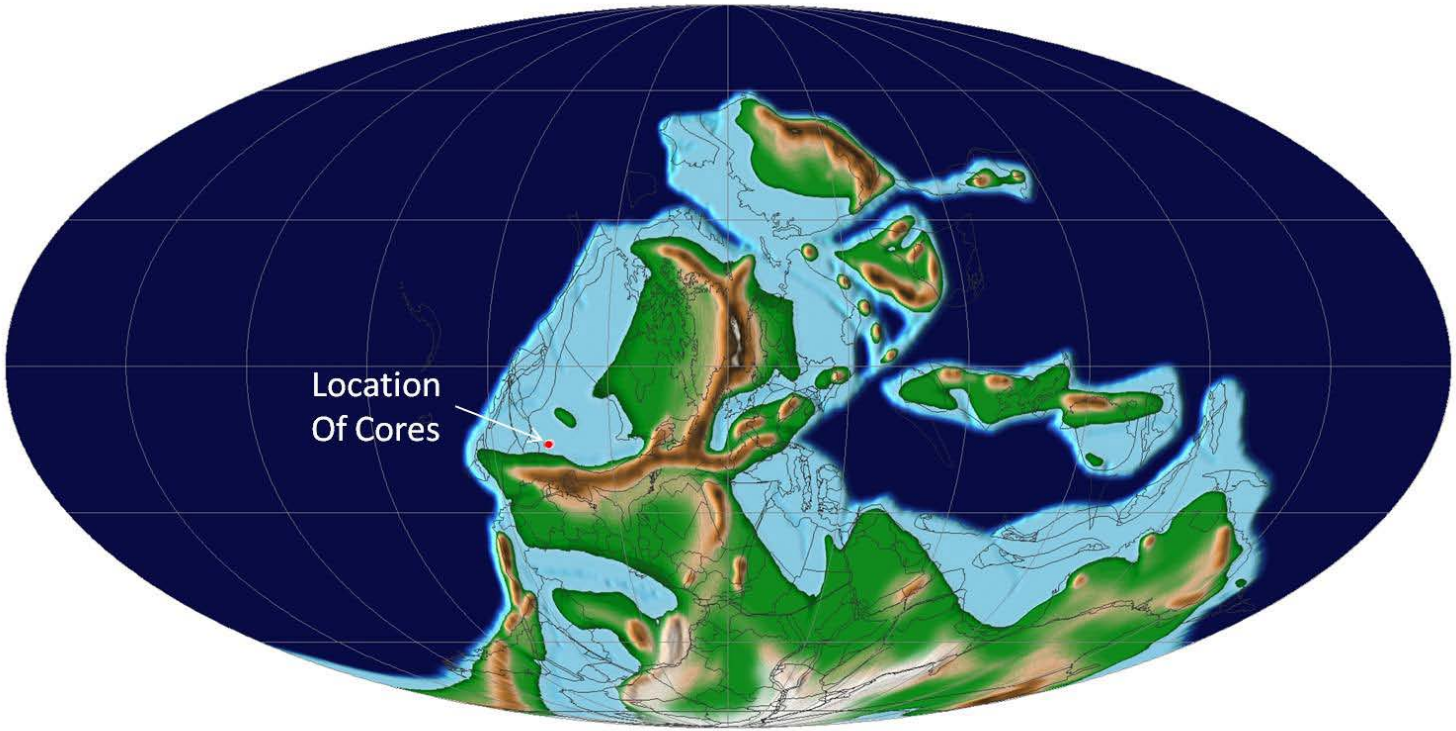

Figure 2. Global paleogeographic reconstruction, 340Ma (Visean) (Scotese, 2010).

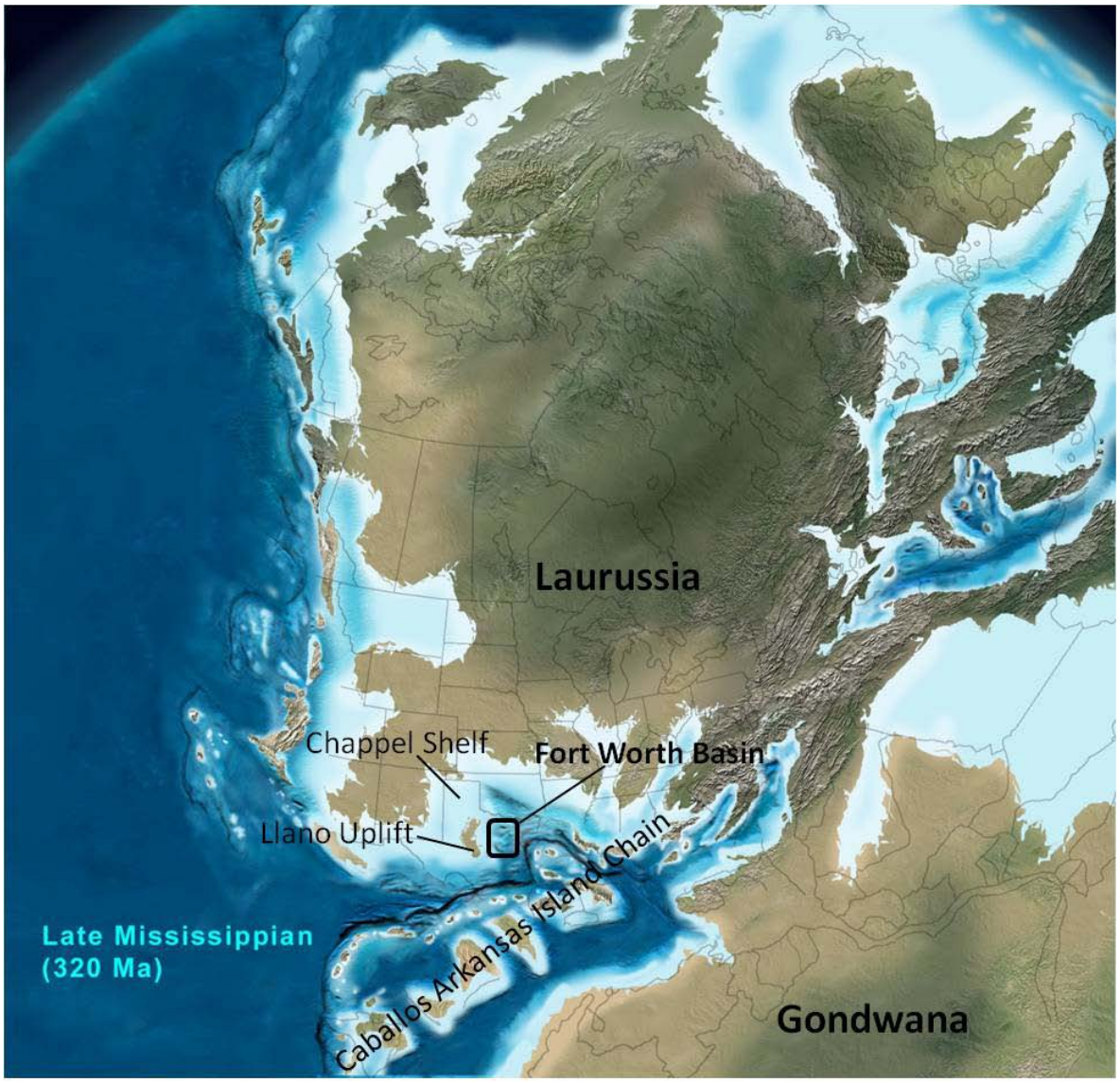

Figure 3. Regional paleogeographic reconstruction, 320Ma (Serpukhovian). (Adapted from Blakely, 2005).

The tectonic history of the Fort Worth Basin consists of several main phases. After Laurentia rifted away from Gondwana in the late Precambrian, the southern margin of Laurentia became a retreating and subsiding plate margin dominated by deposition of carbonates from Cambrian to Ordovician time (Walper, 1982; Jurdy et al., 1995). During Silurian and Devonian time, a reversal in subduction polarity occurred and Laurentia became the subducting plate (Jurdy et al., 1995). The marginal basin strata were scraped into a subduction complex that eventually

overthrusted the subducting margin of Laurentia (Walper, 1982). During the Mississippian period, Gondwana collided with an island arc on the southeastern margin of Laurentia, which was then thrust northward and buried under the sedimentary wedge of the subduction complex (Scotese and McKerrow, 1990). The subduction complex was subsequently uplifted and folded into the Ouachita fold-thrust belt (Walper, 1982). Crustal flexing of the outer rise led to the formation of a hinge line that subsequently migrated toward the craton over time (Walper, 1982). This led to the basin axis also shifting westward toward the craton. Eventually, the basinal trough shifted northwestward adjacent to the Muenster arch due to uplift of the Llano region, continued overthrusting by the Ouachita front, and cessation of downward flexing of the shelf margin (Walper, 1982). Migration of the hinge line and basin axis stopped when the basin margin reached the Concho platform (Walper, 1982).

Formation of the basin is believed to have initiated due to motion along a series of transtensional faults trending along the Muenster Arch from Late Mississippian to Early Pennsylvanian time (Johnson et al., 1988; Erlich and Coleman, 2005). The Fort Worth Basin then subsided substantially during Early to Late Pennsylvanian time, a result of the advancing Ouachita fold-thrust belt (Kier et al., 1979; Walper, 1982; Ehlrich and Coleman, 2005). Subsidence of the basin was asymmetrical to the northern end of the basin and was likely related to flexural loading of the continental crust (Ehlrich and Coleman, 2005). It is important to note that the structural elements that delineate the Fort Worth Basin did not form until Pennsylvanian time because of the influence of the Ouachita Orogeny (Walper, 1982; Thompson, 1988). In the southern part of the basin, Pennsylvanian deformation caused by the Llano Uplift led to the formation of normal faults and a series of grabens and horsts (Belforte, 1971; Thompson, 1988; Montgomery et al., 2005). Evidence of these grabens and horsts has been documented by Dr. Robert Loucks (The University of Texas at Austin, personal communication).

1.3.3 Stratigraphy of the Fort Worth Basin

The Barnett Formation was established as a lithologic unit by Plummer and Moore (1922) based upon outcrops located in San Saba County in Texas (Henry, 1982; Kier et al., 1979). It had been previously known as the Lower Bend Shale (Kier et al., 1979). The Barnett Formation has its greatest thickness in the northeast end of the basin and thins to the south and southwest (Loucks and Ruppel, 2007). The Barnett Formation is conformably overlain by the Pennsylvanian Marble Falls Formation. It is unconformably underlain by the Lower Ordovician Ellenburger Group carbonates or the Middle to Upper Ordovician Viola-Simpson carbonates. The Viola-Simpson carbonates are confined to the northeastern part of the basin (Montgomery et al., 2005). In the southwestern portion of the basin, the Barnett Formation conformably overlies the early Mississippian Chappel Formation above the Ellenburger Group (Henry, 1982; Loucks and Ruppel, 2007; Montgomery et al., 2005). In the northern part of the basin, the Barnett Formation is divided into upper and lower Barnett members by the Forestburg Limestone member. This intervening member is carbonate-rich, but is not a limestone (Loucks and Ruppel, 2007). It is important to note that where the Forestburg Limestone member is absent, the Barnett Formation is considered to be a single, undifferentiated unit (Montgomery et al., 2005; Loucks and Ruppel, 2007). Figure 4 shows the general stratigraphy of the Fort Worth Basin.

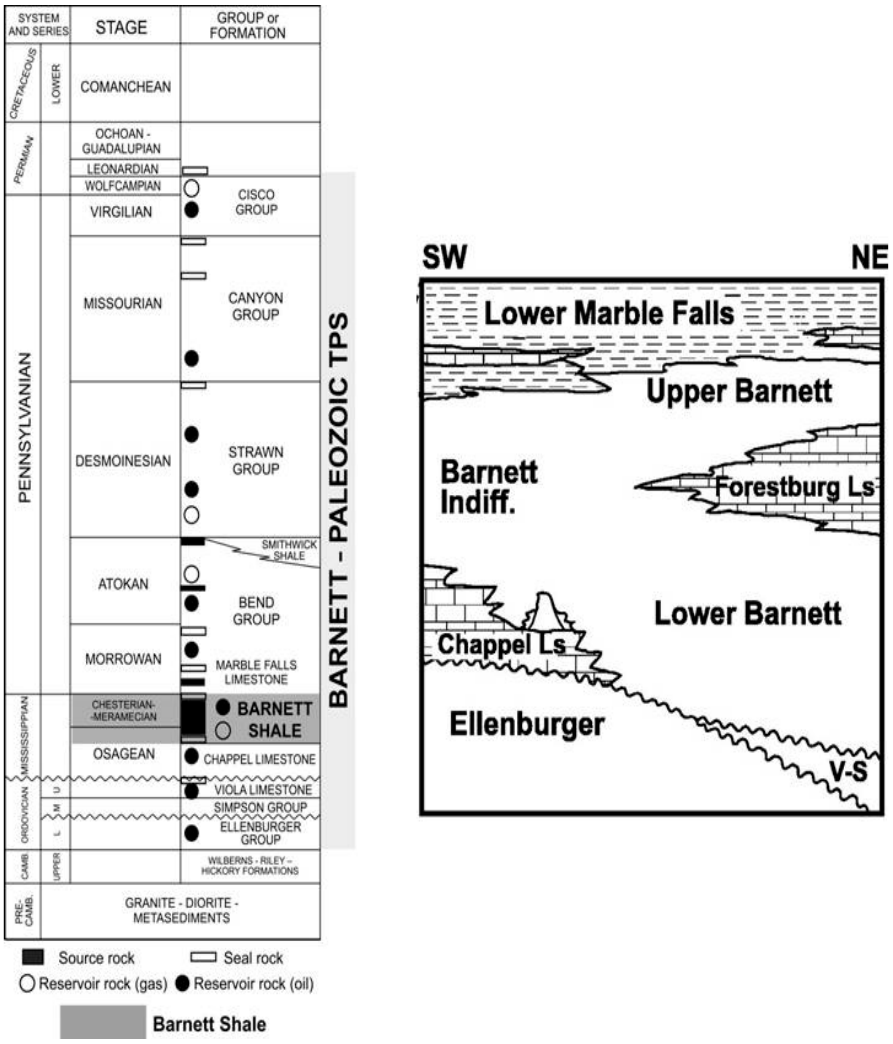

Figure 4. General stratigraphy of the Barnett Formation in the Fort Worth Basin. Left: Generalized stratigraphic column of Fort Worth Basin. (Pollastro et al., 2007) Right: Detailed interpretation of Mississippian stratigraphy. V-S refers to Viola–Simpson interval. (Montgomery et al., 2005)

In the study area, the Barnett Formation is considered a single unit as the Forestburg Limestone member is absent. It is overlain in some localities by a Pennsylvanian detrital member, but it is predominantly overlain by the Pennsylvanian Marble Falls Formation (Loucks, 2008, unpublished). The Barnett Formation is underlain conformably in the study area in some locations by the early Mississippian Chappel Limestone, Devonian Doublehorn Shale, and localized reef buildups of the White's Crossing Formation. It is underlain unconformably in other areas by the Ordovician Ellenburger Group (Montgomery et al., 2005; Loucks and Ruppel, 2007; Loucks, 2008, unpublished). The Barnett Formation has been interpreted as being deposited during a period of sediment starvation (Kier, 1988; Loucks and Ruppel, 2007). The lack of clastic influx has been inferred from the long depositional timeframe (Kier, 1988; Loucks and Ruppel, 2007).

1.3.4 Age of Barnett Formation

The age of the Barnett Formation is known to be mid-late Mississippian in age (Visean-Serpukhovian) based on biostratigraphic studies. Hass (1953) and Merrill (1980) assigned an Osagean-Chesterian age to the Barnett based on conodont studies. Schwarz (1975) assigned a late Osagean to Chesterian age to the Barnett based upon studies of cephalopods. Biostratigraphic studies of the Barnett Formation are still an area of active research (Boardman et al., 2007A; Boardman et al., 2007B; Singh, 2007; Wardlaw and Boardman, 2007). Based upon the timing of eustatic cycles and previous conodont studies, it has been proposed that the Barnett Formation was deposited in the Fort Worth Basin during a second order highstand transgression from the Osagean to Chesterian (late Tournasian-Serpukhovian); approximately 345 to 320 Ma (Ross and Ross, 1987; Loucks and Ruppel, 2007).

1.3.5 Late Paleozoic Paleoclimate

The late Paleozoic was a period of transition from a greenhouse world to an icehouse world (Smith and Read, 2000). The onset and termination of the late Paleozoic ice age has been area of considerable research and debate (Fielding et al., 2008). Previous interpretations of the late Paleozoic ice age viewed it as a single, extended event, but recent research proposes that it was a series of discrete glacial episodes separated by warmer intervening periods (Fielding et al., 2008). Previous interpretations of the late Paleozoic ice age can viewed in Figure 5. These glacial episodes are considered to have been 1-8 My in duration (Fielding et al., 2008). It has been proposed that the paleogeographic changes occurring during the late Paleozoic led to the onset and demise of the late Paleozoic ice age (Fielding et al., 2008; Frank et al., 2008). The demise of the seaway between Laurussia and Gondwana has been proposed as a possible cause for changes in atmospheric and oceanic circulation (Smith and Read, 2000).

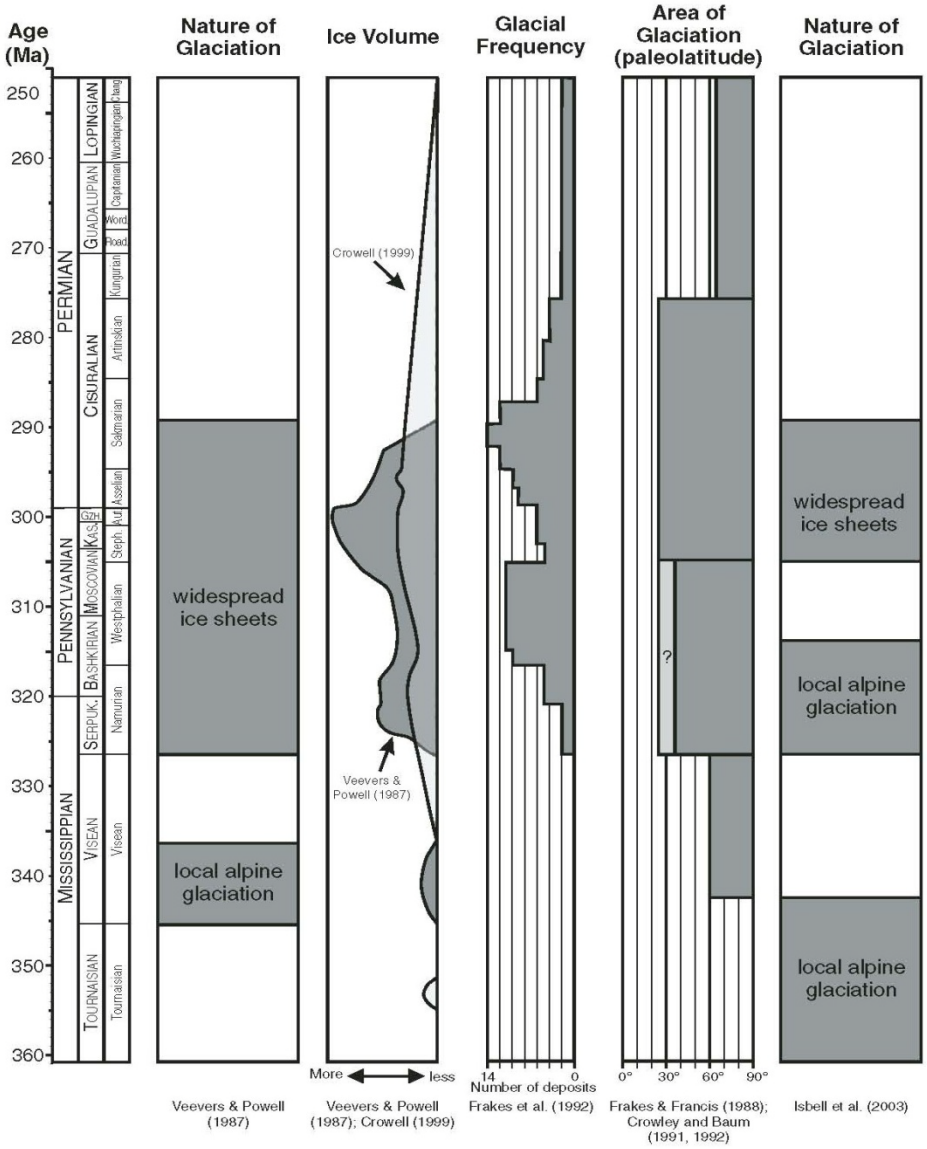

Figure 5. Stratigraphic range chart showing previous interpretations of the extent of glaciation through the Carboniferous and Permian Systems (Fielding et al., 2008).

The first two minor glaciation events occurred in Gondwana at the Late Devonian-Tournasian boundary and during the Visean (Kammer and Matchen, 2008; Fielding et al., 2008). An additional period of glaciation during the middle-late Tournasian at the Kinderhookian-Osagean boundary has been proposed by Kammer and Matchen (2008). The first main

glaciation event during the ice age occurred during the Serpukhovian with the expansion of ice centers in Gondwana (Fielding et al., 2008). The next glaciation event occurred in the early Pennsylvanian (Bashkirian) at the Mississippian-Pennsylvanian boundary with further ice expansion (Fielding et al., 2008). This event left a prominent unconformity across many North American paleoequatorial basins (Blake and Beuthin, 2008). The final major glaciation event occurred at the Pennsylvanian-Permian boundary as the ice sheets became bipolar (Fielding et al., 2008). They reached their apex in the Early Permian before deteriorating during the end of the Middle Permian (Fielding et al., 2008; Frank et al., 2008).

1.4 Research Objectives and Hypotheses

1.4.1 Research Objectives

The purpose of this study is to provide a detailed assessment of the chemostratigraphy and paleoceanography of the Barnett Formation in the southern end of the Fort Worth Basin in Texas. Research objectives that enable this study include: 1) Assessment of the degree of and/or variability of hydrographic restriction in the Fort Worth Basin, 2) Determination of the depositional subenvironments preserved that indicate the range of redox conditions (i.e. oxic-anoxic/euxinic), 3) Characterization of the composition and sources of organic matter in the Barnett Formation, 4) Determination of geochemical conditions in the Barnett strata that reflect changes in paleoclimate during deposition, and 5) Comparison of inferred depositional conditions preserved in the Barnett strata to conditions inferred from organic-rich mudrocks in other restricted basins.

1.4.2 Hypotheses

Based upon personal observations and those of other workers (Hill et al., 2007; Hughes et al., 2009; Loucks and Ruppel, 2007; Rowe et al., 2008; Rowe et al., 2009), the following hypotheses have been made regarding the depositional environments and paleoceanography of the Barnett Formation. First, the Barnett Formation was deposited in the southern Fort Worth Basin during which the basin was severely hydrographically restricted (Rowe et al., 2008). This

basinal restriction led to extended subpyncoclinal water mass renewal times. Second, the Barnett Formation was deposited in a variety of depositional redox subenvironments that were primarily anoxic to euxinic in nature (Loucks and Ruppel, 2007; Rowe et al., 2008; Hughes et al., 2009). Third, the Barnett Formation in the southern Fort Worth Basin is organic rich (>2.5% total organic carbon) and the main source of the organic matter is marine in origin (Hill et al., 2007; Loucks and Ruppel, 2007). Fourth, deposition of the Barnett Formation occurred during an interglacial period. Fifth, the Barnett Formation should have different geochemical and paleoceanographic characteristics compared to other organic-rich mudrocks deposited in modern and ancient anoxic marine basins (Rowe et al., 2008; Rowe et al., 2009). These hypotheses for this study are based upon the research objectives in section 1.4.1.

CHAPTER 2

METHODS

2.1 Core Information

A series of eight drill cores from the southern Fort Worth Basin (FWB) in Central Texas were analyzed. The cores were drilled in Brown, McCulloch, Mills, and San Saba Counties in Texas. All of the drill cores are housed at the Core Research Center of the Texas Bureau of Economic Geology in Austin, TX. Figure 6 has a map of the study area with core locations. Table 1 has general information for each core analyzed. Geologists Dr. Robert Loucks and Dr. Stephen Ruppel of the Bureau of Economic Geology are at present studying the stratigraphy of these cores and descriptions of these cores should be published in the near future.

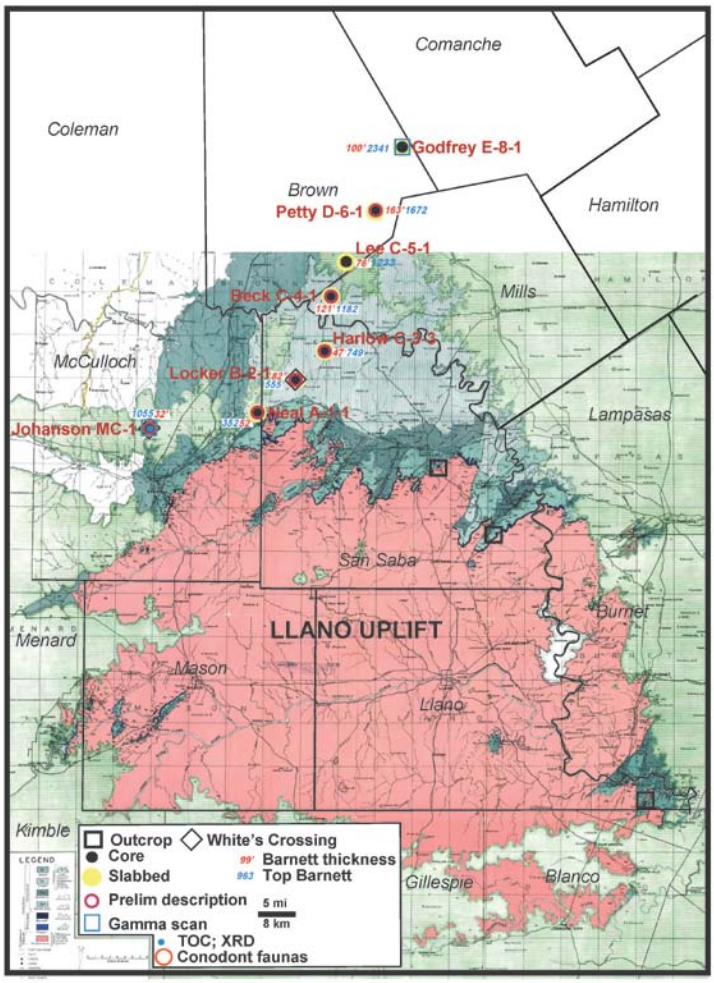

Figure 6. Map of study area with core locations. (Adapted from Loucks, R.G. 2009. Unpublished.)

2.2 Energy Dispersive X-ray Fluorescence (ED-XRF) Analysis

2.2.1 ED-XRF Analysis

Core samples from five cores were marked prior to ED-XRF analysis at an approximately one-foot (~0.3m) interval. A Bruker Tracer III-V handheld ED-XRF spectrometer was used to measure metal concentrations in each sample. Samples were placed on the nose of the instrument immediately above the 3 by 4 mm elliptical beam window and stabilized using a platform that surrounded the instrument's nose. Because the measurement sensitivity of the ED-XRF instrument decreases by the inverse square of the distance from the silicon detector (SiPIN), located directly beneath the sampling window, a flat sample surface is needed in order to optimize measurement consistency and accuracy. Core samples were analyzed on the slabbed side whenever possible. Samples that were unslabbed were given a flat surface area for analysis using a Dremel grinding hand tool. The instrument was stabilized using a plastic platform supplied by Bruker.

Major element data acquisition, which includes V and Cr measurements, was undertaken using a low-energy, vacuum-pumped instrument setting. Each sample was analyzed for major and trace element concentrations for 180 seconds each. For additional information on energy dispersive X-ray fluorescence techniques and X-ray fluorescence in general, see Potts and Webb (1992).

Low-energy spectrum acquisition includes elements that emit characteristic x-rays between 1.25 to 7.06 kV. In order to obtain the elements in this range, and allow for backscatter that does not interfere with the peaks of interest, the voltage on the instrument was set to 15 kV. The BEG instrument current was set to 42 μA; however, while the voltage settings remain constant for this elemental range, regardless of the Tracer III-V used, the current settings vary between instruments because of inter-instrument variability associated with the manufacture of the x-ray tube and electronics.

Trace element data acquisition was undertaken using a filtered, high-energy instrument setting. The characteristic x-rays between 6.92 and 19.80 kV were measured in the high-energy

acquisition mode (40 kV and 28 μA). For the trace element analyses, a Cu-Ti-Al filter inserted into the instrument was utilized to attenuate greatly the low-energy x-rays from reaching the detector.

2.2.2 Mudstone Calibration of ED-XRF

Calibration for major and trace elemental analysis was undertaken using a suite of ninety reference materials. The ninety reference materials include: five international shale standards, seven from the Devonian-Mississippian Ohio Shale, twenty from the Pennsylvanian Smithwick Formation of Central Texas, twenty-seven from Devonian-Mississippian Woodford Formation from West Texas, fifteen from the Late Cretaceous Eagle Ford formation of South Texas, and sixteen from the Mississippian Barnett Formation of North Central Texas. Each of the ninety reference materials was pressed in a Carver press to forty tons with a forty millimeter die using a boric acid backing. Each reference material was pulverized to a 200 mesh powder using a TM Engineering pulverizer with trace metal grade stainless steel pulverizing cups and pucks. Approximately eight grams of powdered reference material were used in each reference material. The finished reference pellets were analyzed for major and trace elements using wavelength-dispersive x-ray fluorescence (WD-XRF) and inductively-coupled plasma mass spectrometry (ICP-MS), respectively.

The standard pellets were analyzed on the Bruker Tracer III-V for six minutes at three different locations on the pellet face under both low- and high-energy settings. All 270 raw x-ray spectra (90 references x 3 analyses) were loaded into Bruker's CalProcess software along with the accepted (WD-XRF & ICP-MS) elemental concentrations for all standards. A low-energy and a high-energy calibration were developed by making inter-element corrections (slope and background) for each element in each calibration. Certain standards were omitted after the implementation of the inter-element corrections using statistical analysis for each element to determine the outliers with a studentized value greater than 3.0 standard deviations from the mean.

The completed calibration yields quantified values using the raw ED-XRF spectra from unknown samples. The low energy calibration quantifies the following elements: Mg, Al, Si, P, S, K, Ca, Ba, Ti, V, Cr, Mn, and Fe. The high energy calibration quantifies the following elements: Ni, Cu, Zn, Th, Rb, U, Sr, Y, Zr, Nb, and Mo. The limits of determination of a method (LDM) for each element are provided in Table 2 (Rousseau, 2001). Raw spectra from unknowns are processed through a calibration spreadsheet (Rowe et al., 2011, in review).

2.3 Wavelength Dispersive X-ray Fluorescence (WD-XRF) Analysis

2.3.1 WD-XRF Analysis

A preliminary suite of samples from three cores (Johansen MC-1, Lee C-5-1, Locker B-2-1) were collected for wavelength-dispersive x-ray fluorescence analysis at an approximately one foot (~0.3m) interval. Samples were air-dried and powdered to 200-mesh using a hardened steel pulverizer. Samples were pressed automatically to 40 tons into pellets and analyzed for major and trace elemental composition using the Bruker S4 Pioneer WD-XRF unit, housed at the Kentucky Geological Survey. A suite of USGS and internationally accepted standards and a suite of Kentucky Devonian black shales previously analyzed by ICP-MS were used for standardization of unknowns. The internationally accepted standard SARM-41 was analyzed for quality control.

2.4 Additional Geochemical Analysis

2.4.1 Sample Preparation

Samples for additional analyses were collected from each analysis location at an approximately one foot (~0.3m) interval along the cores using a standard rock saw to cut discrete samples. These samples were subsequently pulverized using a TM Engineering pulverizer with trace metal grade stainless steel pulverizing cups and pucks. The samples were then stored in standard plastic liquid sample cups.

2.4.2 Total Inorganic Carbon (TIC)

Samples were analyzed for their total inorganic carbon (TIC) content using a UIC, Inc. coulometer equipped with a CM5230 acidification module with average unknown standard deviations of less than 0.5 percent (Engleman et al 1985). Samples were weighed out between 5 to 50 mg. For TIC analysis, weighed samples are acidified at 70^{o}C with ten percent (10%) phosphoric acid (H_3PO_4). A subset of samples was analyzed for TIC using this method (Table 3).

2.4.3 TOC/TN/Carbon Isotopes/Nitrogen Isotopes

Total organic carbon (TOC), total nitrogen (TN), and stable isotopic compositions of TOC ($\delta^{13}C$) and TN ($\delta^{15}N$) were performed on powdered samples that were weighed into silver capsules (Costech Analytical, Inc. #41067) and subsequently acidified repeatedly with six percent (6%) sulfurous acid (H_2SO_3) in order to remove carbonate phases (Verardo et al., 1990). Samples were analyzed at the University of Texas at Arlington using a Costech 4010 elemental analyzer interfaced with a Thermo Finnigan Conflo IV device to a Thermo Finnigan Delta-V isotopic ratio mass spectrometer (IRMS). Isotopic results are reported in per mil (‰) relative to V-PDB for $\delta^{13}C$ and air for $\delta^{15}N$. The average standard deviations were 0.11‰ and 0.07‰ for $\delta^{13}C$ and $\delta^{15}N$ of USGS-40 glutamic acid (IAEA-8573), respectively, and 1.07% and 0.08% for the TOC and TN of USGS-40, respectively, and 0.13 for C/N. The average standard deviations for unknown samples analyzed in triplicate were 0.10‰ for $\delta^{13}C$, 0.12‰ $\delta^{15}N$, 0.02% for TOC, 0.01% for TN, and 0.18 for C/N. A subset of samples was analyzed for TOC, TN, and stable isotopic compositions of TOC ($\delta^{13}C$) and TN ($\delta^{15}N$) (Table 3).

2.4.4 LECO Sulfur

Sulfur analyses were conducted using a LECO C-S analyzer at the Kentucky Geological Survey, with the standard deviation of unknowns averaging less than 0.01%. A subset of samples was analyzed for sulfur using this method (Table 3).

Table 1. General Core Information.

Core Name	County Location (Texas)	Location (Latitude/Longitude in digital degrees)	API #	BEG Box Numbers	Total Interval Length (Feet)	Interval Analyzed (Depth in feet)	Total Interval Length (Meters)	Interval Analyzed (Depth in meters)	XRF Unit Utilized
J.D. Godfrey E-8-1	Brown County	31.7897096 / 98.7526216	420493181500	27-42	150	2296-2446	46	700-746	BEG (ED-XRF)
N. Petty D-6-1	Brown County	31.6616639 / 98.8204053	420493178500	7-26	181	1652-1833	55	503-559	BEG (ED-XRF)
Lee C-5-1	Brown County	31.5665283 / 98.8867703	420493171600	N/A	77	1231-1308	23	375-399	WD-XRF
Beck C-4-1	Mills County	Not Available	423333019400	12-23	111	1174-1285	34	358-392	UTA1 (ED-XRF)
Harlow C-3-3	San Saba County	31.388902 / 98.9430736	424113010200	10-17	76	736-812	23	224-247	UTA1 (ED-XRF)
Locker B-2-1	San Saba County	31.3371293 / 99.011035	424113010100	N/A	52	585-637	16	178-194	WD-XRF
Neal A-1-1	McCulloch County	31.2726216 / 99.0941208	423073042900	30-37	77	342-419	23	104-128	BEG (ED-XRF)
Johansen MC-1	McCulloch County	31.2457553 / 99.3386624	423073048700	N/A	24	1055-1079	7	322-329	WD-XRF

Table 2. Lowest Detectable Measurements (LDM) for Elements Analyzed.

Element	Accepted Value[a]	Instrument 1 (UTA-1)			Instrument 2 (1st UTA-2)		
		Measured Value[b]	σ (n=7)[b]	LDM[c]	Measured Value[b]	σ (n=7)[b]	LDM[c]
Mg (%)	0.67	0.80	0.09	0.17	0.85	0.14	0.28
Al (%)	4.96	5.39	0.14	0.28	5.32	0.11	0.22
Si (%)	32.6	33.7	0.2	0.5	33.1	0.4	0.8
P (%)	0.07	0.05	0.03	0.07	0.09	0.03	0.06
S (%)	3.34	2.18	0.10	0.20	2.27	0.09	0.18
K (%)	2.07	2.31	0.09	0.18	2.22	0.07	0.14
Ca (%)	0.13	0.23	0.03	0.06	0.24	0.02	0.04
Ti (%)	0.23	0.27	0.02	0.04	0.27	0.02	0.03
Mn (%)	0.015	0.012	0.001	0.002	0.013	0.001	0.003
Fe (%)	2.93	2.55	0.06	0.12	2.52	0.06	0.13
Ba (ppm)	2090	1884	376	753	1706	300	600
V (ppm)	928	1114	68	137	1110	80	159
Cr (ppm)	110	98	13	26	106	14	27
Ni (ppm)	130	153	26	52	150	20	40
Cu (ppm)	83	147	20	40	87	12	23
Zn (ppm)	823	844	96	191	880	74	147
Th (ppm)	8.4	9	1	2	9	1	2
Rb (ppm)	122	123	12	25	131	12	25
U (ppm)	18.1	17	6	11	22	4	8
Sr (ppm)	75.5	87	5	10	93	9	18
Y (ppm)	35.4	34	3	5	36	2	4
Zr (ppm)	80.3	95	7	13	96	6	13
Nb (ppm)	9	9	1	2	9	1	2
Mo (ppm)	79	83	4	9	82	3	6

a - Values for major elements from lithium borate-fused disc analysis by WD-XRF at SGS; values for trace elements (ppm) from sodium borate fusion dissolution and analysis by ICP-MS.

b - Average HH-ED-XRF measured values (n = 7) and standard deviations (s) for reference material RTC-W-260, a black shale from the Devonian Woodford Formation of West Texas.

c - Limit of Determination of a Method (LDM) calculated according to Rousseau (2001).

Table 3. Types and Number of Analyses Performed By Core

Core Name	XRF	Total Inorganic Carbon (TIC)	Total Organic Carbon (TOC)	Total Percent Nitrogen (TN)	Carbon Isotopes ($\delta^{13}C$)	Nitrogen Isotopes ($\delta^{15}N$)	Percent Sulphur (LECO)	X-Ray Diffraction (XRD)
J.D. Godfrey E-8-1	162	162	162	162	162	162	N/A	N/A
N. Petty D-6-1	208	208	208	208	208	208	N/A	N/A
Lee C-5-1	36	36	36	36	36	36	36	N/A
Beck C-4-1	117	N/A	N/A	N/A	N/A	N/A	N/A	N/A
Harlow C-3-3	79	N/A	N/A	N/A	N/A	N/A	N/A	N/A
Locker B-2-1	100	100	100	100	100	100	100	N/A
Neal A-1-1	82	N/A	N/A	N/A	N/A	N/A	N/A	N/A
Johansen MC-1	24	24	24	24	24	24	24	N/A

CHAPTER 3

RESULTS

3.1 General X-Ray Fluourescence and Non-XRF Data

All the graphs contained in this section come from the X-ray fluorescence spectrometry and other geochemical analyses described in Chapter two. All plots relative to core depth have units in weight percent (e.g. % Si), degree of pyritization (DOP_T), parts per mil (‰), whole number ratio (C/N), or are expressed as an enrichment factor. Enrichment factors (EF) are expressed per the following equation:

$$EF = (\text{element in ppm/Al in ppm})_{sample} / (\text{element in ppm/Al in ppm})_{standard}$$

All cross-plots are expressed in weight percent, parts per million (ppm), or a combination of the two. Cross-plot data include data from all cores when available. Degree of pyritization (DOP) values are approximated using DOP_T. DOP_T is defined as pyritic iron/total iron (Raiswell and Berner, 1986). Both ternary and cross plots utilize data only from the Barnett interval in each core and excludes interval data from other formations (e.g. Marble Falls). Samples with negative and zero metal values were excluded from the analysis dataset in cross-plots and in down core plots.

3.2 X-Ray Fluorescence and Sulfur-Iron-TOC Ternary Graph Information

All ternary plots represent the use of normalized data. Ternary diagrams utilizing calcium oxide (CaO), alumina (Al_2O_3), and silica (SiO_2) are used to compare the composition of the Barnett to that of average gray shale. A ternary diagram utilizing total organic carbon (TOC), sulfur (S), and iron (Fe) is used to determine the amount of iron held in pyrite.

3.3 Chemostratigraphic Data

Chemostratigraphic information for all eight cores is plotted in two to three pages depending on the types of geochemical data available for that particular core. The first page of chemostratigraphic data is for major elements. These are used to determine changes in mineralogy over time. The second page is for trace elements expressed as enrichment factors (EF). These are used to determine changes in redox conditions over time. The third page is for non-XRF data including total organic carbon, total inorganic carbon, stable isotope ratios for organic carbon and nitrogen, total carbon/total nitrogen ratios, and degree of pyritiztion (DOP_T). These are used to determine changes in organic matter richness, presence of carbonate, organic matter provenance, and redox conditions respectively over time.

Figure 7. Core colors for cross-plots.

3.4 Cross-Plot Diagrams

Cross-plots of major elements versus aluminum are used to identify the presence of each element in clay and non-clay mineral phases. Aluminum is used as a proxy for clay mineral phases (e.g. illite). A cross-plot of total inorganic carbon (TIC) versus calcium is used to determine the presence of calcium in carbonate and non-carbonate phases. Cross-plots of copper, nickel, and zinc versus total organic carbon (TOC) are used to determine partially the phases where these elements are present. A cross-plot of sulfur versus total organic carbon (TOC) is used to assess the relative redox conditions of the cores. Sulfur is plotted against iron to indicate the association of iron with sulfur in sulfide phases. A cross-plot of DOP_T versus enrichment factors for molybdenum is used to determine the relationship between iron sulfurization and molybdenum enrichment. A cross-plot of DOP_T versus total organic carbon (TOC) is used to determine the relationship between iron sulfurization and organic matter preservation. A cross-plot of molybdenum versus total organic carbon (TOC) is used to determine the degree of hydrographic restriction in the basin. A cross-plot of Mo/TOCx10-4 versus the log of time (t) in years is used to estimate deep-water renewal times (τ_{dw}) for the basin. Figure 7 shows the colors used to represent each core in the cross-plots with the exceptions of Figures 8, 9 and 51.

CHAPTER 4

DISCUSSION

4.1 Bulk Geochemistry

The bulk geochemistry of the Barnett Formation is useful in identifying the mineralogy of the formation. Cross-plots of major elements versus aluminum are used to identify the mineral phases where the element is present. A cross plot of total inorganic carbon (TIC) versus calcium is used to determine partially the mineral phases where calcium is present. Cross-plots of copper, nickel, and zinc versus total organic carbon (TOC) are used to determine presence of these minerals in mineral and non-mineral phases (i.e. organic matter).

4.1.1 Major Elements

Aluminum is often used as a geochemical proxy for clay minerals such as illite. XRD patterns from the Texas United 1 Blakely core in the Barnett Formation of the northern Fort Worth Basin indicate the presence of illite, calcite, pyrite, and quartz (Rowe et al., 2008). Strong linear relationships between potassium and titanium with aluminum (Figures 41 and 42) suggest that these elements predominately reside in clay mineral phases including illite.

Silicon also exhibits a strong linear trend with aluminum (Figure 40), however, there are many data points to the left of the trend indicating an enrichment of silicon relative to aluminum. This is an indication that silicon resides in another mineral phase apart from clays, most likely silica (quartz). It is not clear whether the source of this excess silica is biogenic or detrital in origin.

Iron shows a very strong linear relationship with aluminum (Figure 39) indicating that iron resides in clay mineral phases. The enrichment of iron relative to aluminum, however, points to the presence of iron in other mineral phases apart from clays. The cross-plot of iron versus sulfur shows a fairly strong linear trend indicating that iron resides in an iron sulfide phase (i.e.

pyrite). Previous researchers have observed the presence of pyrite in cores from the southern Fort Worth Basin (Loucks and Ruppel, 2008). In addition, the author observed numerous pyrite nodules in several of the study's cores. The enrichment of iron relative to sulfur (Figure 43) indicates the presence of iron in other phases (i.e. clays).

Total inorganic carbon (TIC) is used as a geochemical proxy for carbonates such as calcite. There is a good sublinear trend between total inorganic carbon and calcium. The enrichment of calcium relative to total inorganic carbon (Figure 48) indicates the presence of calcium in other mineral phases. The most likely other phase for calcium is in Ca-phosphates found in phosphatic layers and phosphate nodules (Loucks and Ruppel, 2008; Loucks, 2009).

4.1.2 Trace Elements and Total Organic Carbon

Total organic carbon (TOC) is commonly used as a geochemical proxy for organic matter. Trace elements such as copper, nickel, and zinc are micronutrients and often associated with preserved organic matter. Cross-plots of copper, nickel, and zinc versus total organic carbon (Figures 45-47) indicate a linear trend and thus a strong association of these elements with organic matter. Enrichment of these elements relative to total organic carbon indicates their presence in another mineral phase. SEM images from the Locker B-2-1 core suggest the presence of a zinc sulfide phase (Hughes et al., 2009).

4.1.3 Calcite-Clay-Quartz Ternary Diagrams

Ternary diagrams for all eight cores were plotted to determine the composition of the Barnett Formation relative to average marine gray shale. The composition of average marine gray shale (Wedepohl, 1971, 1991) is represented by the red rectangle on each ternary plot. The solid line on each ternary plot represents a carbonate/phosphate dilution line. All of the cores indicate varying degrees of dilution by carbonate and non-clay silica phases.

4.2 Paleoceanography

The physical and chemical paleoceanography of the sea in which the Barnett Formation was deposited can be looked at both temporally and spatially. The paleoceanography can be examined on a temporal basis by examining differences in the chemostratigraphy of each core. The paleoceanography of the Barnett can be examined spatially by comparing differences between the cores across the southwest-northeast transect. The chemical paleoceanography of the Barnett can be revealed primarily through the use of several redox indicators and stable isotope ratios of nitrogen. The physical paleoceanography of the Barnett Formation can be studied using molybdenum-total organic carbon ratios to reveal the degree of hydrographic restriction and the scale of deepwater renewal times.

4.2.1 Chemical Paleoceanography

4.2.1.1 Redox Indicators

Trace metal concentrations in the form of enrichment factors (EFs) were used to evaluate the redox character of the Barnett. Enrichment factors of one represent levels similar to that of average crustal abundance and represent deposition under oxic conditions, while higher enrichment factors represent deposition under anoxic or even euxinic conditions (Calvert and Pedersen, 1993; Crusius et al., 1996).

Molybdenum generally shows moderate degrees of enrichment with a few peaks representing higher levels of enrichment in the Barnett interval. Moderate enrichments tend to indicate suboxic deposition (McManus et al., 2006). However, given the general conclusion that the Barnett was deposited under anoxic-euxinic conditions with high levels of organic matter accumulation (e.g. Loucks and Ruppel, 2007; Rowe et al., 2008), the moderate levels of molybdenum enrichment are likely the result of aqueous molybdenum being removed to the sediment without compensatory resupply (Algeo and Lyons, 2006). Molybdenate ions are sequestered to sediments in the presence of sulfide minerals, organic matter, or sulfidized organic matter (Helz et al., 1996; Erickson and Helz, 2000; Tribovillard et al., 2004). The strong

correlation between molybdenum and total organic carbon in Figure 8 indicates that organic matter's importance in scavenging molybdenum (Lyons et al., 2003). The lack of resupply is most likely due to hydrographic restriction during Barnett deposition (Rowe et al., 2008; Algeo and Rowe, 2011). This will be discussed further in section 4.3.2.

Uranium, zinc, and vanadium also show similar patterns of enrichment molybdenum. These metals have a strong euxinic affinity (Algeo and Maynard, 2004). The enrichment of these metals, especially molybdenum, is indicative of anoxic to euxinic (free H_2S) conditions during the deposition of the Barnett (Calvert and Pedersen, 1993; Piper, 1994; Crusius et al., 1996; Tribovillard et al., 2006). The strong level of agreement between molybdenum, vanadium, uranium, and zinc are also indicative of deposition under anoxic-euxinic conditions versus oxic or suboxic conditions (Algeo and Maynard, 2004; Tribovillard et al., 2008; Piper and Calvert, 2009). Zinc, copper, and nickel all show a strong degree of correlation. This likely reflects their strong association with organic matter in the form of micronutrients (Figures 45-47). Peaks of the first set of trace elements likely represent periods of intensified anoxia or more likely, periods of euxinia.

Sulfur-iron-organic carbon relationships were also used to evaluate redox conditions in the Barnett. A cross-plot of iron versus sulfur was used to determine the association of iron with sulfur. A fairly strong linear trend along the pyrite line in Figure 43 indicates the presence of iron in a sulfide phase (i.e. pyrite). Pyrite commonly forms in stages from bacterial sulfate reduction, the formation of Fe monosulfides by reaction of H_2S with Fe minerals, and by reaction of Fe monosulfides with elemental sulfur (Berner, 1970). A cross-plot of total organic carbon (TOC) versus sulfur (Figure 44) was used to assess relative redox conditions. Significant portions of the data in Figure 44 points plotted to the left of the normal marine line with a positive intercept. This enrichment of sulfur relative to total organic carbon (TOC) is an indication of anoxic or euxinic redox conditions during deposition (Berner and Raiswell, 1983). A ternary diagram of sulfur-iron-organic carbon (Figure 51) was used to determine the degree of iron in pyrite. The sublinear trend above the pyrite line indicates that less than one hundred percent of iron resides

in the pyrite phase (Dean and Arthur, 1989). The sublinear trend also indicates iron limitation or deficiency (Dean and Arthur, 1989).

The use of degree of pyritization (DOP_T) was also used to assess bottom water redox conditions. DOP levels are defined as oxic ($DOP_T<0.42$), dyoxic ($0.46<DOP_T<0.80$), and anoxic/euxinic ($0.55<DOP_T<0.93$) (Raiswell and Berner, 1986; Raiswell et al., 1988). DOP_T for the Barnett samples ranged from 0-0.98 with a couple samples above 1.0. The average DOP_T for the samples below 1.0 was 0.64 which places Barnett bottom water oxygen at dysoxic or anoxic-euxinic levels. The relatively high DOP_T is likely the result of persistent anoxic conditions with episodes of euxinia, in addition to decreased siliciclastic accumulation (Lyons et al., 2003; Lyons and Severmann, 2006). The Barnett is considered to have been deposited during a period of sediment-starvation making this plausible scenario (Kier, 1988; Loucks and Ruppel, 2007). Plots of DOP_T versus molybdenum enrichment factors and total organic carbon (Figures 49 and 50) reveal positive relationships between iron sulfurization with molybdenum enrichment and organic matter preservation.

The existence of framboidal pyrite in the 2-4 micron size-range in other Barnett samples from other areas of the Fort Worth Basin also suggests the possibility of periods of water column euxinia during deposition (Papazis, 2005; Loucks and Ruppel, 2007). In addition, authigenic pyrite nodules and pyrite fracture fills in several of the cores were observed. All of these features point to persistent anoxia with episodes of euxinia during Barnett deposition.

4.2.1.2 Stable Nitrogen Isotope Ratios

Stable nitrogen isotope ratios were used to evaluate nitrogen cycling during the deposition of the Barnett. $\delta^{15}N$ ratios for the Barnett range from slightly negative (-1.75‰) to highly positive (12.77‰) with predominately positive values and with an average of 7.76‰. The $\delta^{15}N$ values are relatively constant in most of the cores. The high $\delta^{15}N$ values are indicative of intensified denitrification during deposition (Algeo et al., 2008). Denitrification is the nitrogen cycle process by which nitrate and nitrite are reduced to nitrogen gas (N_2). This process is

particularly important in areas with low oxygen levels in the water column such as oxygen-minimum zones (OMZs) (Algeo et al., 2008). It is, therefore, an indicator of lower oxygen levels in the water column. Denitrification usually has been associated with suboxic conditions in the water column (Twichell et al., 2002).

4.2.2 Physical Paleoceanography

4.2.2.1 Basinal Restriction

The degree of hydrographic restriction in marine basins and the associated increased stratification of the water column has been an area of intense recent study. Algeo and Lyons (2006) noted that molybdenum-total organic carbon ratios can be used to reflect the degree of hydrographic restriction of the subpycnoclinal water mass in marine basins. Hydrographic circulation in marine basins plays an important role in the basin environment and in biogeochemical cycles (Algeo and Rowe, 2011). The geometry of basins plays an important role in controlling hydrographic restriction. In particular, the ratio of a basin's size to the depth of underwater sills controls restriction. Restriction is higher in basins with a large area and shallow sills (e.g. Black Sea) than in basins with a smaller area and a deeper sill (e.g. Saanich Inlet) (Algeo and Lyons, 2006; Algeo and Rowe, 2011).

Figure 8 shows the cross-plot of total organic carbon versus molybdenum concentrations. The low Mo/TOC ratios of the Barnett in the southern Fort Worth Basin indicate a high degree of hydrographic restriction. This conclusion is consistent with paleoenvironmental evidence in the Fort Worth Basin that indicate watermass restriction. This evidence includes high levels of total organic carbon (TOC), laminated sediments, the abundance of pyrite, and various redox indicators noted in section 4.3.1. Although previous interpretations saw the Barnett Formation as being deposited under normal marine conditions (Henry, 1982; Thompson, 1988), other interpretations including more recent ones (Kier et al., 1979; Loucks and Ruppel, 2007; Rowe et al., 2008) interpreted the deposition of the Barnett as occurring under restricted marine conditions. Based upon this data, there was a higher degree of hydrographic restriction in the

southern Fort Worth Basin than all similar modern anoxic basins (e.g. Saanich Inlet). The southern Fort Worth Basin also appears to be slightly more restricted than the northern Fort Worth Basin (Rowe et al., 2008).

Although the geometry of the Fort Worth Basin during the deposition of the Barnett is somewhat unknown due to the speculative nature of paleogeographic reconstructions, it is known that the Fort Worth Basin area was at least partially encircled by various tectonic elements (e.g. Laurussian craton). It is possible that the existence of a sill or sills on the basin periphery could have contributed to hydrographic restriction. Another possible factor influencing hydrographic restriction is the set of third-order eustatic sea-level changes that occurred during the Barnett's deposition (Ross and Ross, 1987; Loucks and Ruppel, 2007). Lower sea level over a basin's sill could lead to greater basinal restriction and stratification (Algeo and Rowe, 2011). Eustatic rise often leads to sediment starvation, organic matter accumulation, and reduced seasonal mixing (Sageman et al., 2003). Reduced seasonal mixing due to eustatic rise in particular could lead to increased stratification of the water column.

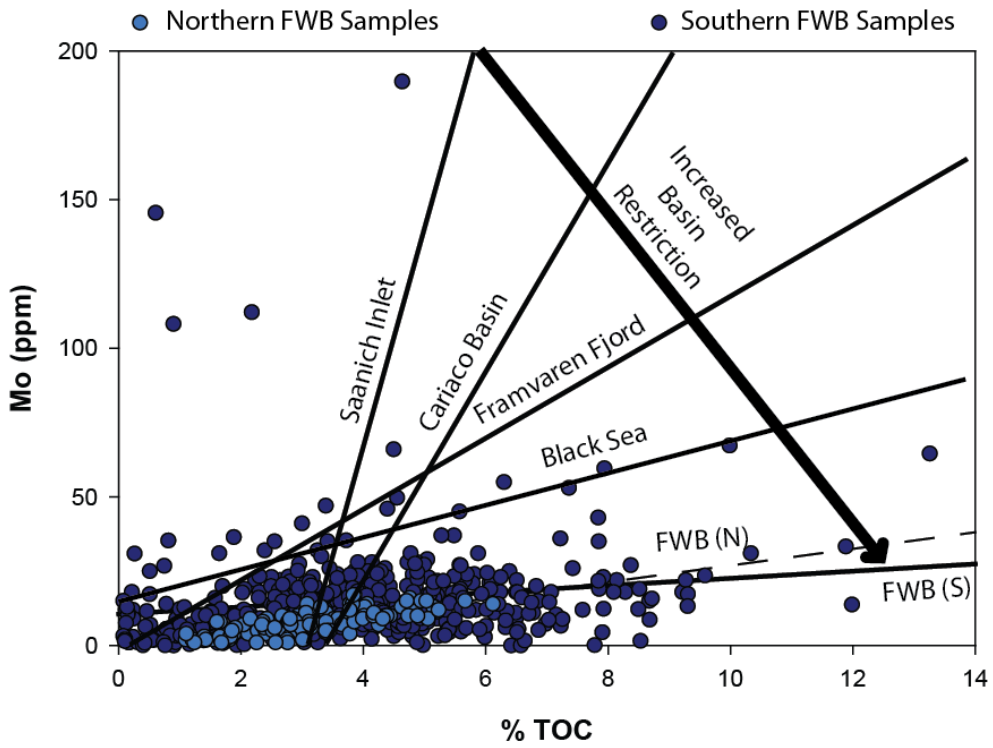

Figure 8. Cross-plot of total organic carbon (TOC) versus Mo (Algeo and Lyons, 2006).

4.2.2.2 Subpycnoclinal Water-Mass Renewal Time

Another physical parameter that can be determined using molybdenum-total organic carbon (TOC) ratios is renewal time for the subpycnoclinal water mass. Algeo and Lyons (2006) plotted the molar ratio of molybdenum to total organic carbon versus a logarithmic scale for time. Using a regression line equation (Algeo and Rowe, 2011) slightly modified from that used by Algeo and Lyons (2006), deep-water renewal times for the various Barnett cores were calculated. The results for the southern Fort Worth Basin cores listed in Figure 9 show that deep-water renewal times were generally greater than the modern anoxic basins with the exception of the Johansen MC-1 core. The southern cores have much shorter deepwater renewal times compared to the Blakely core in the northern Fort Worth Basin (Rowe et al., 2008).

The results for the southern cores in Figure 9 generally show a low degree of temporal variation in deep-water renewal times. There is a higher degree of spatial variation in deep-water

renewal times across the core transect. In particular, the Johansen MC-1 core shows a significantly shorter renewal time than the other Barnett cores. This is likely due to the situation of the Johansen core closer to the perceived basin margin (Loucks and Ruppel, 2008). The proximity to the basin margin likely meant shallower water depths and thus a higher degree of water-mass circulation and water column ventilation. The low DOP_T values for the Johansen MC-1 core are likely the result of increased water mass circulation and thus higher levels of oxygenation in the water column.

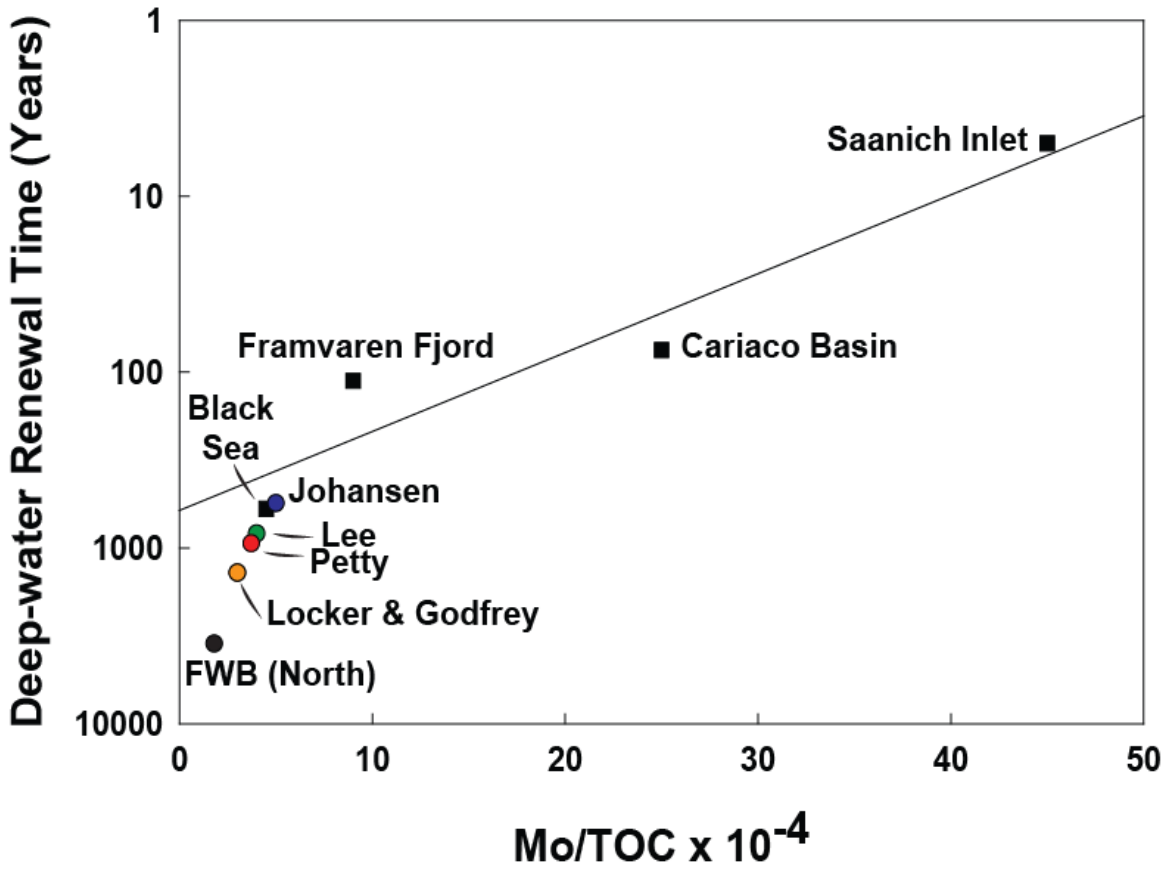

Figure 9. Cross-plot of Mo/TOC x 10^{-4} versus deep-water renewal time (τ_{dw}) (Algeo and Lyons, 2006). Updated deep-water renewal values for modern basins from Algeo and Rowe, 2011.

4.3 Paleoclimate

Using stable isotopes of nitrogen, a reconstruction of changes in paleoclimate was made. The high $\delta^{15}N$ values indicative of denitrification have been used in a previous study to indicate deposition during an interglacial period (Algeo et al., 2008). It has been proposed that intensified denitrification could lead to greater concentration of greenhouse gases, most notably carbon dioxide and nitrogen oxide (Algeo et al., 2008). There is a pronounced peak in $\delta^{15}N$ values prior to the contact between the Barnett and the overlying Marble Falls before it declines substantially. This peak seen on several of the study's cores (e.g. Figure 37) may represent the maximum transgression prior to a return to a period of glaciations during the Pennsylvanian period (Algeo et al., 2008; Fielding et al., 2008). The peak may correspond to one of the last two peaks in the second-order highstand curve published by Ross and Ross (1987). The lack of accurate timing from biostratigraphic control makes this association speculative, however.

4.4 Organic Composition

Using total organic carbon (TOC), stable isotopes of organic carbon, and carbon-nitrogen ratios (C/N), the organic character of the Barnett Formation in the southern Fort Worth Basin was examined. The Barnett in the southern Fort Worth Basin is organic rich (TOC>2.5%) with total organic carbon (TOC) ranging from 0.07-13.25% with an average TOC of 4%. This degree of organic enrichment roughly matches that of the Barnett Formation in the northern Fort Worth Basin (Henk et al., 2000; Loucks and Ruppel, 2008).

The organic richness of the Barnett samples is likely primarily because of higher primary productivity with enhanced preservation of organic matter related to the low oxygen levels in the bottom waters. The strong association of copper, nickel, and zinc with total organic carbon (Figures 45-47) and their relative enrichment along with high levels of total organic carbon (TOC) could be construed as being the result of higher primary productivity. The higher productivity is a possible result of seasonal upwelling related to an increased temperature contrast between the sea and land during a warmer interglacial period (Algeo et al., 2008). This periodic upwelling

would have led to the transport of nutrient-rich bottom waters to the surface. These nutrient-laden waters would then have led to enhanced primary production (Sageman et al., 2003). Previous studies have indicated that upwelling may have occurred during the deposition of the Barnett (Hill et al., 2007; Loucks and Ruppel, 2007).

Using stable isotopes of carbon from organic matter (C_{org}), the provenance of the Barnett organic matter was investigated. The $\delta^{13}C_{org}$ values ranged from -24‰ to -32‰ with an average $\delta^{13}C_{org}$ value of -30‰. This $\delta^{13}C_{org}$ value is higher than one would expect for organic matter primarily of marine origin (Meyers, 1994). $\delta^{13}C_{org}$ values for marine algae are typically in the -22‰ to -20‰ range. These values could be construed as the result of significant terrestrial organic matter input from C3 plants which have more negative $\delta^{13}C_{org}$ values (-27‰ on average) (Meyers, 1994). The geographic isolation of the Fort Worth Basin area from potential sources of terrestrial organic matter makes this unlikely, however. Previous studies of the petroleum geochemistry of the Barnett also have failed to find any significant terrestrial input to organic matter in the Barnett and indicated a marine origin for the organic matter present (Hill et al., 2007; Rodriguez and Philp, 2010). A possible explanation of the more negative $\delta^{13}C_{org}$ values is bacterial methanogenesis. The reduction of carbon dioxide to methane by bacteria during methanogenesis increases the fractionation of carbon isotopes and can lead to far more negative $\delta^{13}C_{org}$ values (Whiticar, 1999).

The provenance of the organic matter in the study's cores also was examined using carbon-nitrogen ratios. The carbon-nitrogen values ranged from 1.6 to 92.3 with an average C/N ratio of 21.78. Carbon-nitrogen ratios for marine algae typically range from 4 to 10 (Meyers, 1994). The C/N ratios in the Barnett are more typical of organic matter derived from terrestrial plants. The lack of evidence for substantial terrestrial organic matter inputs makes this unlikely (Hill et al., 2007). A more likely scenario producing the higher C/N ratios is the selective degradation of nitrogen-containing elements of organic matter (Meyers, 1994; Meyers, 1997; Twichell et al., 2002; Meyers et al., 2006; Meyers et al., 2009B). High C/N ratios are commonly seen in areas of high primary productivity (Meyers, 1994; Meyers, 1997; Twichell et al., 2002).

High C/N ratio values also have been interpreted as an indicator of low oxygen levels in the water column (Meyers et al., 2006; Meyers et al., 2009A). If high primary productivity and denitrification were occurring during deposition of the Barnett Formation, nitrogen-containing organic compounds likely were preferentially removed from organic matter, thus leading to higher carbon-nitrogen ratios.

CHAPTER 5

CONCLUSIONS

5.1 Conclusions

The use of geochemical proxies has allowed the reconstruction of the paleoceanography of the Barnett Formation during the mid-late Mississippian period. The reconstruction of the chemical paleoceanography provides insight into the redox conditions of the bottom waters and sediments during Barnett deposition. Reconstruction of the physical paleoceanography of the Barnett Formation provides insight into marine circulation patterns that have influences on biogeochemical cycles and the production and preservation of organic matter. Geochemical data has provided the foundation to reconstruct the chemostratigraphy of the Barnett Formation in the southern Fort Worth Basin. Studying the chemostratigraphy of the formation allows the determination of changes in paleoceanography and paleoclimate over time. The use of several cores in southwest-northeast transect allows for the determination of paleoceanographic and paleoenvironmental changes across this part of the basin.

1. The physical paleoceanography of the Barnett Formation reveals that the area of Barnett deposition in the southern Fort Worth Basin was hydrographically restricted based upon Mo/TOC ratios. The southern basin was more restricted than comparable modern anoxic basins and the northern Fort Worth Basin during Barnett time. This basinal restriction led to longer deep-water renewal times. These deep-water renewal times are longer than those of comparable modern anoxic basins and shorter than those for the Barnett Formation of the northern Fort Worth Basin. Deep-water renewal times for the southern basin range from 557-1383 years.

2. The chemical paleoceanography of the Barnett Formation reveals that the Barnett strata were deposited under anoxic to euxinic conditions for essentially the entire depositional timeframe in the mid-late Mississippian. The southernmost end of the transect was deposited initially under anoxic conditions and later under oxic conditions. A variety of redox and paleoenvironmental indicators support this conclusion.

3. The Barnett strata in the southern Fort Worth Basin were determined to be organic rich (4% on average) in total organic carbon (TOC). The organic matter was determined to be primarily marine origin based on stable isotope ratios and carbon-nitrogen ratios. Carbon-nitrogen ratios also indicate the selective degradation of organic matter and low oxygen levels in the water column.

4. The Barnett Formation was deposited during a second-order eustatic high stand during a warmer, interglacial period based upon stable nitrogen isotope ratios.

5. The bulk geochemistry of the Barnett Formation indicates that it is composed primarily of siliceous mudstone and calcareous siliceous mudstone with significant phosphate and sulfide phases present.

5.2 Areas for Future Study

Future work in this general area of study should include the production of additional geochemical datasets from other mudrock formations for comparison. For the Barnett Formation, three main areas of future work should be addressed. First, additional paleontological studies of the Barnett Formation need to be undertaken in order to provide greater biostratigraphic control. This would allow better timing of geologic events indicated by changes in chemostratigraphy. Second, additional structural geology and tectonic studies should be undertaken to determine the Fort Worth Basin's geometry to validate assumptions (i.e. presence of a sill or sills in the basin).

Finally, additional geochemical data from the northern and central Fort Worth Basin should be obtained in order to better understand the geologic and paleoceanographic evolution of the Barnett Formation in the Fort Worth Basin.

APPENDIX A

ADDITIONAL FIGURES

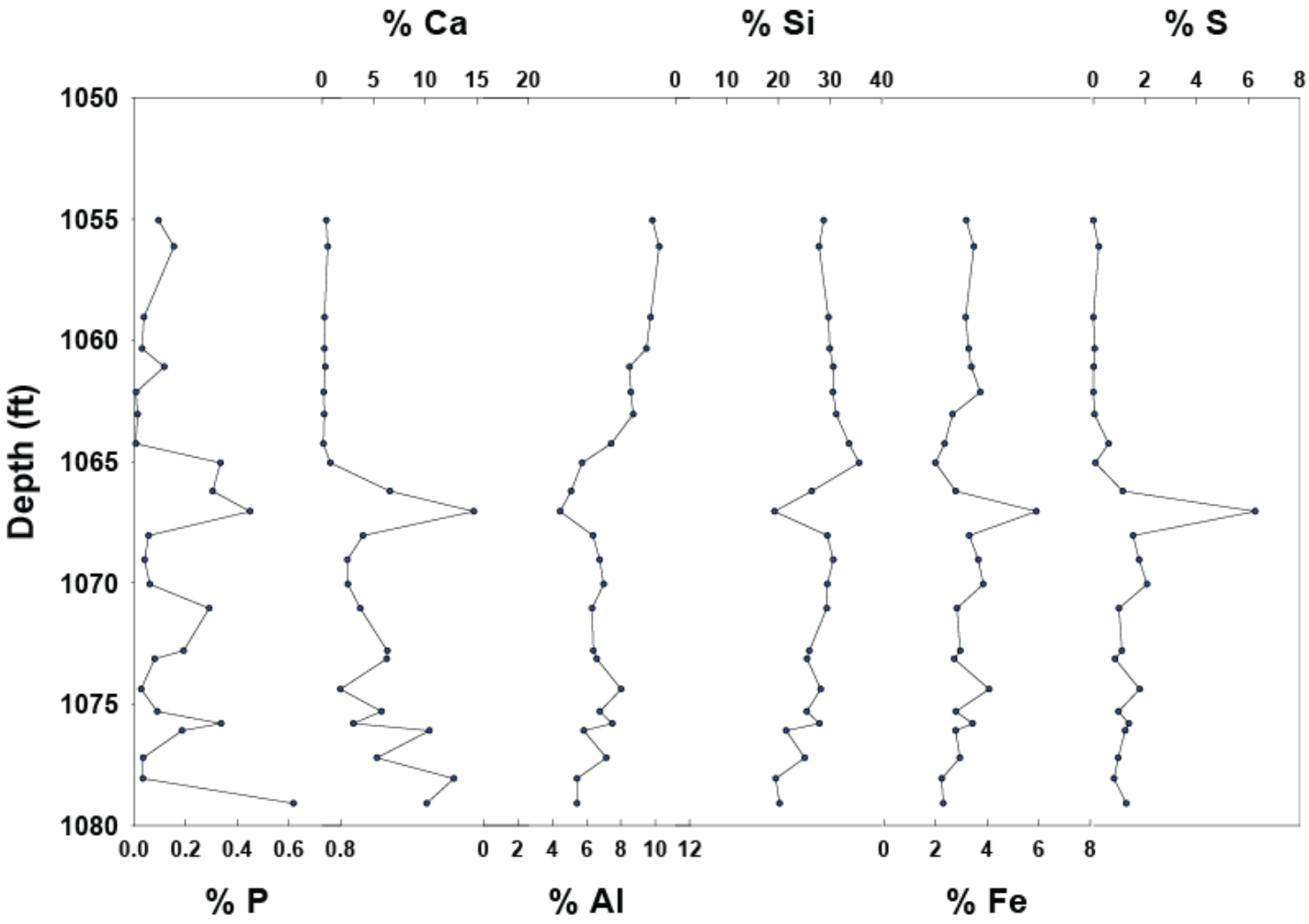

Figure 10. Major elements for Johansen MC-1.

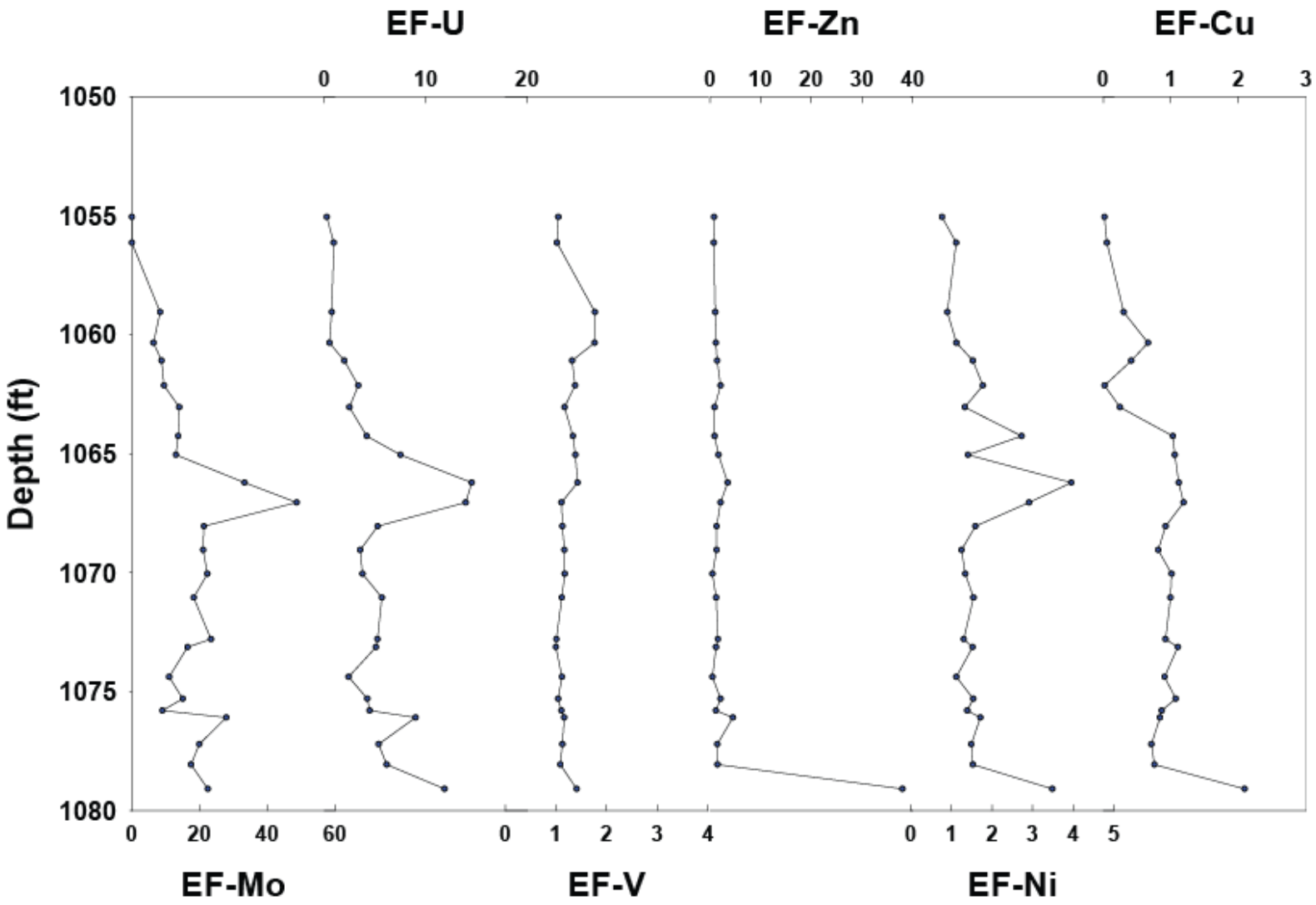

Figure 11. Trace elements for Johansen MC-1.

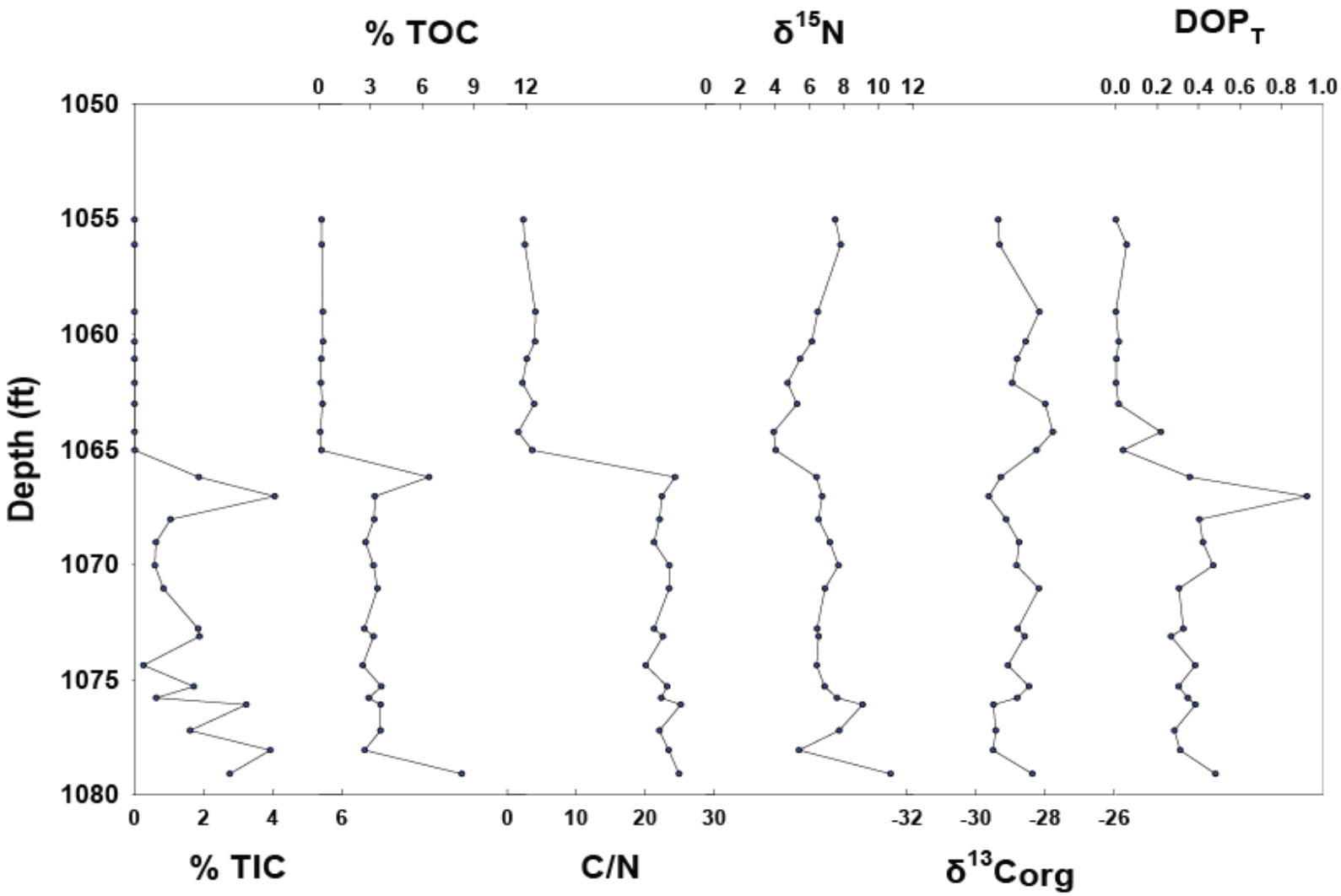

Figure 12. Non-XRF data for Johansen MC-1.

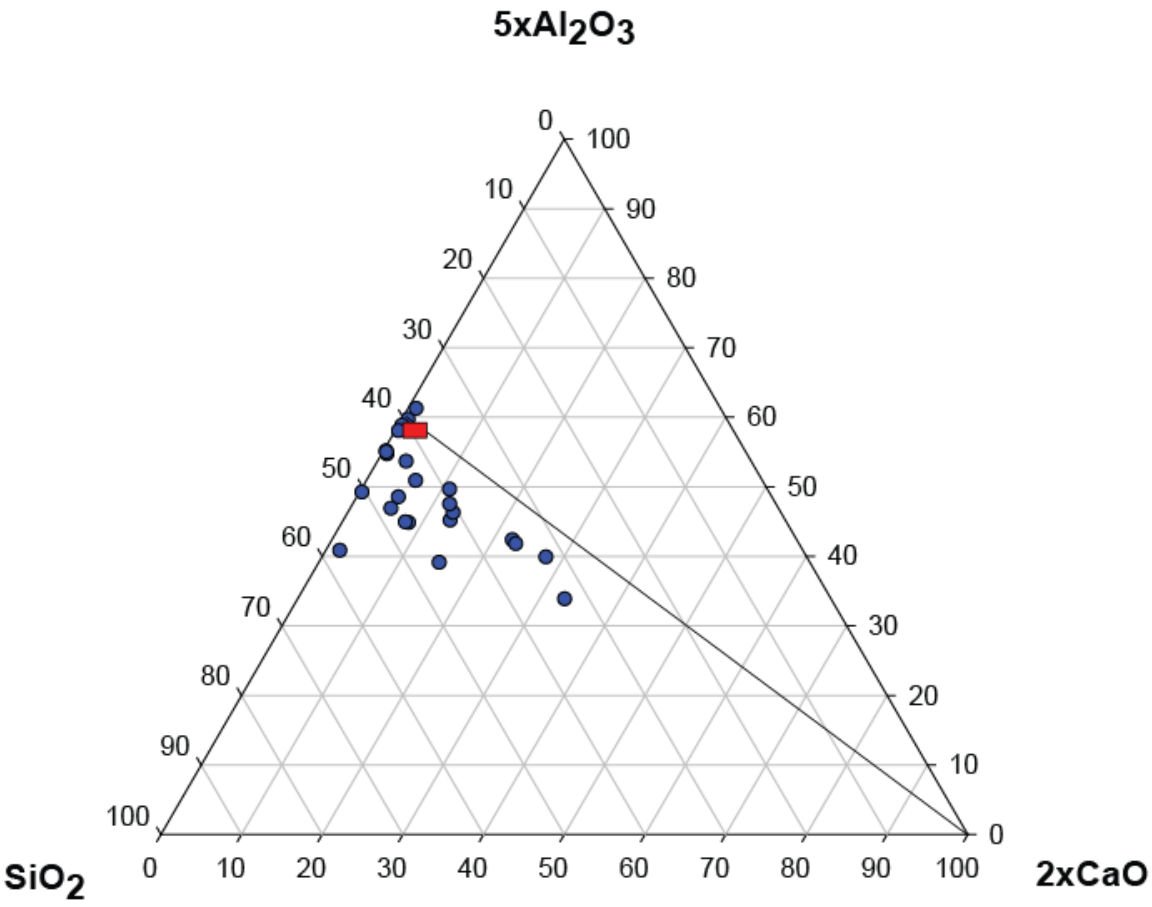

Figure 13. Calcite-clay-quartz ternary for Johansen MC-1.

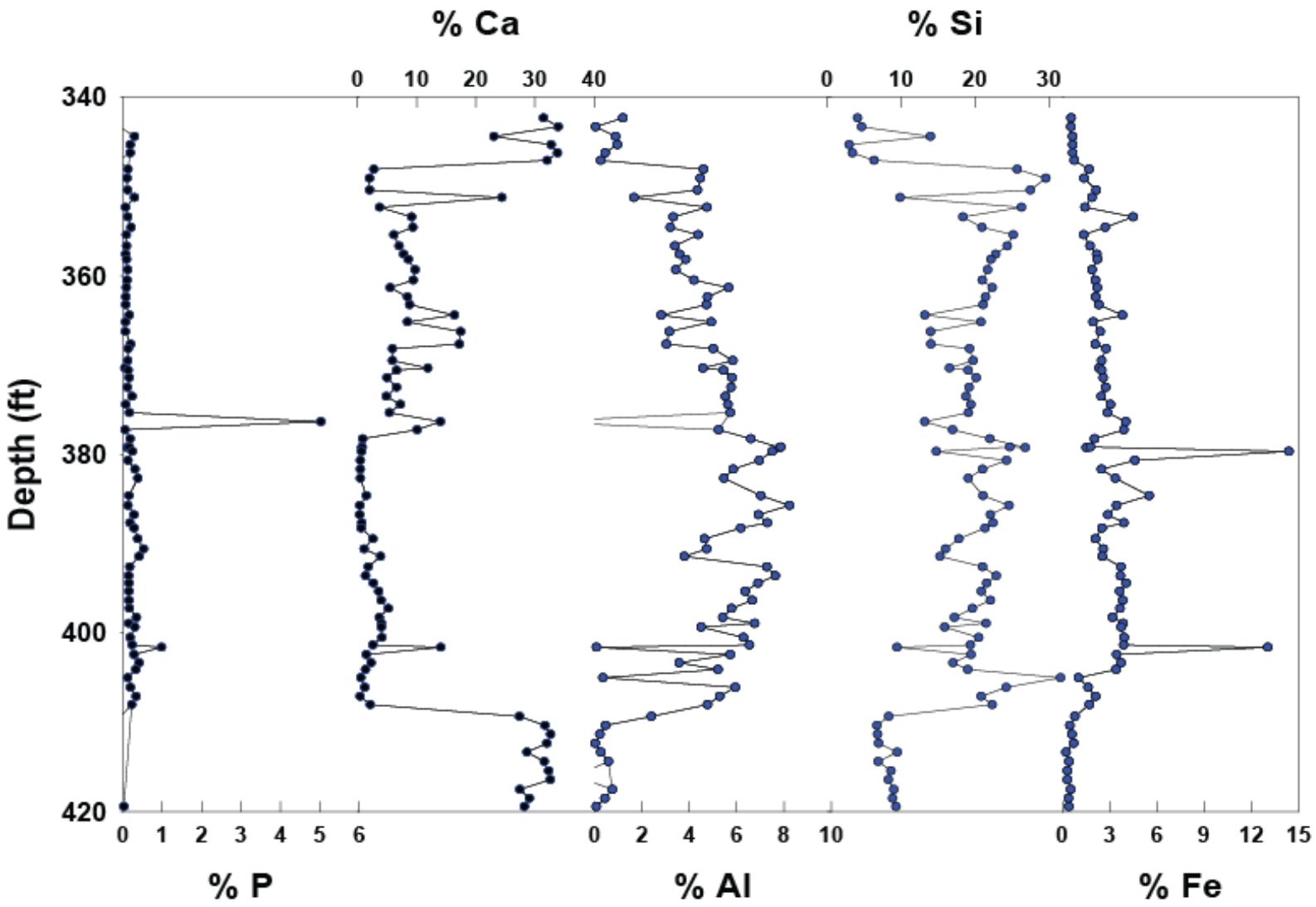

Figure 14. Major elements for Neal A-1-1.

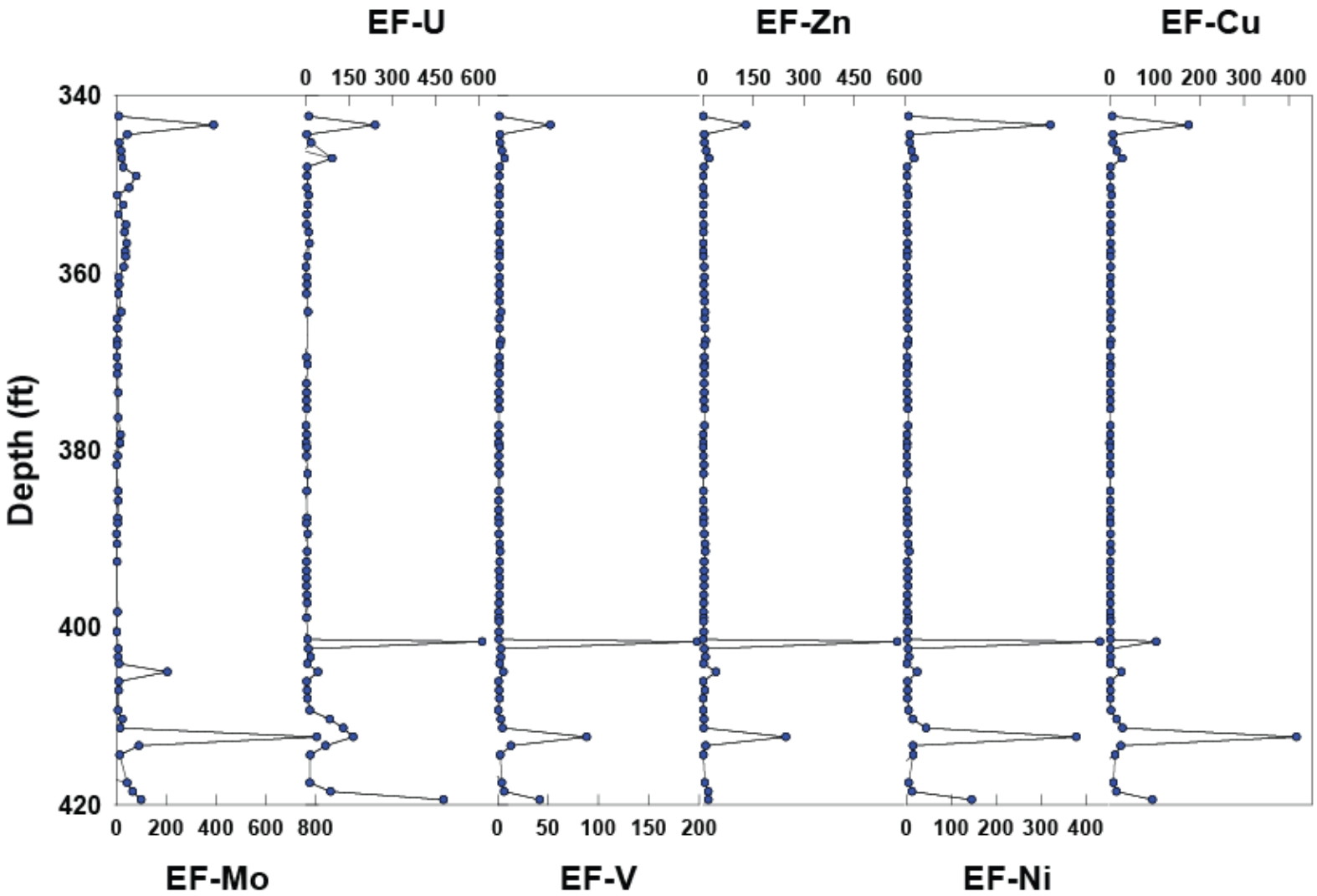

Figure 15. Trace elements for Neal A-1-1.

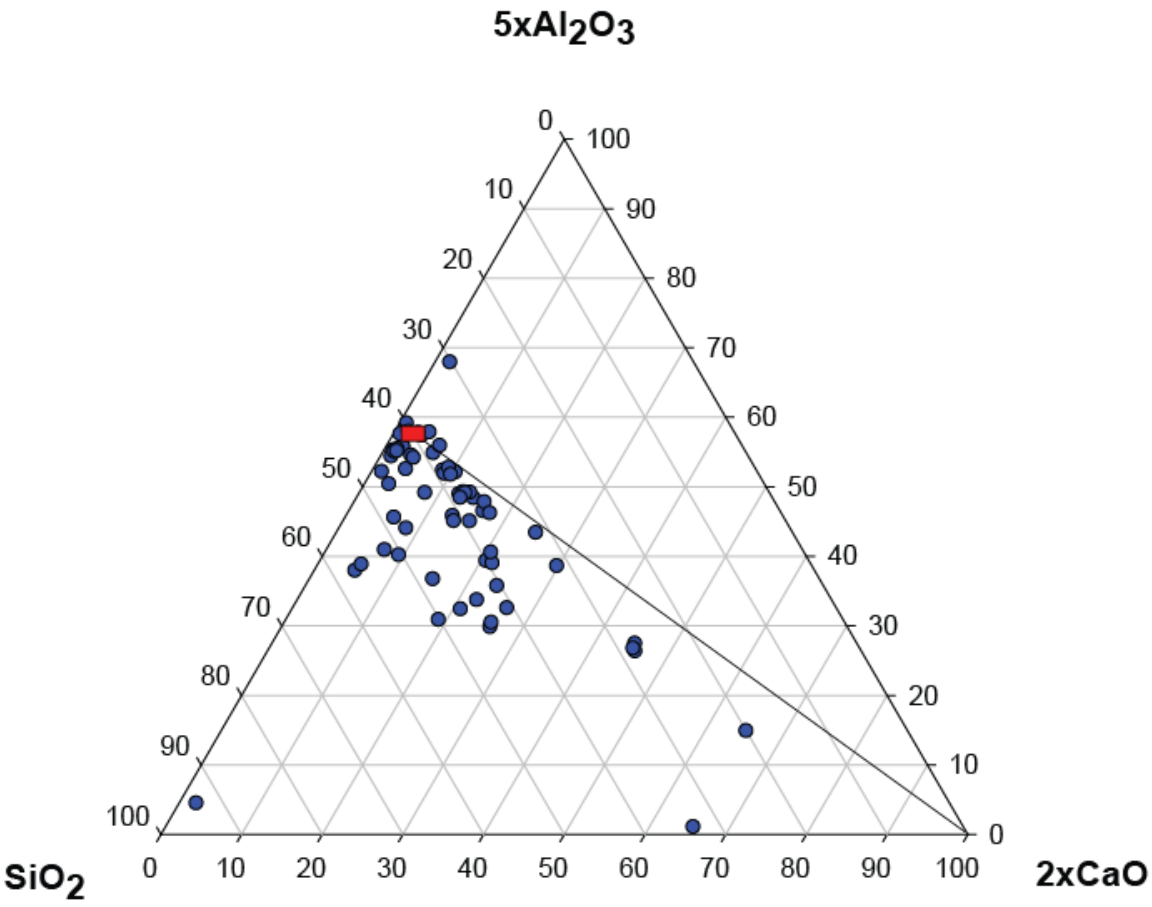

Figure 16. Calcite-clay-quartz ternary for Neal A-1-1.

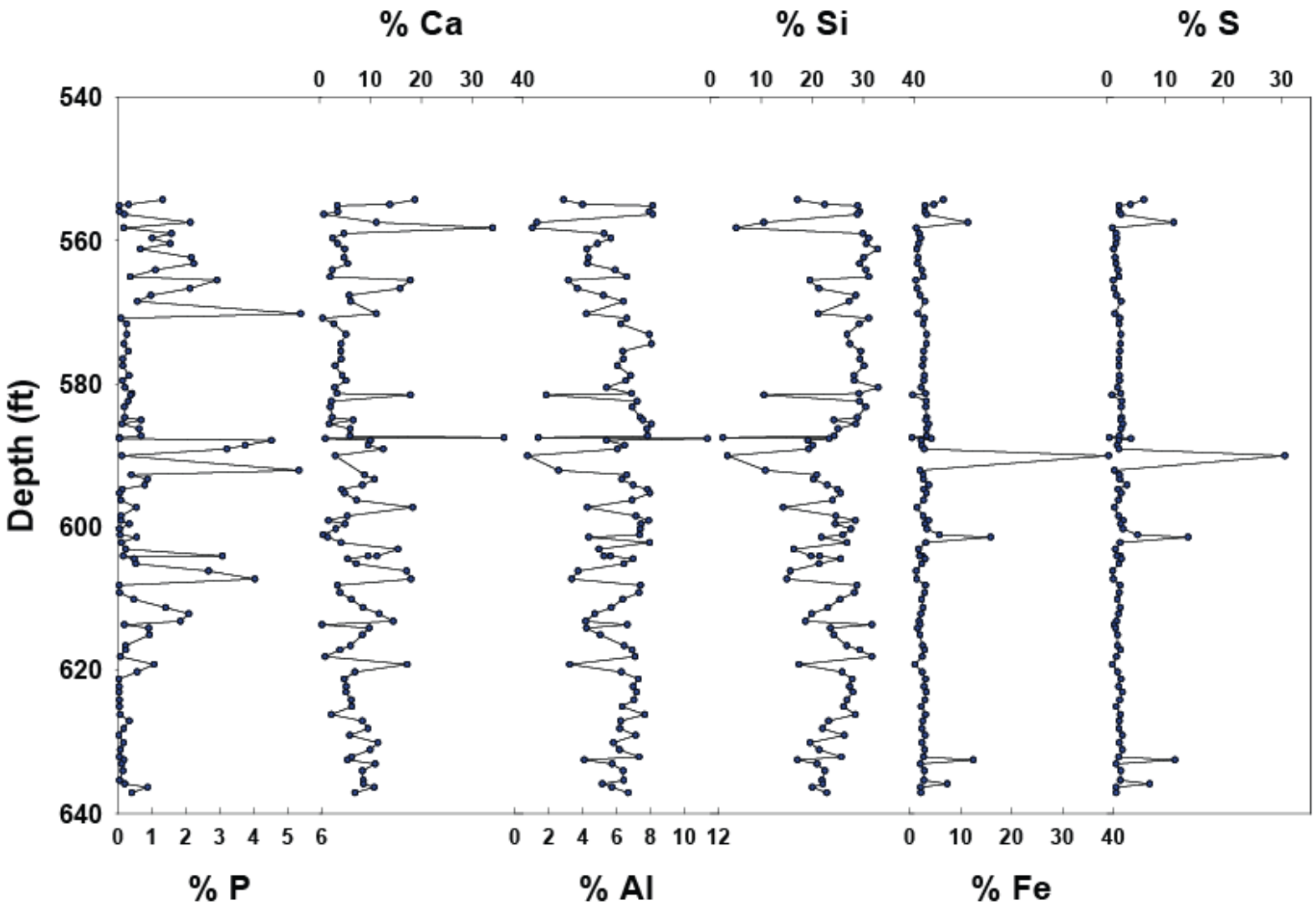

Figure 17. Major elements for Locker B-2-1.

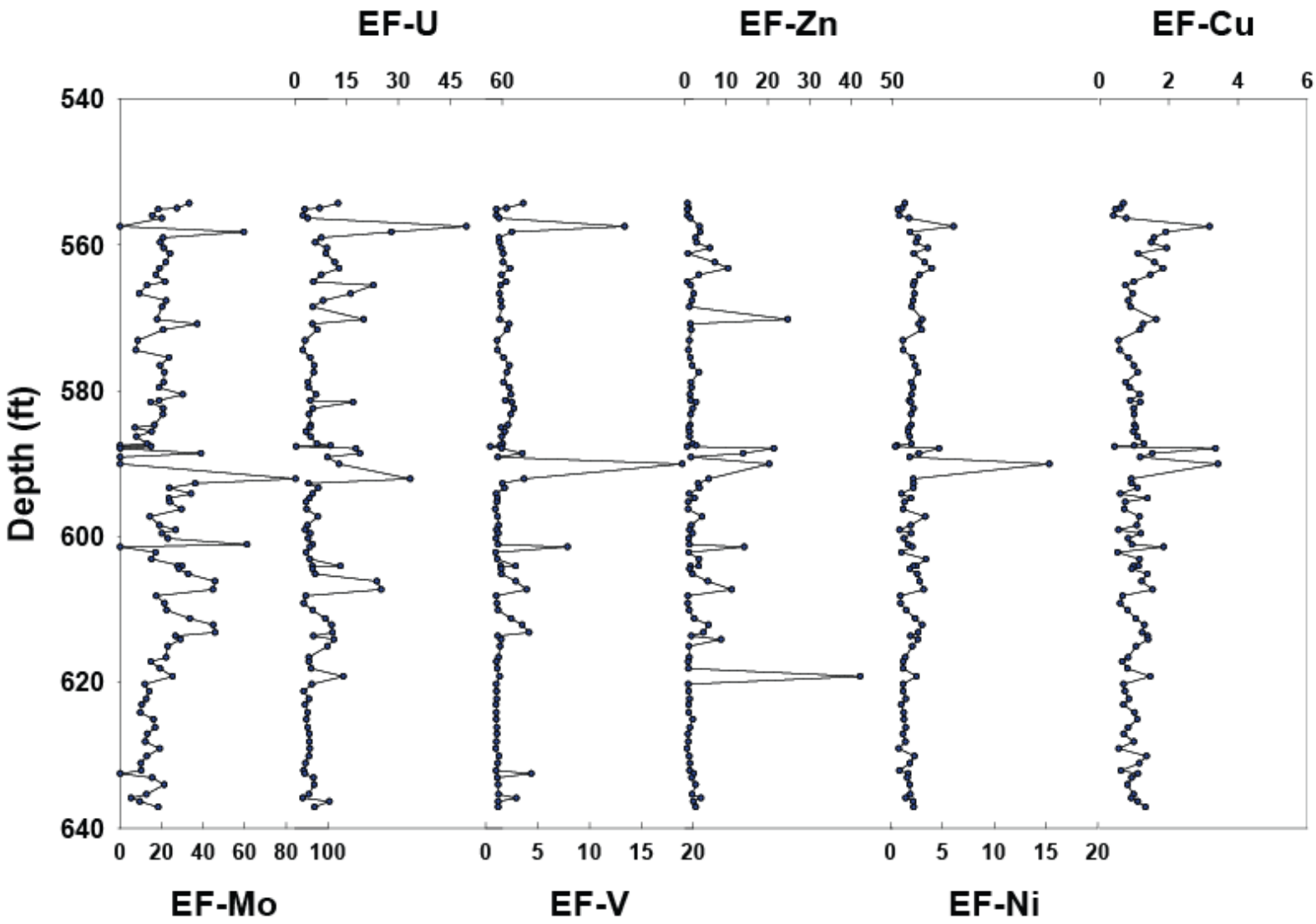

Figure 18. Trace elements for Locker B-2-1.

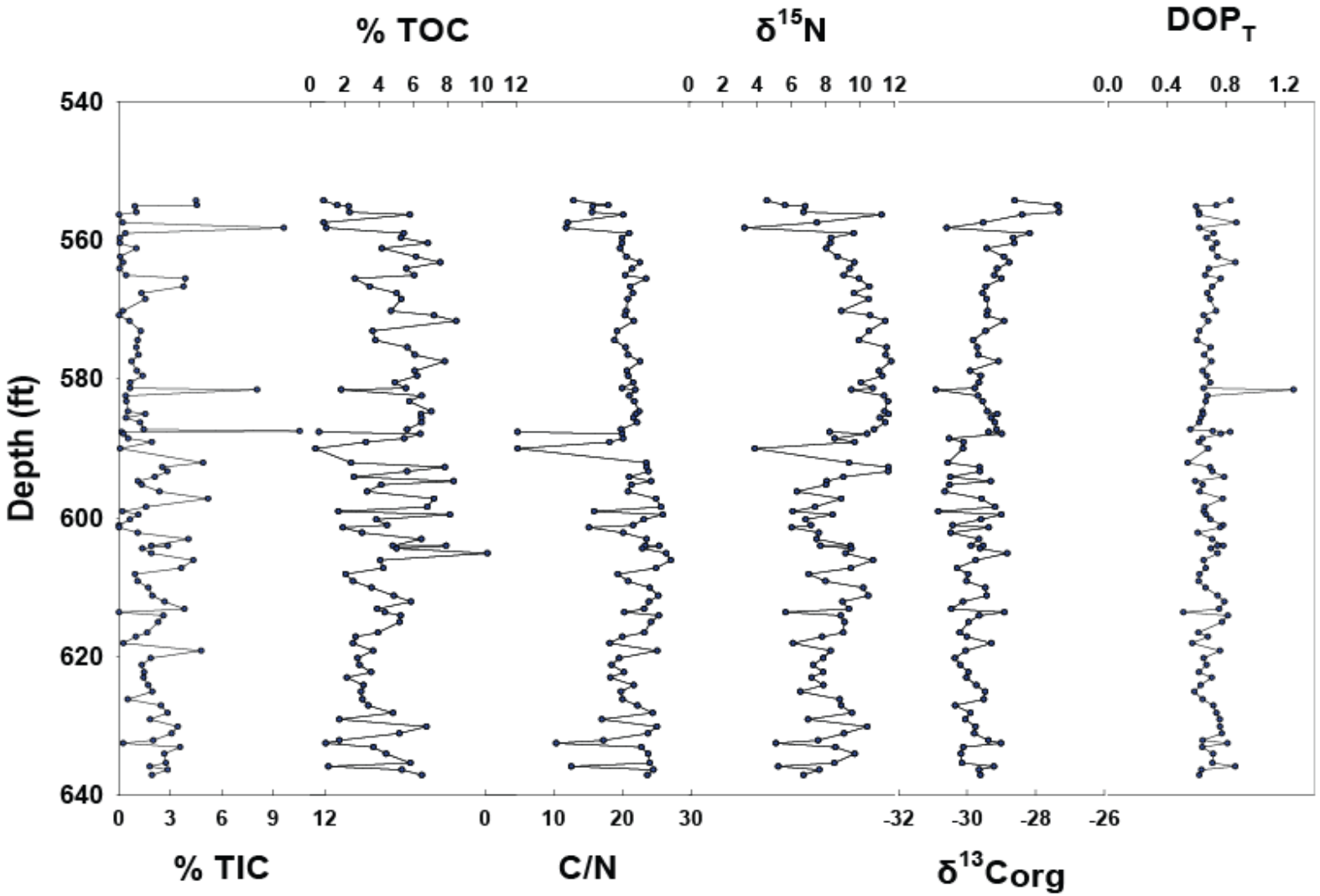

Figure 19. Non-XRF data for Locker B-2-1.

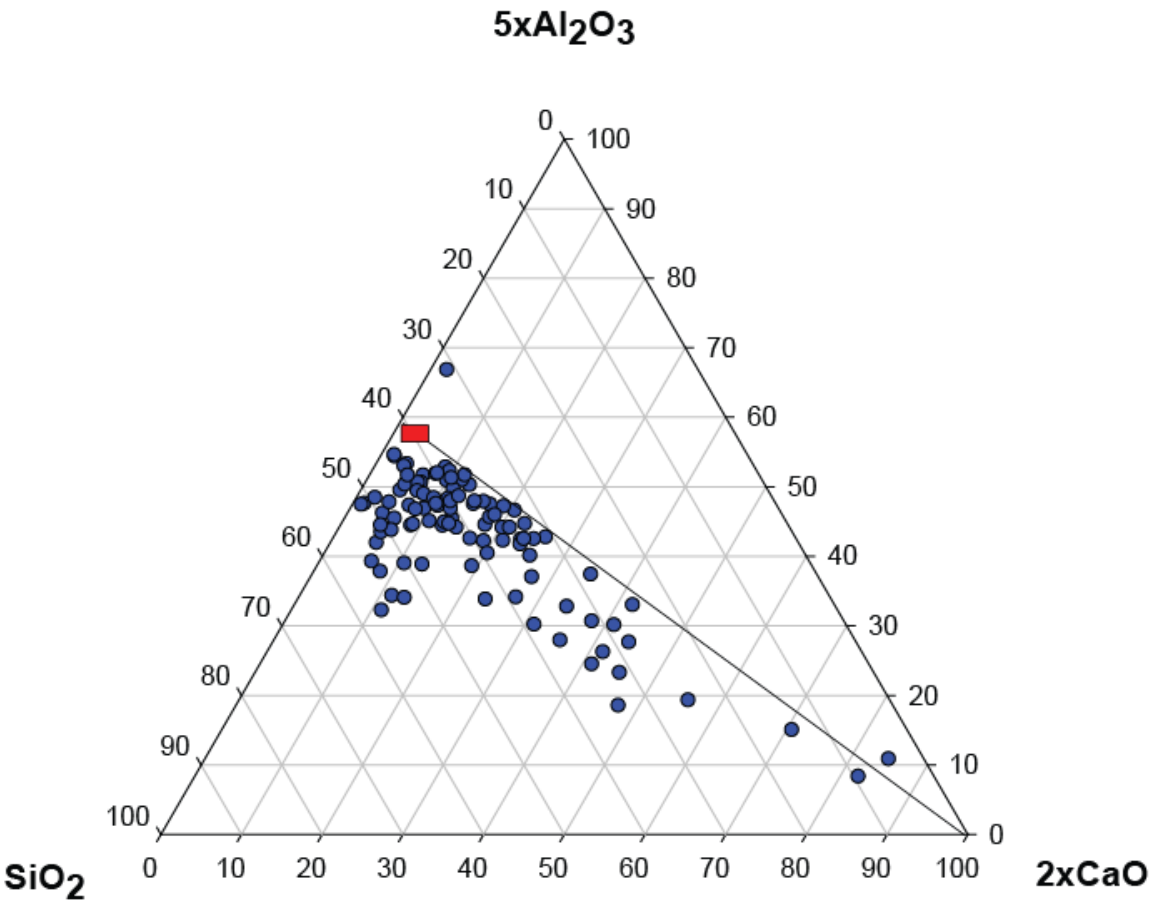

Figure 20. Calcite-clay-quartz ternary for Locker B-2-1.

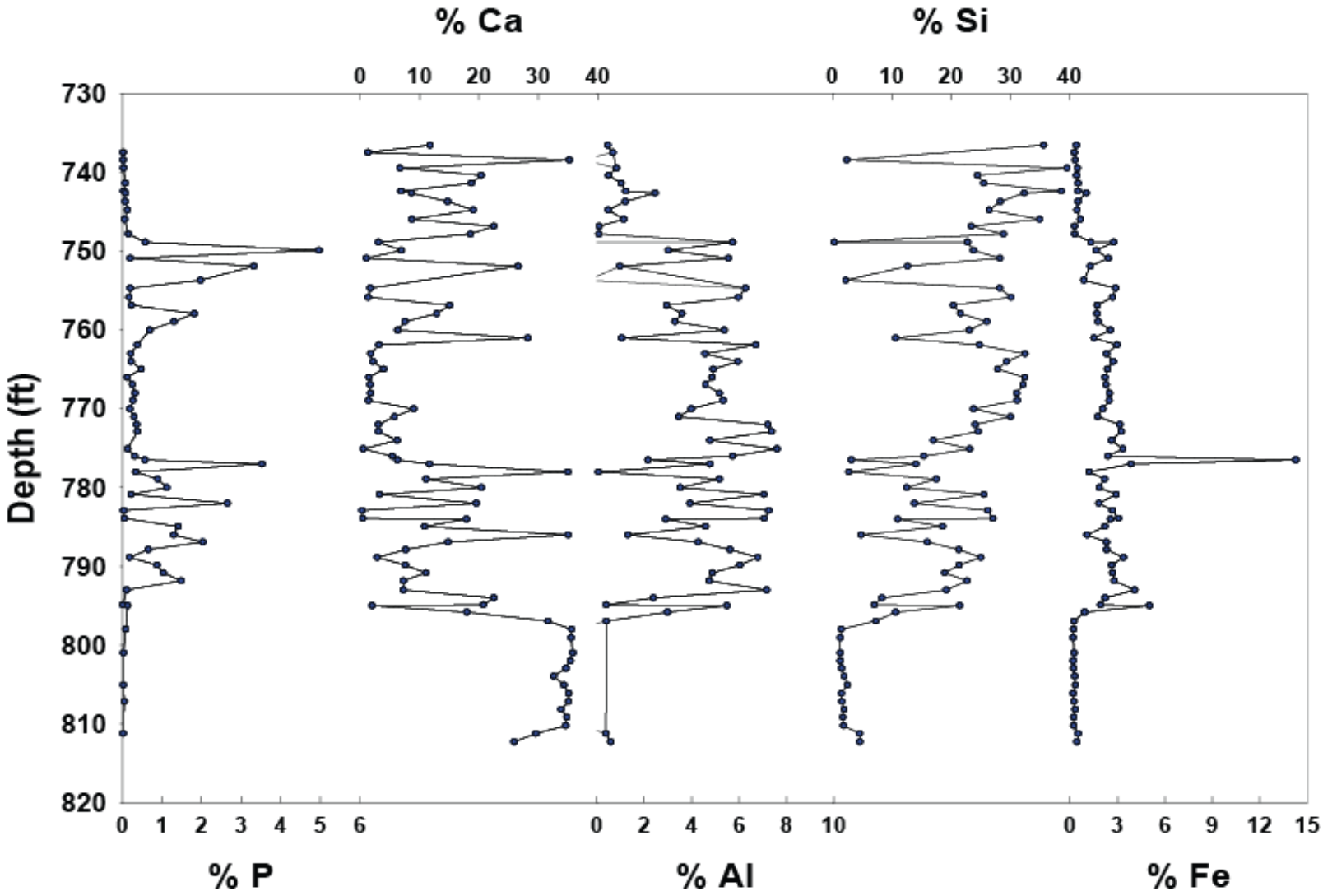

Figure 21. Major elements for Harlow C-3-3.

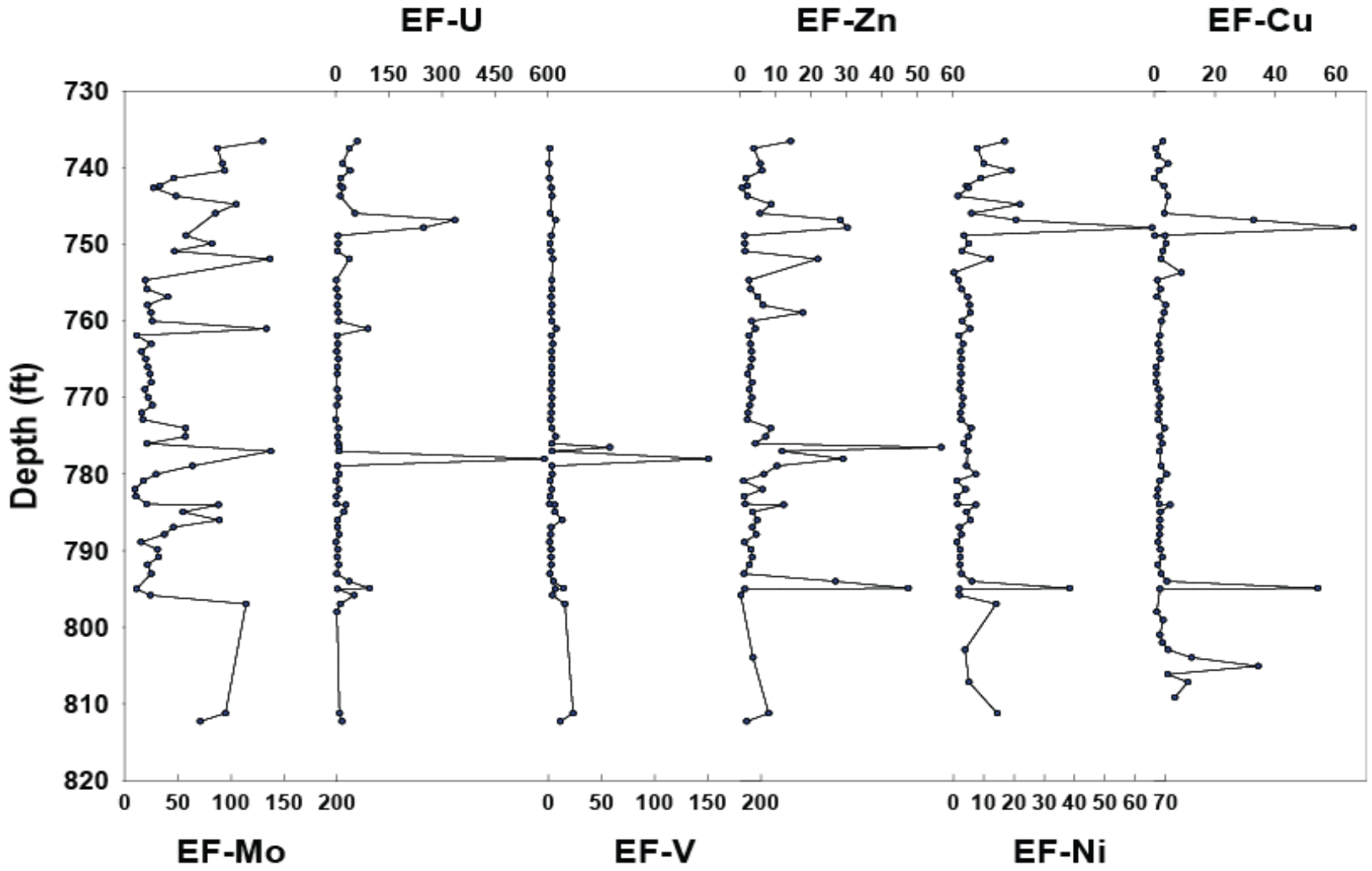

Figure 22. Trace elements for Harlow C-3-3.

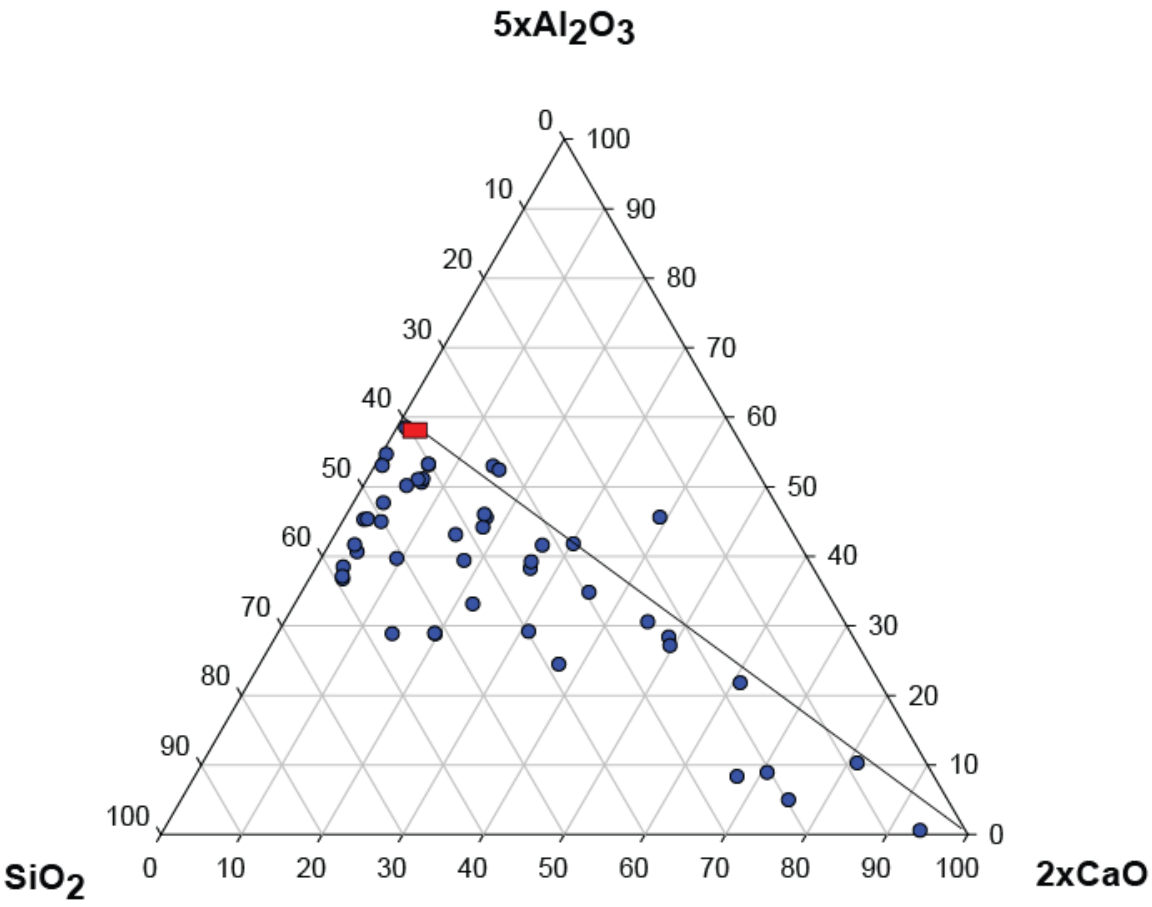

Figure 23. Calcite-clay-quartz ternary for Harlow C-3-3.

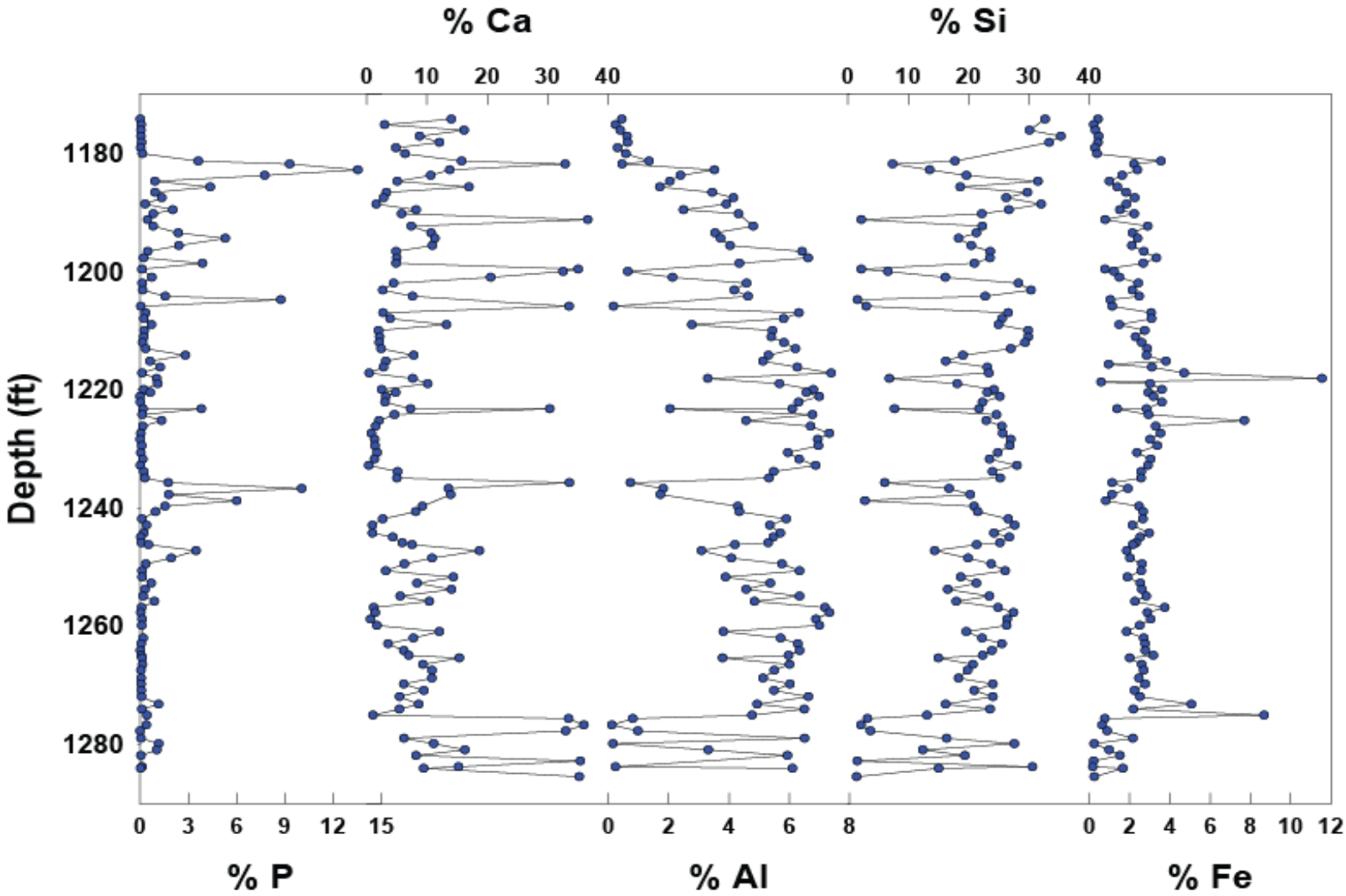

Figure 24. Major elements for Beck C-4-1.

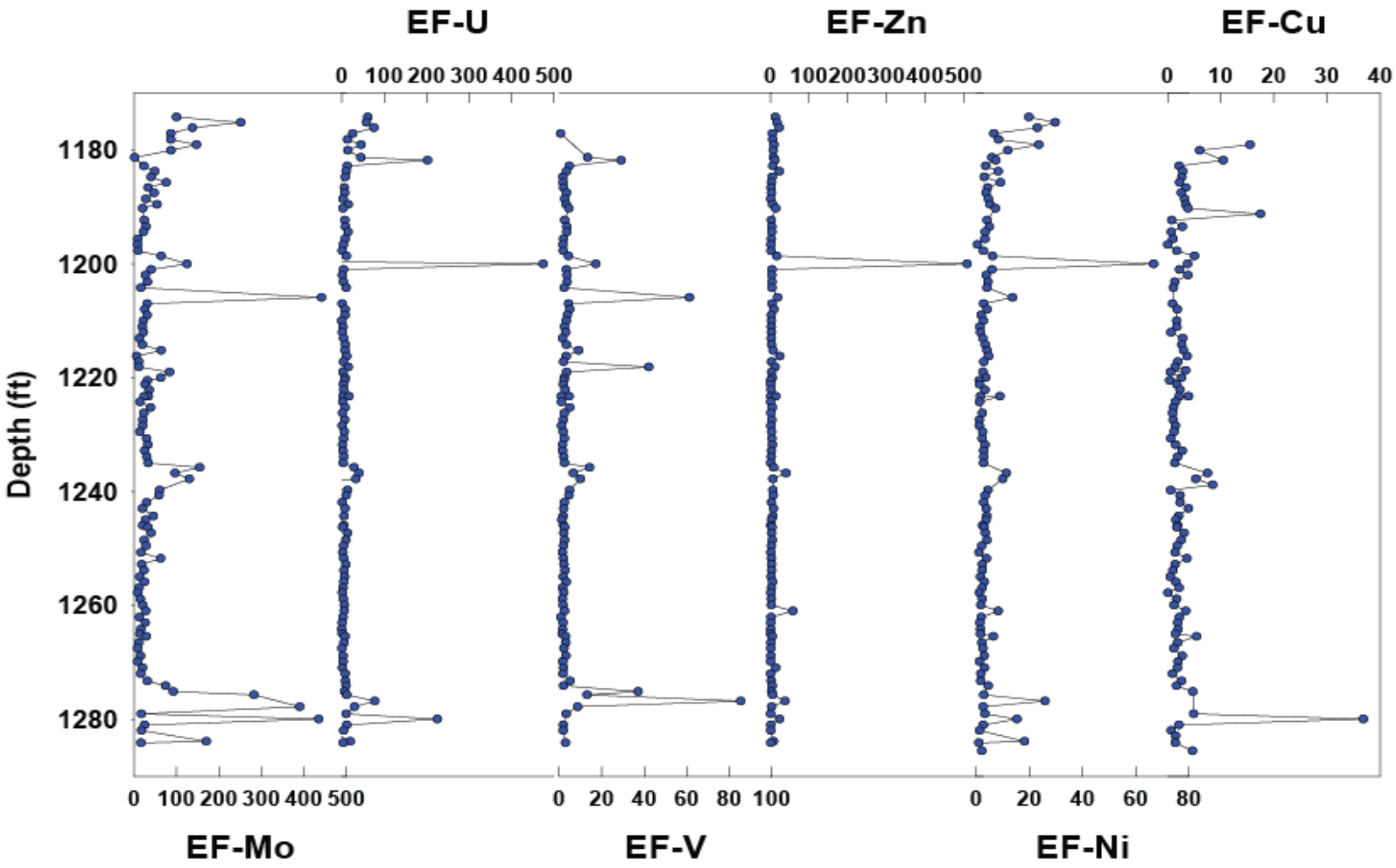

Figure 25. Trace elements for Beck C-4-1.

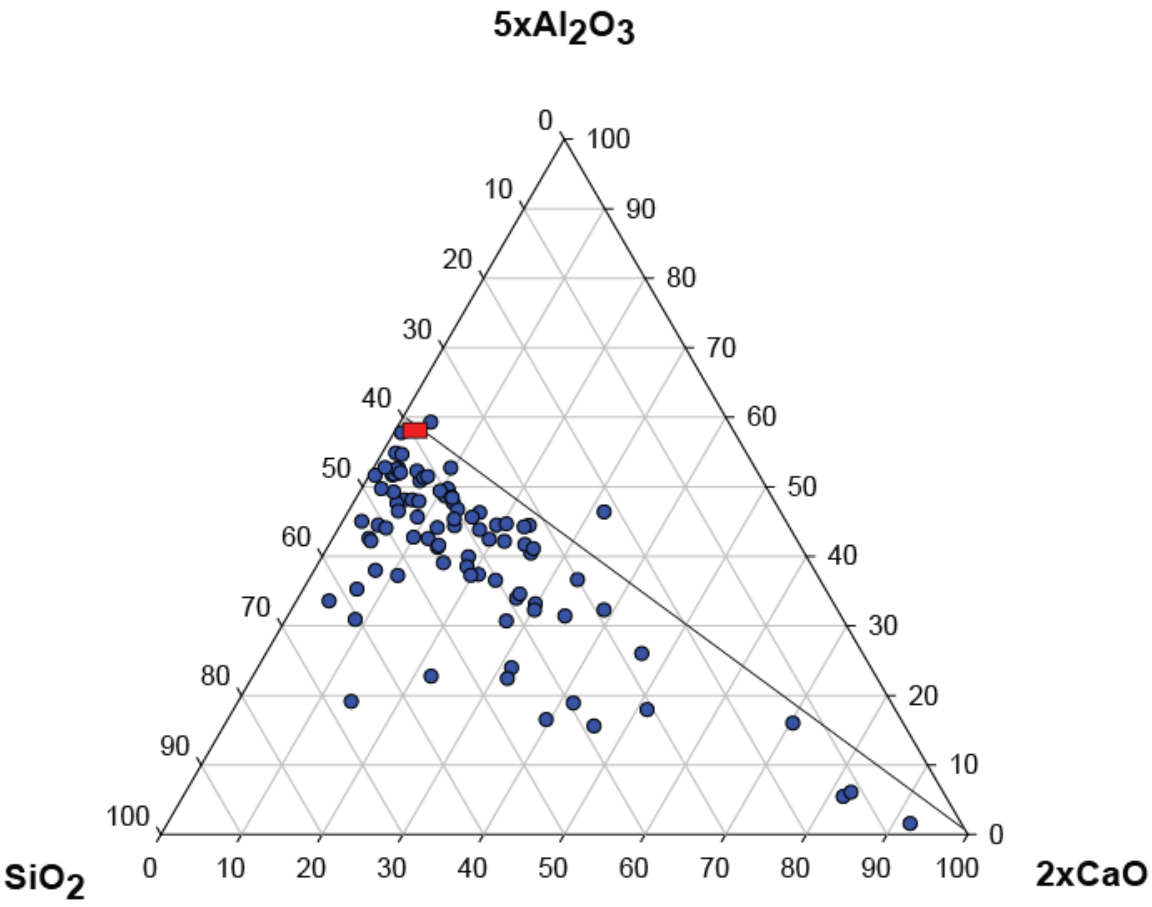

Figure 26. Calcite-clay-quartz ternary for Beck C-4-1.

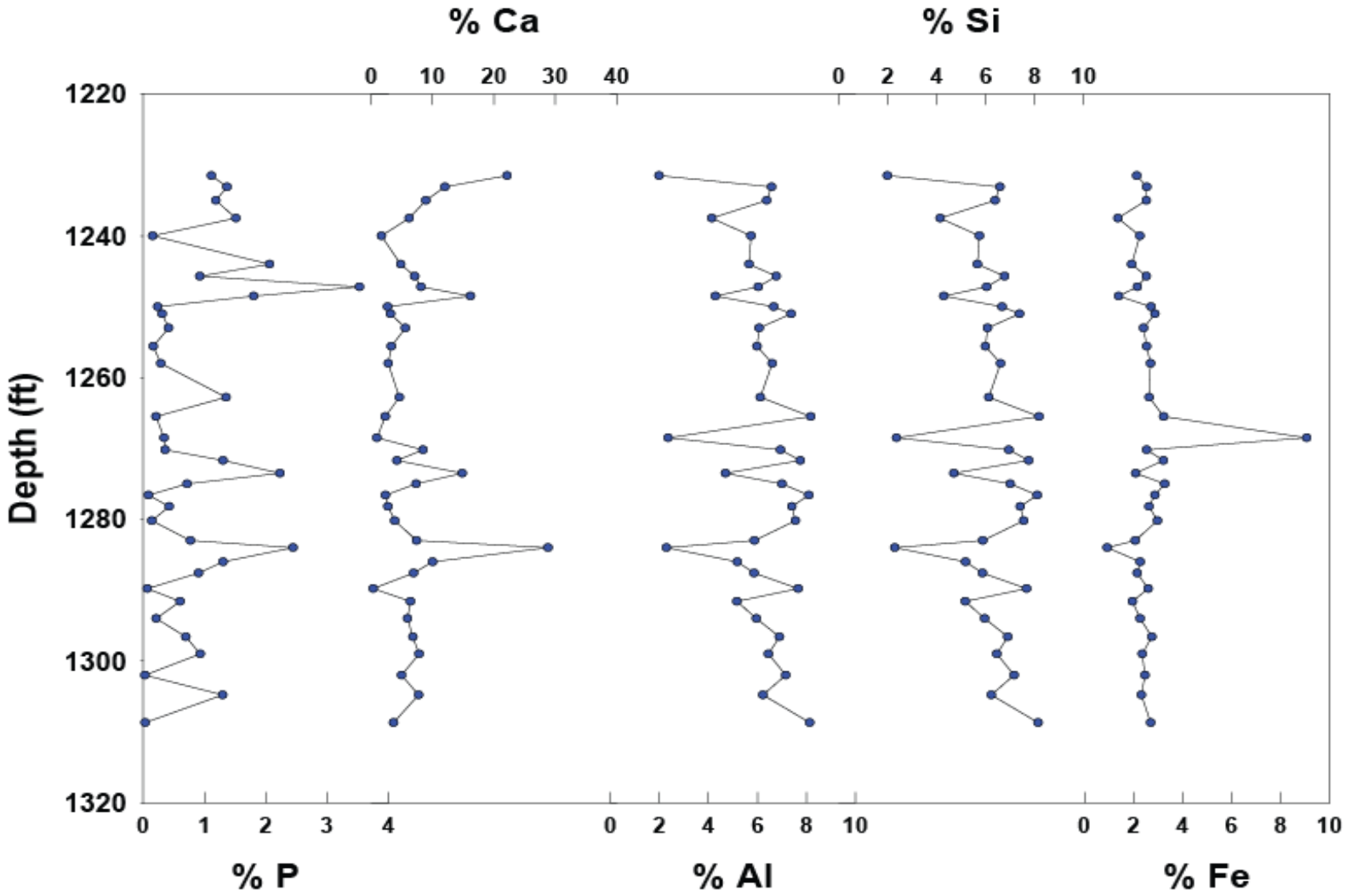

Figure 27. Major elements for Lee C-5-1.

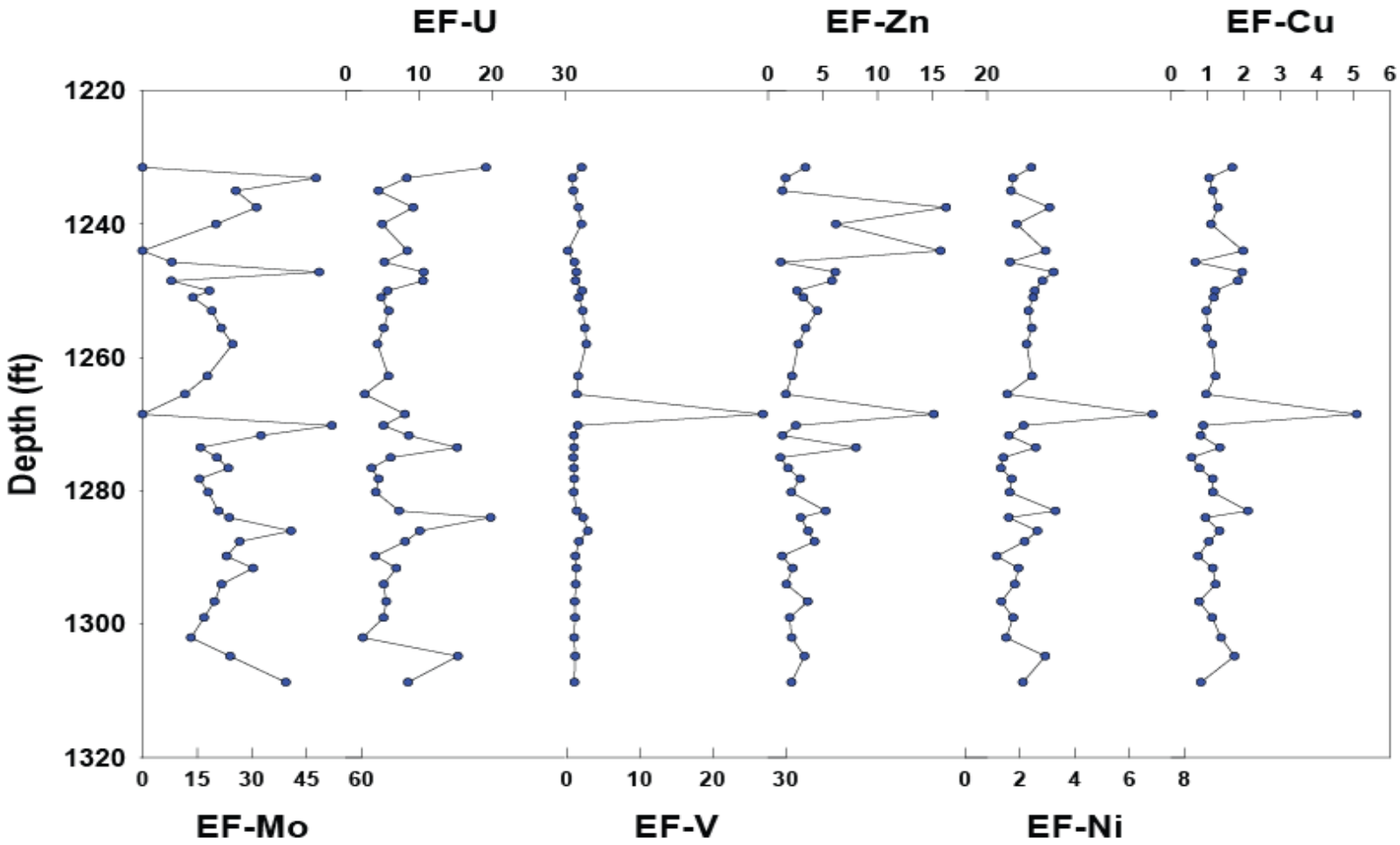

Figure 28. Trace elements for Lee C-5-1.

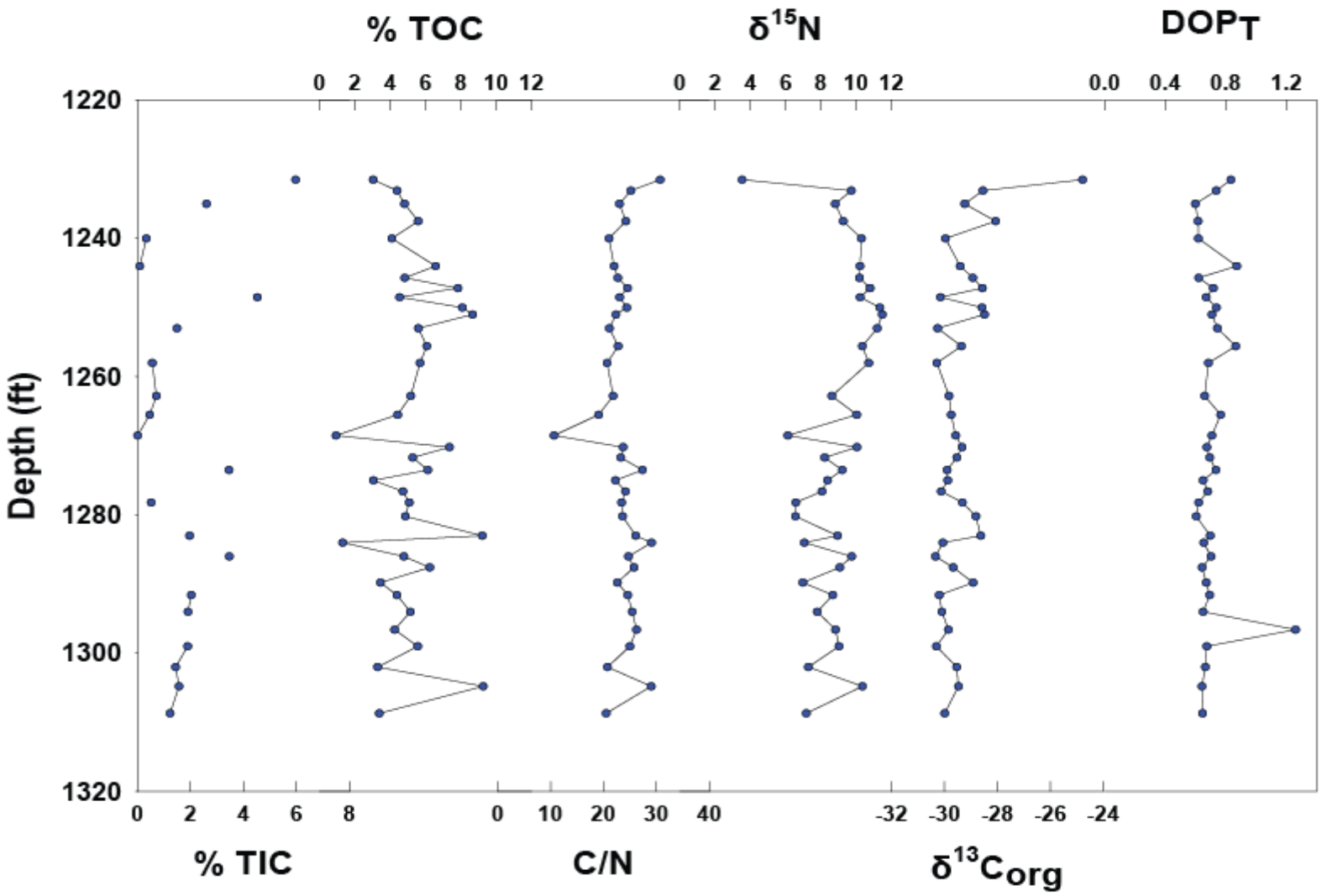

Figure 29. Non-XRF data for Lee C-5-1.

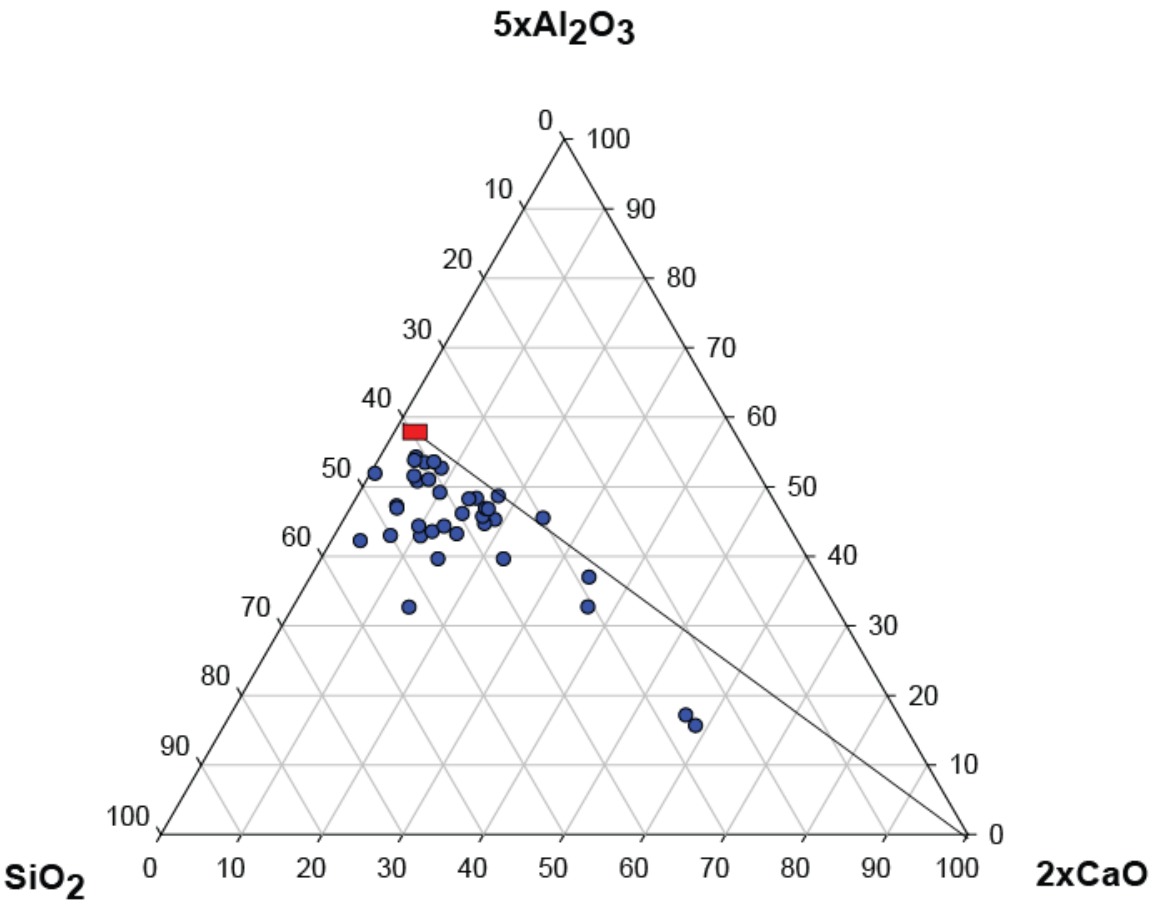

Figure 30. Calcite-clay-quartz ternary for Lee C-5-1.

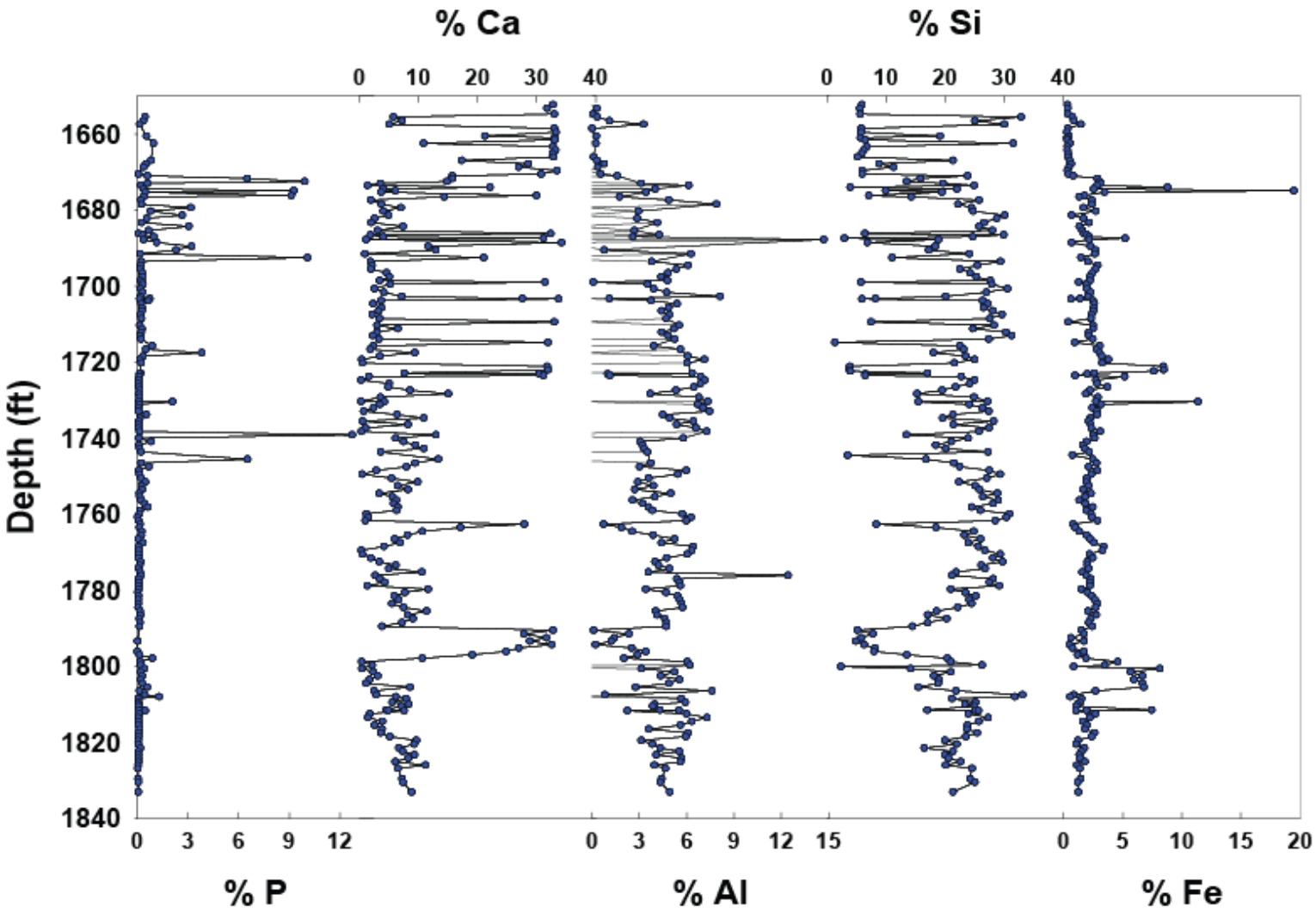

Figure 31. Major elements for Petty D-6-1.

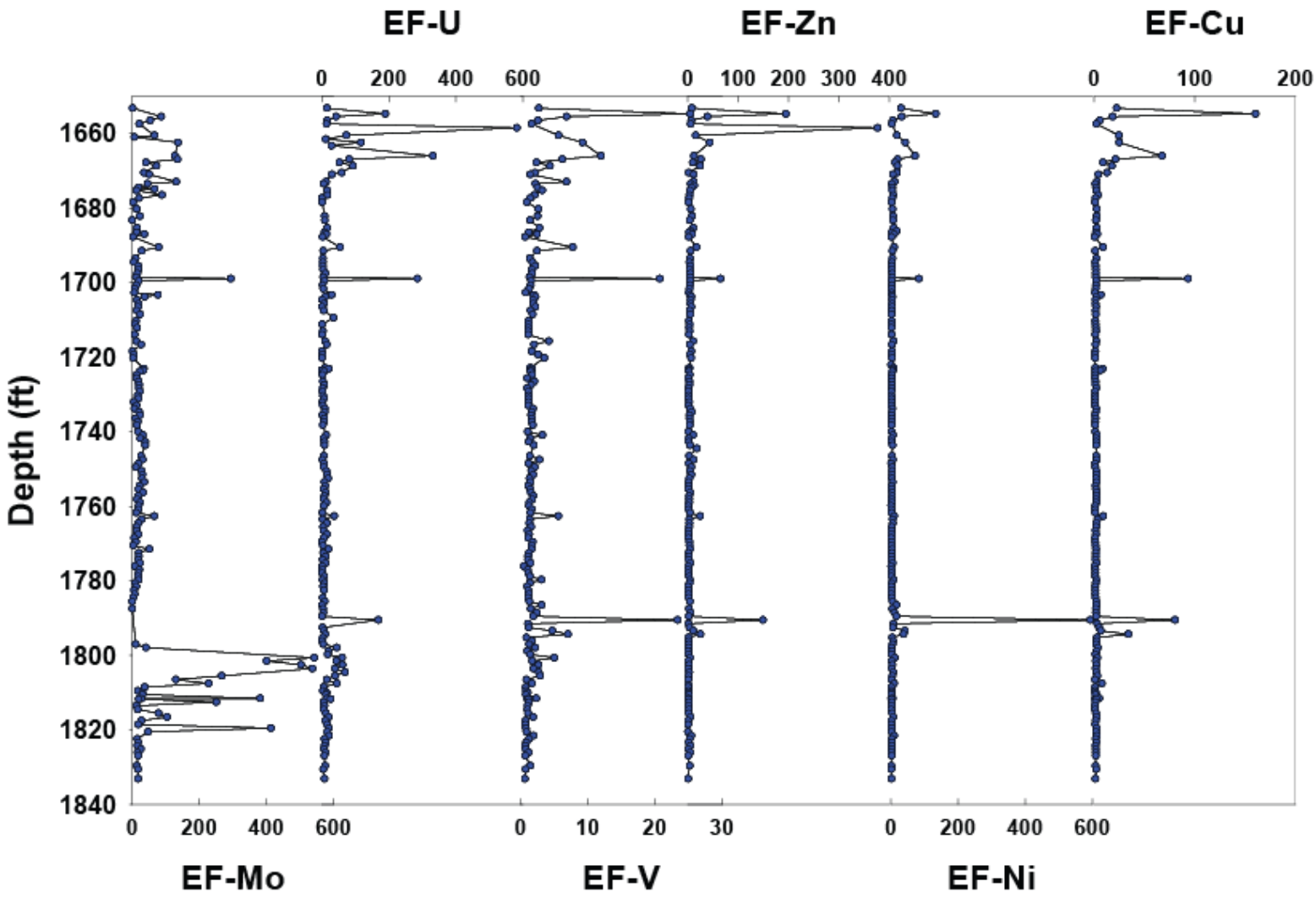

Figure 32. Trace elements for Petty D-6-1.

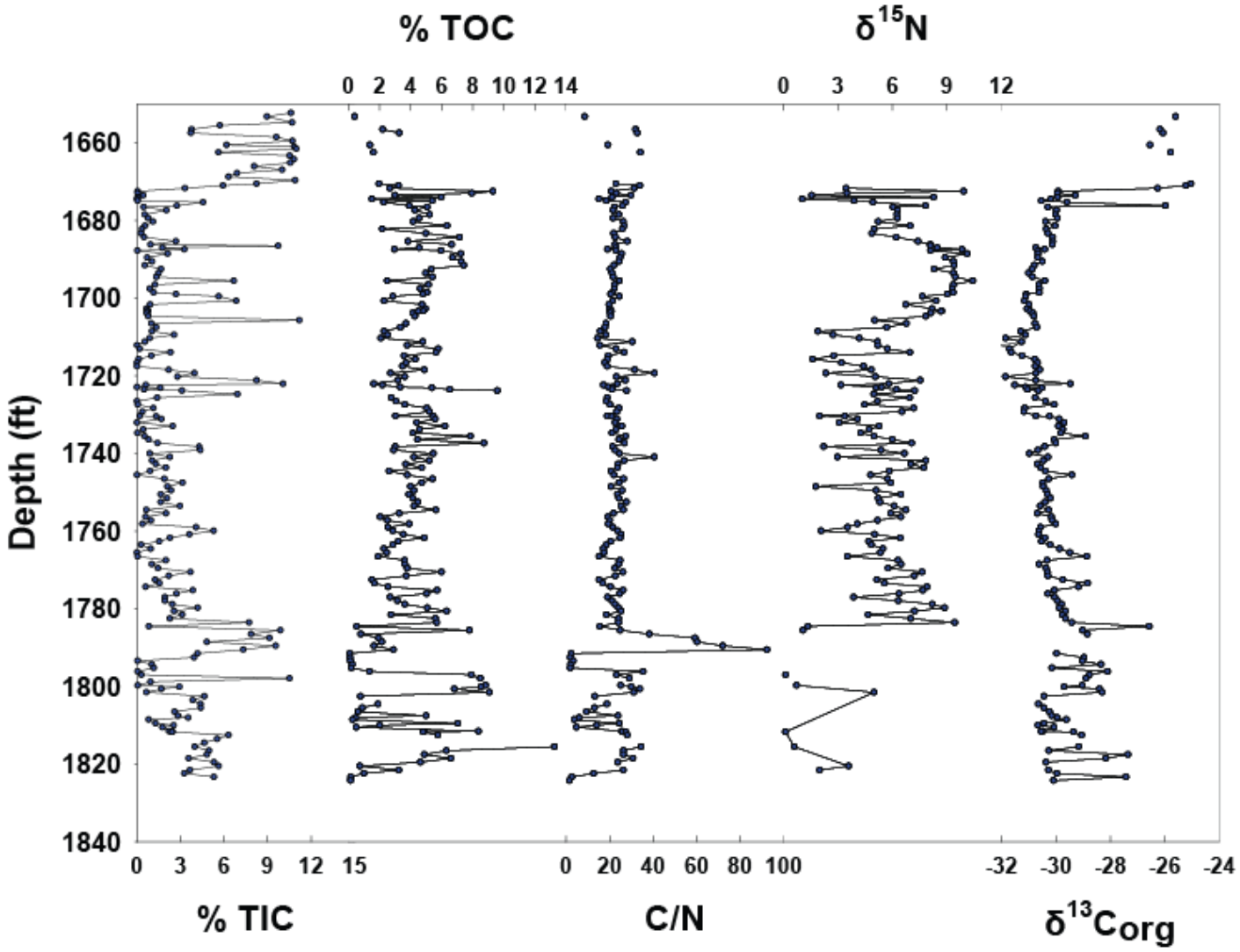

Figure 33. Non-XRF data for Petty D-6-1.

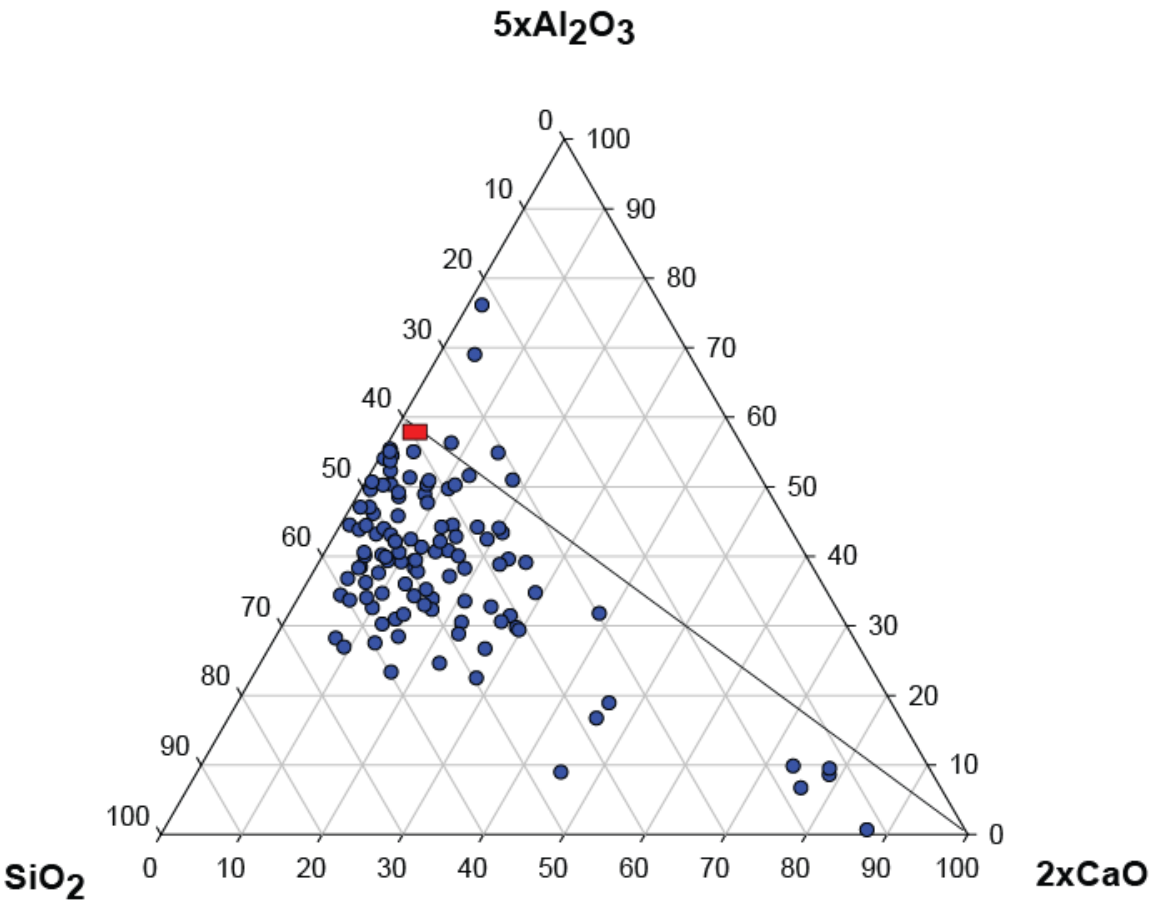

Figure 34. Calcite-clay-quartz ternary for Petty D-6-1.

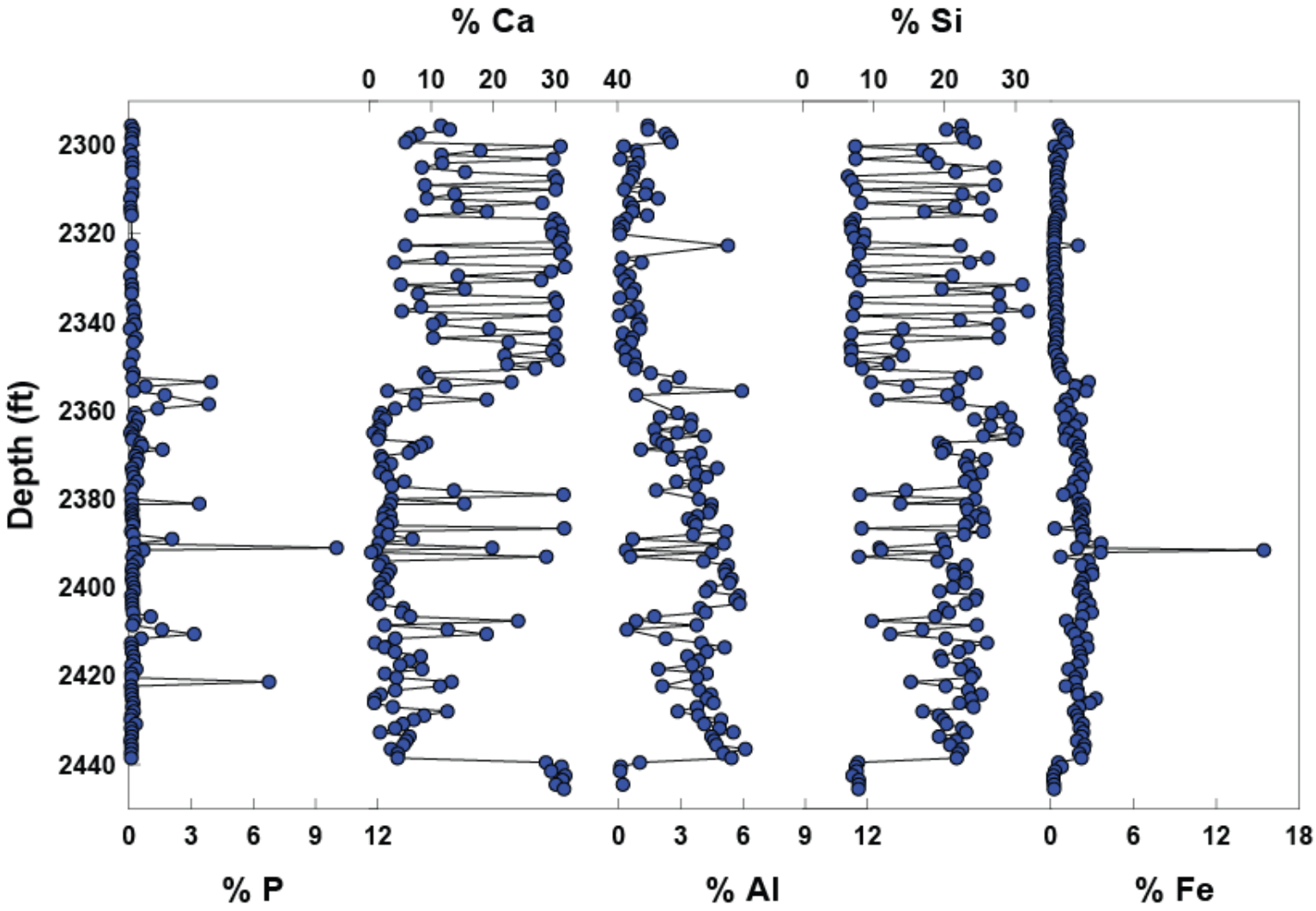

Figure 35. Major elements for Godfrey E-8-1.

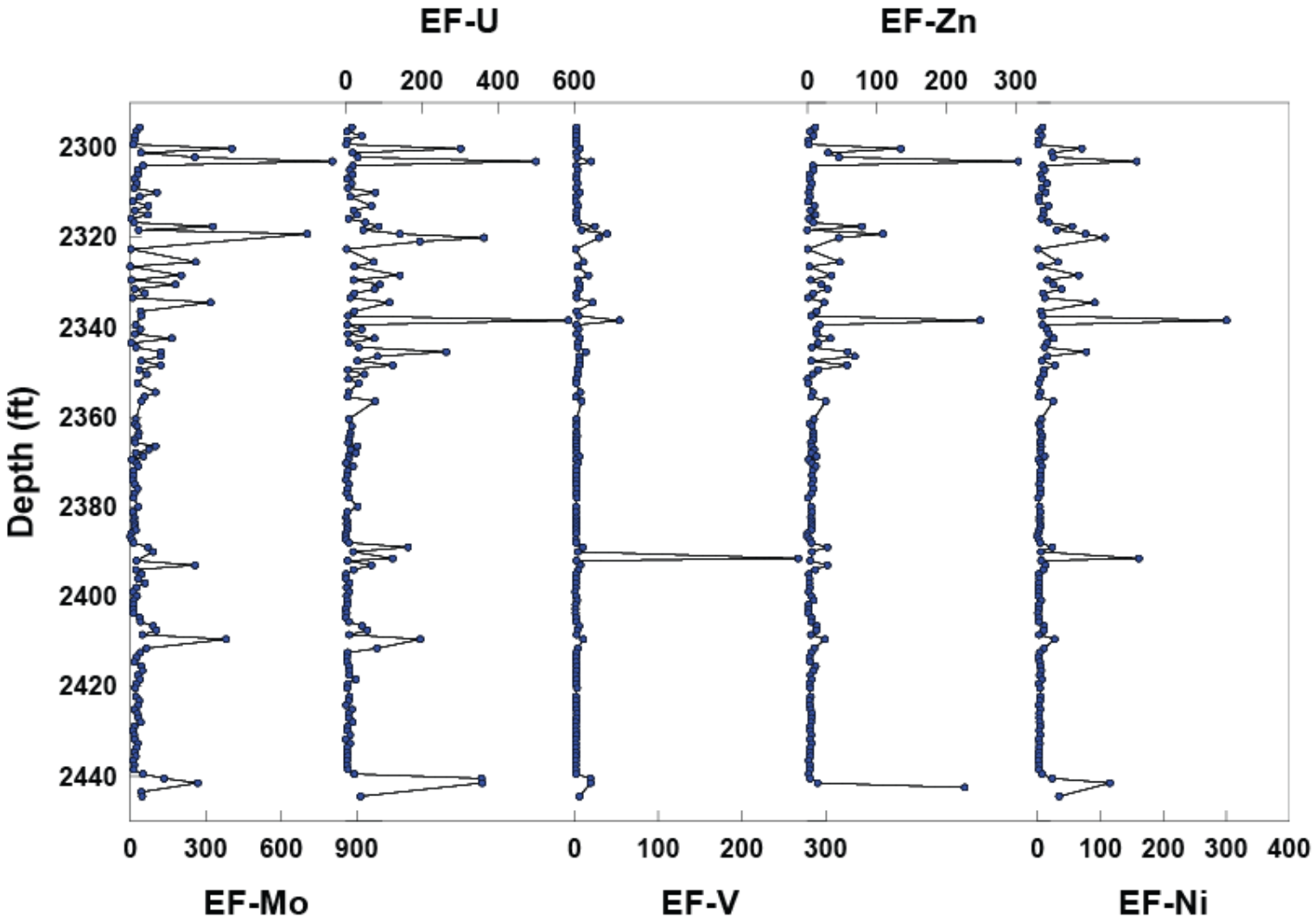

Figure 36. Trace elements for Godfrey E-8-1.

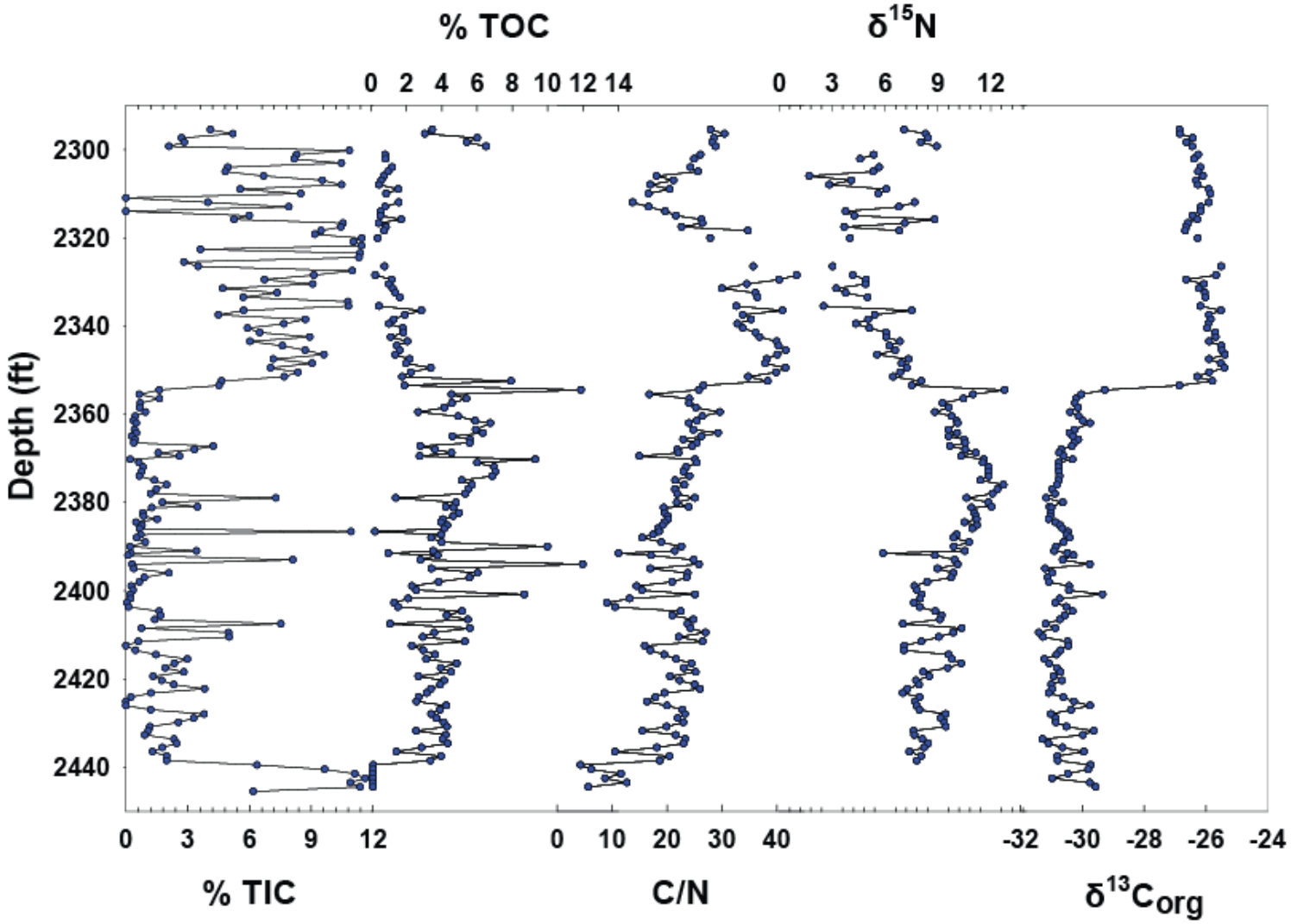

Figure 37. Non-XRF data for Godfrey E-8-1.

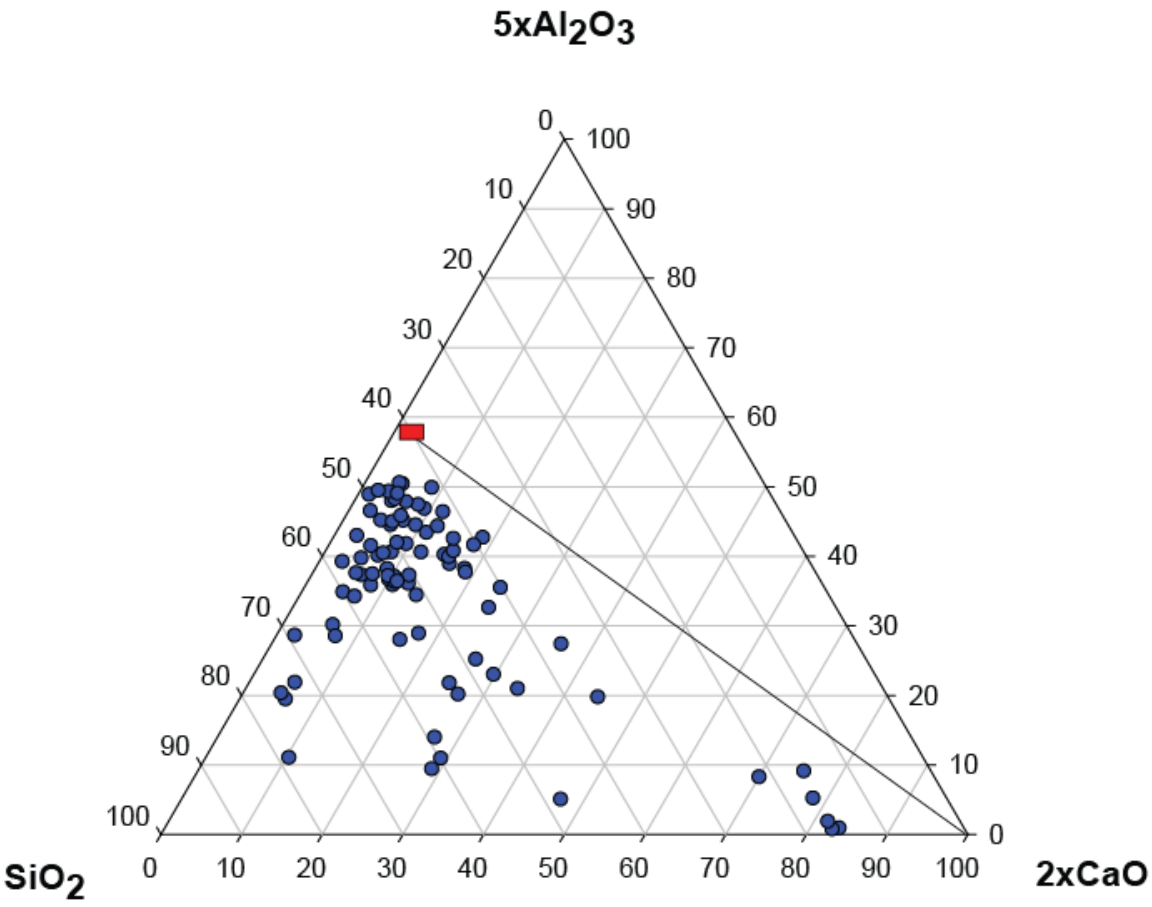

Figure 38. Calcite-clay-quartz ternary for Godfrey E-8-1.

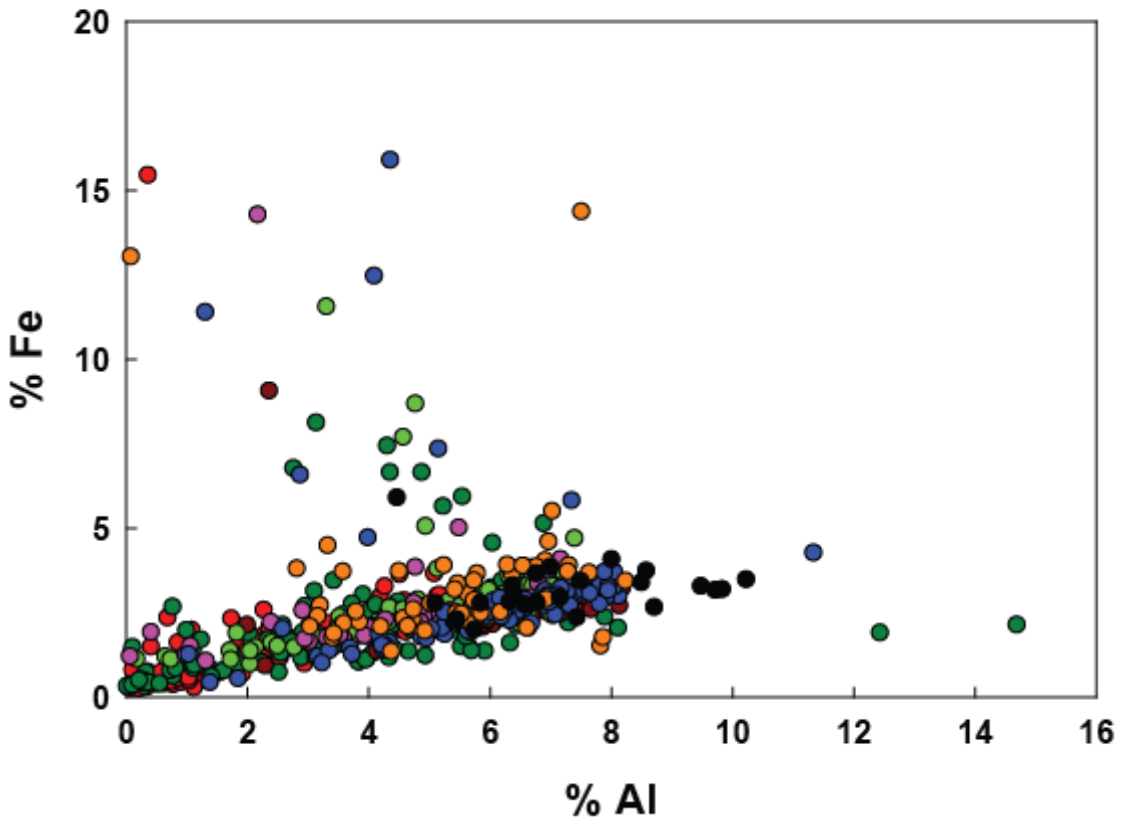

Figure 39. Cross-plot of Al versus Fe.

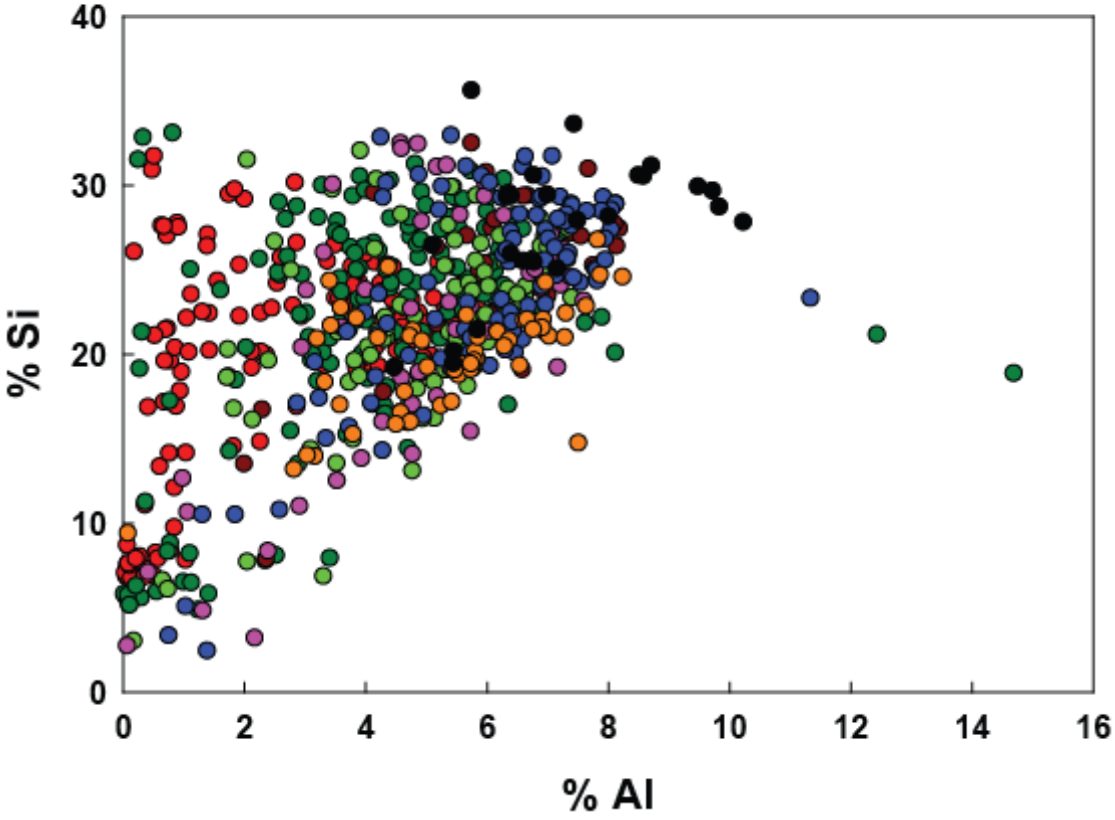

Figure 40. Cross-plot of Al versus Si.

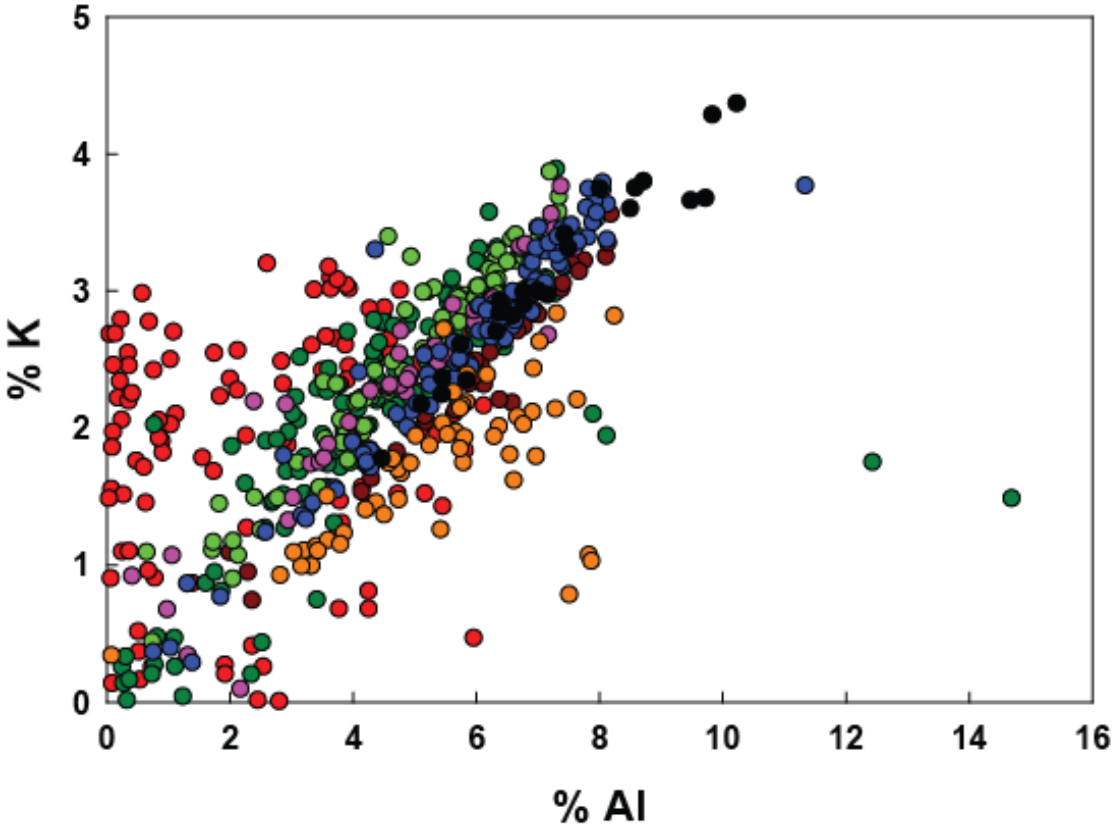

Figure 41. Cross-plot of Al versus K.

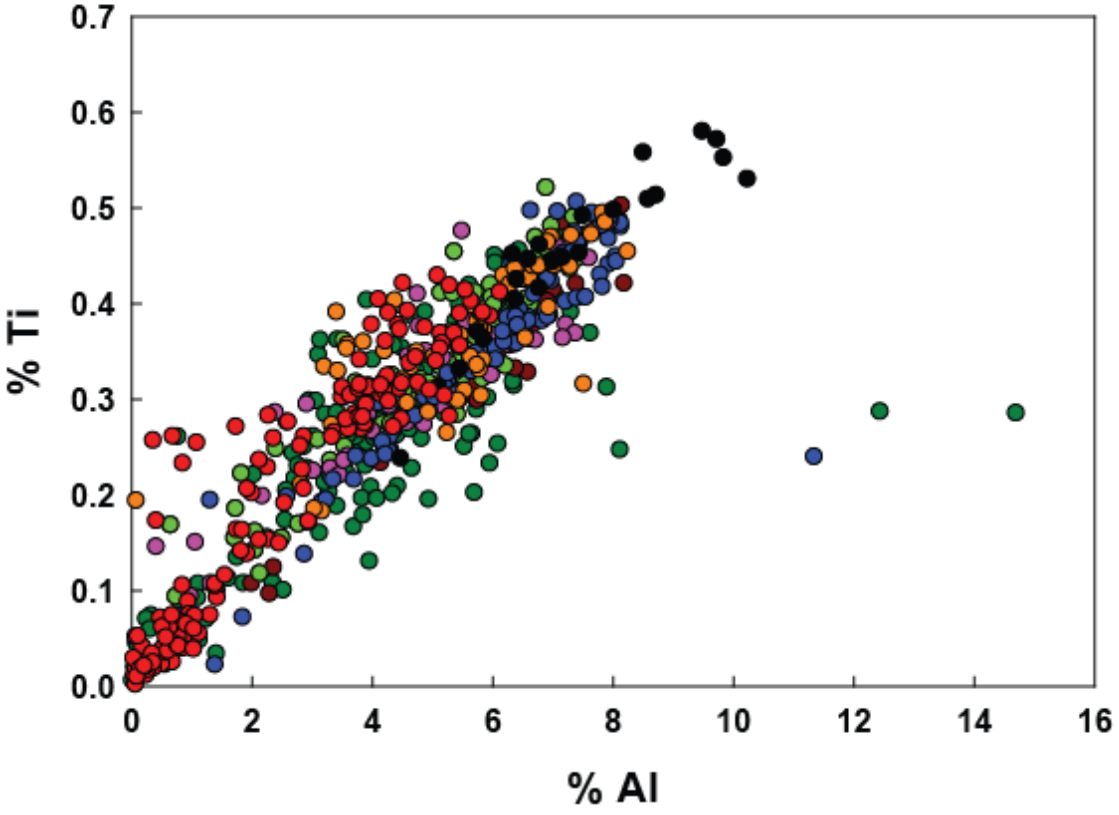

Figure 42. Cross-plot of Al versus Ti.

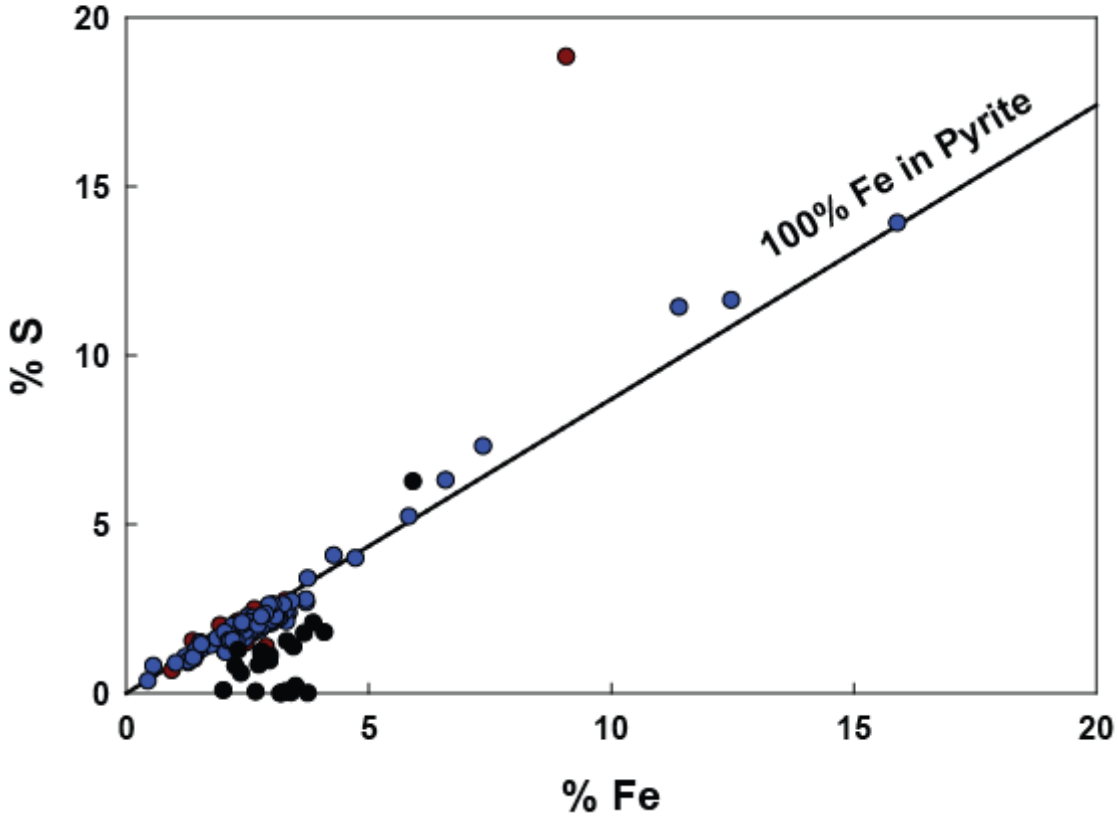

Figure 43. Cross-plot of Fe versus S (Dean and Arthur,1989).

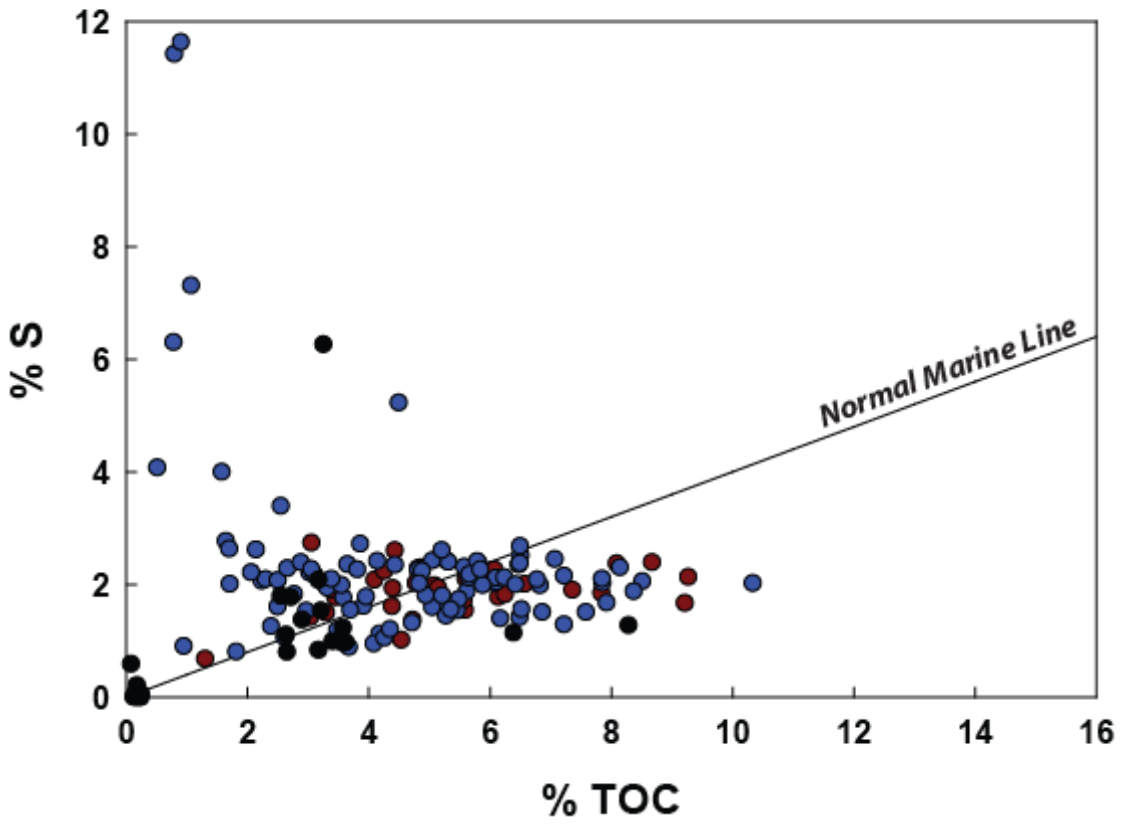

Figure 44. Cross-plot of total organic carbon (TOC) versus S (Berner and Raiswell,1983).

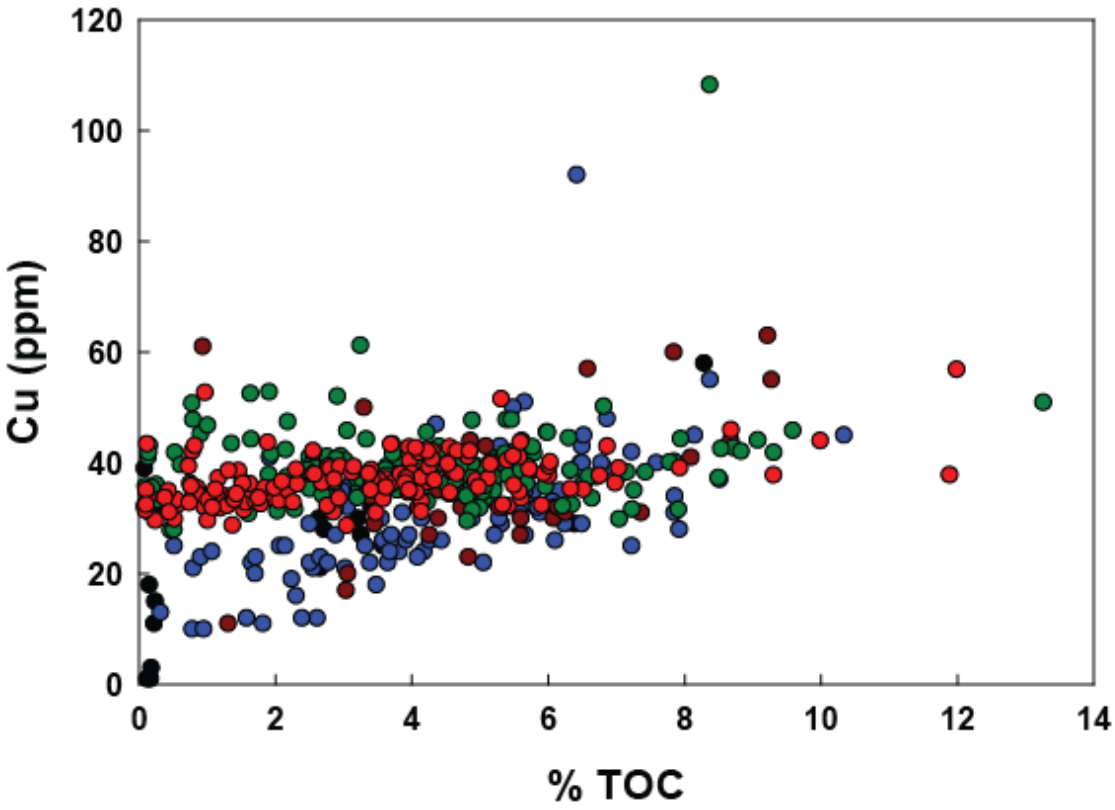

Figure 45. Cross-plot of total organic carbon (TOC) versus Cu.

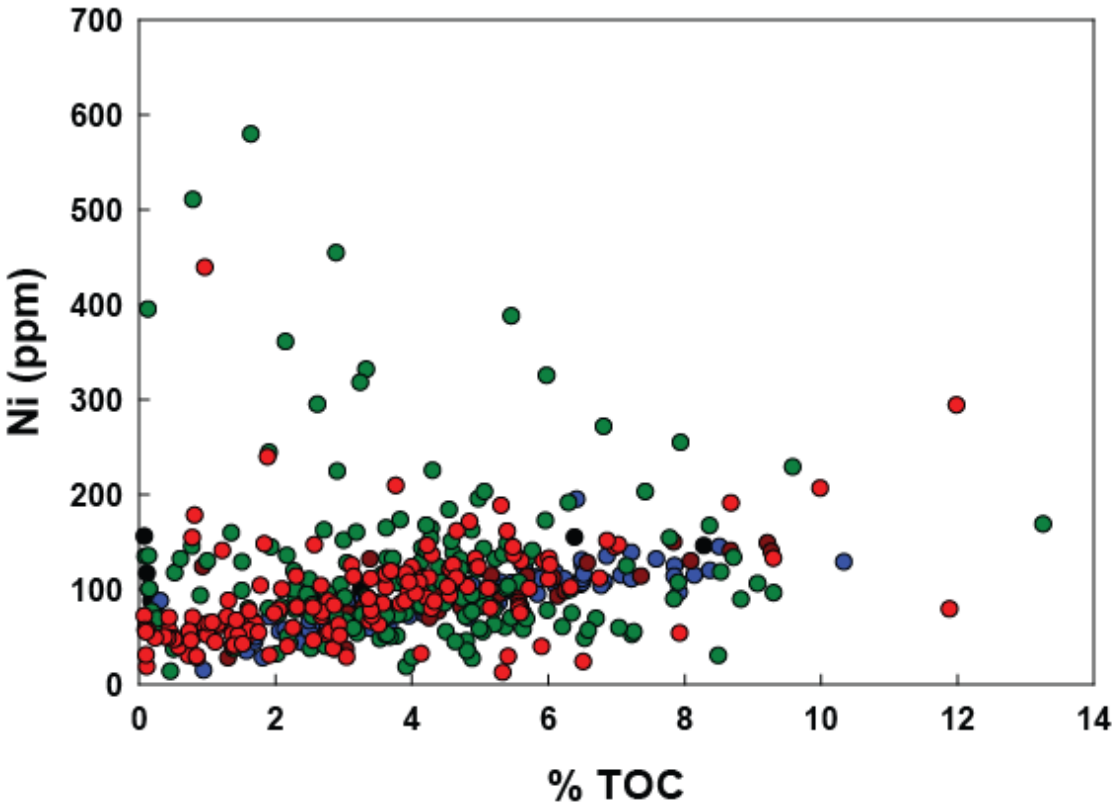

Figure 46. Cross-plot of total organic carbon (TOC) versus Ni.

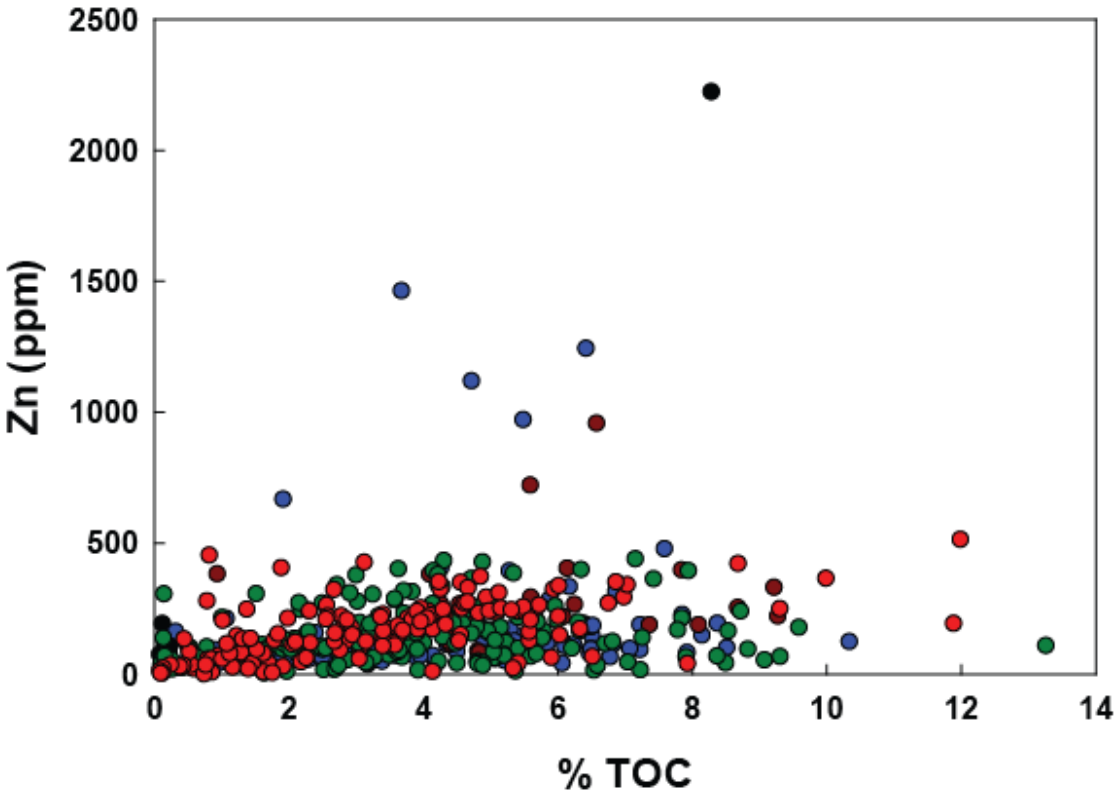

Figure 47. Cross-plot of total organic carbon (TOC) versus Zn.

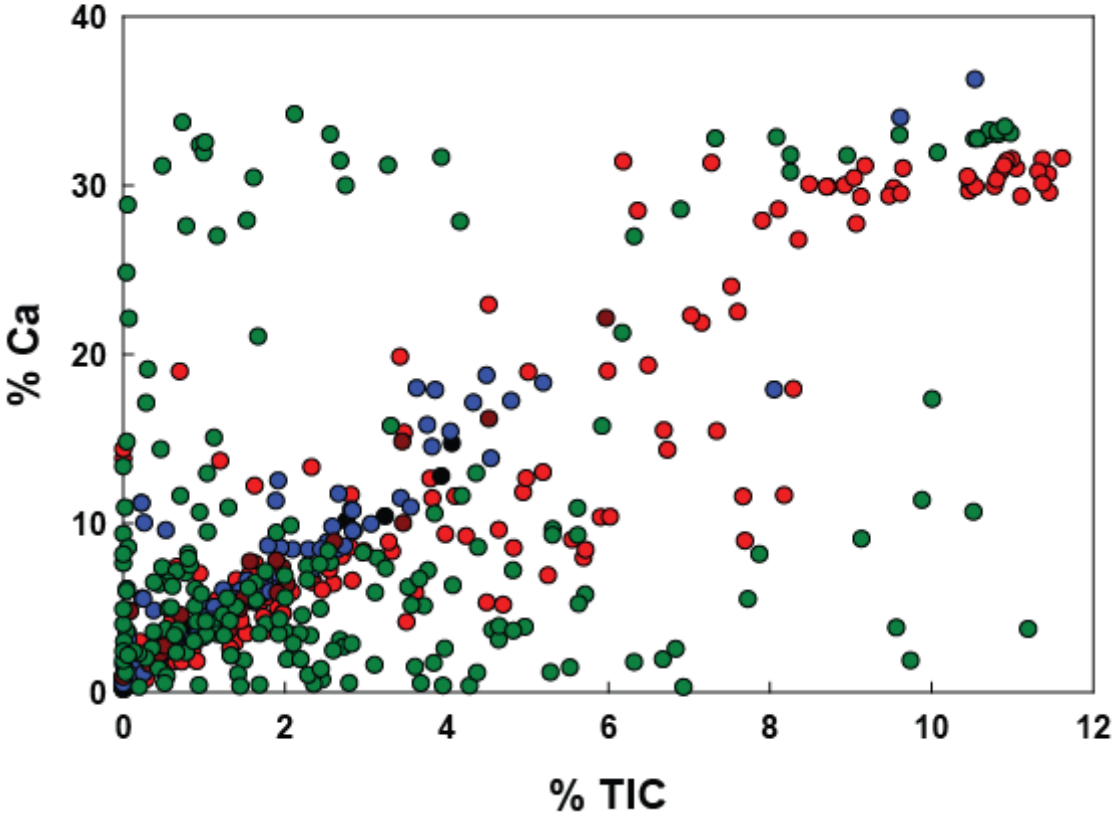

Figure 48. Cross-plot of total inorganic carbon (TIC) versus Ca.

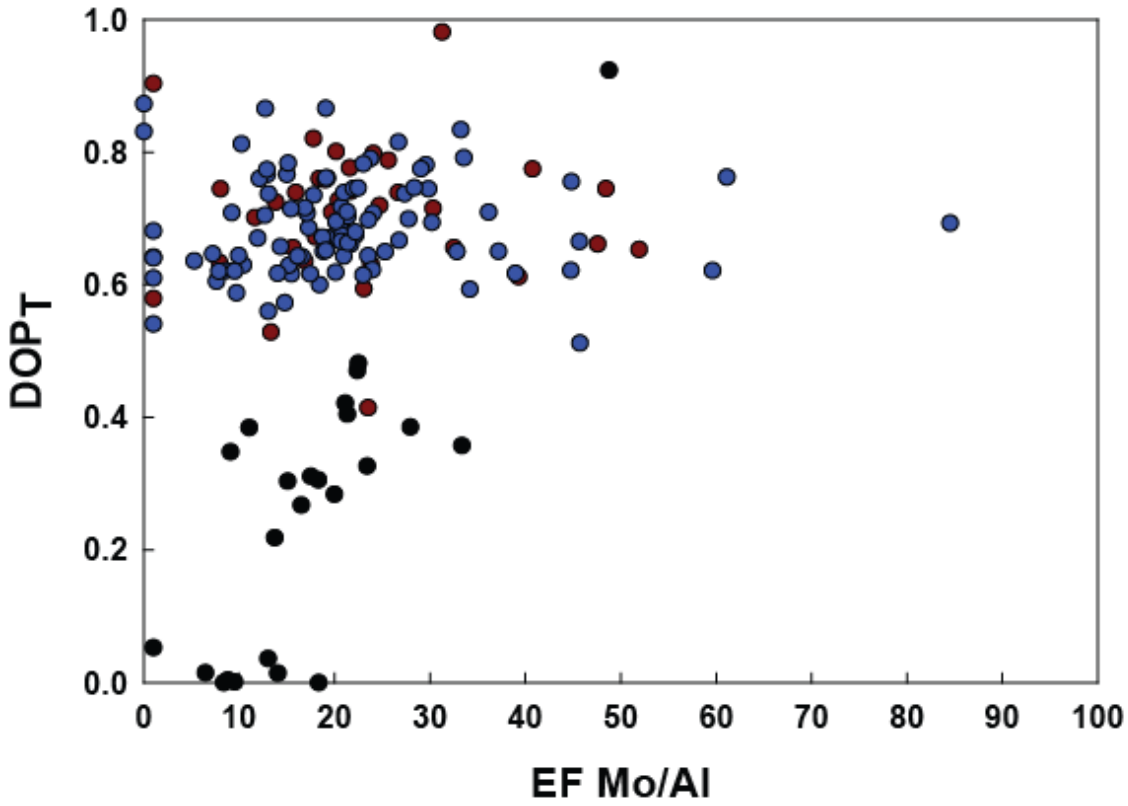

Figure 49. Cross-plot of enrichment factor for Mo versus DOP_T.

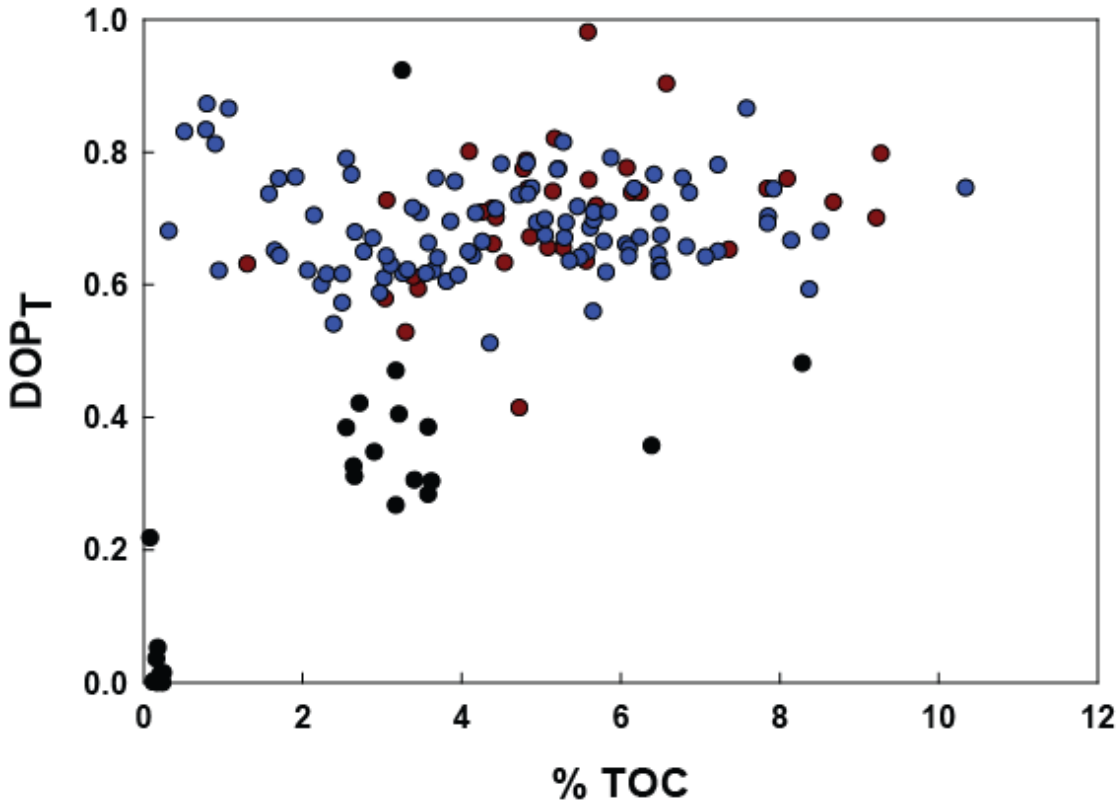

Figure 50. Cross-plot of total organic carbon (TOC) versus DOP_T.

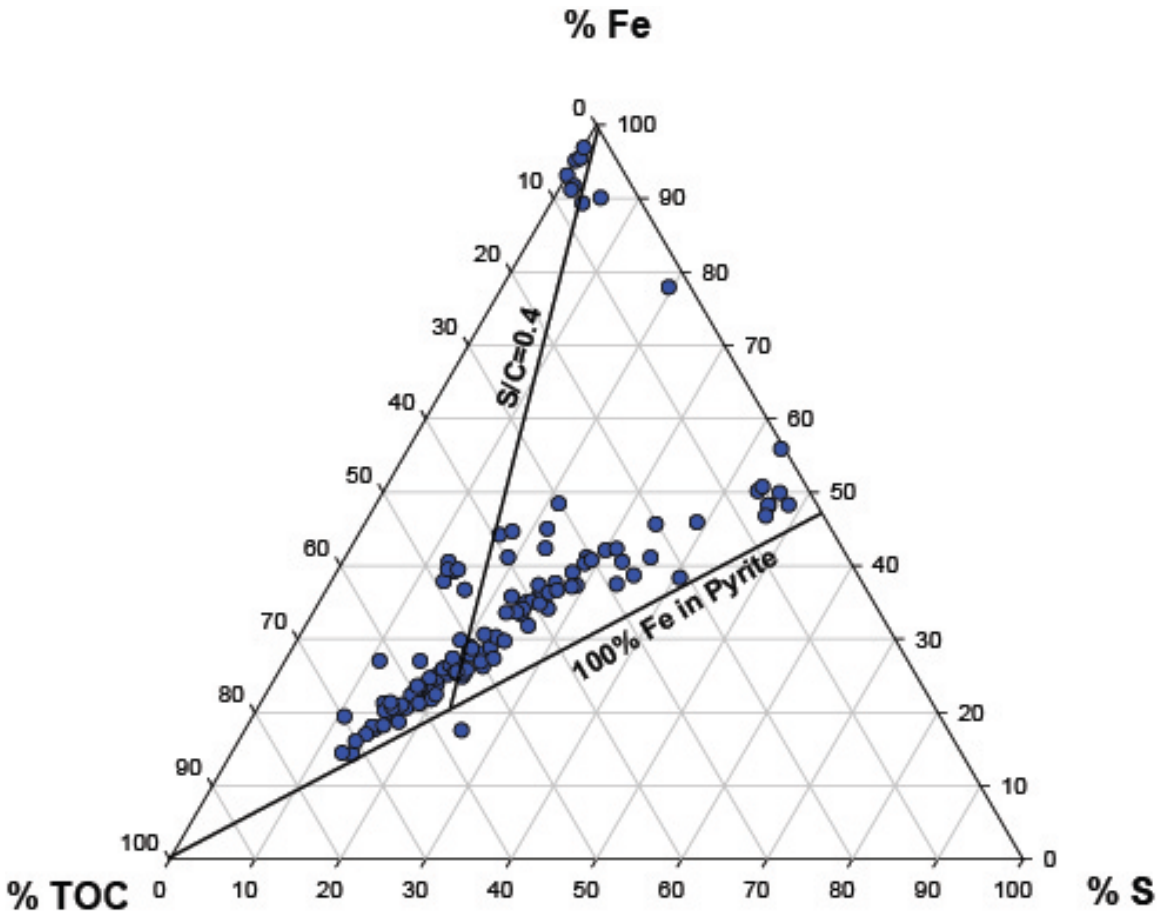

Figure 51. Ternary diagram of S-Fe-TOC (Dean and Arthur,1989).

REFERENCES

Algeo, T.J. and Maynard, J.B., 2004. Trace-metal behavior and redox facies in core shales of Upper Pennsylvanian Kansas-type cyclothems. Chemical Geology. 206: 289-318.

Algeo, T.J. and Lyons, T.W., 2006. Mo-total organic carbon covariation in modern anoxic marine environments: implications for analysis of paleoredox and paleohydrographic conditions. Paleoceanography, v. 21, PA1016.

Algeo, T.J., Lyons, T.W., Blakey, R.C., and Over, D.J. 2007. Hydrographic conditions of the Devono–Carboniferous North American Seaway inferred from sedimentary Mo–TOC relationships. Palaeogeography, Palaeoclimatology, Palaeoecology. 256: 204–230.

Algeo, T.J., Maynard, J.B., 2008. Trace-metal covariation as a guide to water-mass conditions in ancient anoxic marine environments. Geosphere. Oct 2008, v. 4, no. 5; 872-887.

Algeo, T.J. Rowe, H., Hower, J.C., Schwark, L., Herrmann, A., and Heckel, P. 2008. Changes in ocean denitrification during Late Carboniferous glacial-interglacial cycles. Nature Geoscience. v.1, October 2008; 709-714.

Algeo, T.J. and Tribovillard, N. 2009. Environmental analysis of paleoceanographic systems based on molybdenum–uranium covariation. Chemical Geology. 268: 211–225.

Algeo, T.J. and Rowe, H.D. 2011. In press. Paleoceanographic applications of trace-metal concentration data. Chemical Geology.

Aplin, A.C., Fleet, A.J., and Macquaker, J.H.S. 1999. Muds and mudstones: physical and fluid-flow properties. Geological Society, London, Special Publications, v. 158, p. 1-8.

Arthur, M.A., Sageman, B.B., 1994. Marine black shales: depositional mechanisms and environments of ancient deposits. Annual Reviews in Earth and Planetary Science. 22: 499–551.

Belforte, A. S. 1971. Pre-Canyon structural geology of the southern end of Fort Worth Basin, Central Texas. M.A. thesis: The University of Texas at Austin. 74p.

Berner, R.A. 1970. Sedimentary pyrite formation. American Journal of Science. 268: 1–23.

Berner, R.A. and Raiswell, R., 1983. Burial of organic carbon and pyrite sulfur in sediments over Phanerozoic time: a new theory. Geochimica et Cosmochimica Acta. 47: 855–862.

Blake Jr, B.M. and Beuthin, J.D. 2008. Deciphering the mid-Carboniferous eustatic event in the central Appalachian foreland basin, southern West Virginia, USA. Geological Society of America Special Paper 441. Pp. 249-260.

Blakey, R. 2005. Paleogeography and geologic evolution of North America; images that track the ancient landscapes of North America. Online. http://jan.ucc.nau.edu/~rcb7/nam.html (accessed March 26, 2010).

Blatt, H. 1980. Origin of Sedimentary Rocks. Englewood Cliffs, Prentice-Hall. 782 p.

Boardman, D.R., Puckette, J., Coffey, B., Gerding, E., Kamman, P., Aryal, N., Singh, M., and Rihn, A. 2007A. Cyclic stratigraphy and conodont biostratigraphy of the Barnett Shale from the type locality of the Chappel Limestone and near-surface cores from the Llano Uplift. Abstracts: Annual Meeting - American Association of Petroleum Geologists. 2007, 14.

Boardman, D.R., Puckette, J.O., and Cemen, I. 2007B. Middle and late Paleozoic organic-rich shales from the North American Midcontinent. Abstracts with Programs - Geological Society of America (October 2007), 39(6):356-357.

Brumsack, H.J. 2006. The trace metal content of recent organic carbon-rich sediments: Implications for Cretaceous black shale formation. Palaeogeography, Palaeoclimatology, Palaeoecology. 232: 344-361.

Calvert, S.E. and Pedersen, T.F. 1993. Geochemistry of recent oxic and anoxic marine sediments: implications for the geological record. Marine Geology. 113: 67–88.

Catuneanu, O. et al. 2009. Towards the standardization of sequence stratigraphy. Earth-Science Reviews. 92: 1-33.

Crusius, J., Calvert, S., Pedersen, T., Sage, D., 1996. Rhenium and molybdenum enrichments in sediments as indicators of oxic, suboxic and sulfidic conditions of deposition. Earth and Planetary Science Letters. 145: 65–78.

Dean,W.E. and Arthur, M.A. 1989. Iron–sulfur–carbon relationships in organic-carbon-rich sequences I: Cretaceous western interior seaway. American Journal of Science. 289: 708–743.

Demaison, G.J. and Moore, G.T. 1980. Anoxic environments and oil source bed genesis. American Association of Petroleum Geologists Bulletin. 64: 1179–1209.

Engleman, E.E., Jackson, L.L., Norton, D.R. and Fischer, A. G. 1985. Determination of carbonate carbon in geological materials by coulometric titration. Chemical Geology. 53: 125-128.

Erickson, B.E. and Helz, G.R. 2000. Molybdenum(VI) speciation in sulfidic waters: stability and lability of thiomolybdates. Geochimica et Cosmochimica Acta. 64: 1149–1158.

Erlich, R.N. and Coleman Jr., J.L. 2005. Drowning of the Upper Marble Falls carbonate platform (Pennsylvanian), central Texas: A case of conflicting “signals?” Sedimentary Geology. 175: 479-499.

Fielding, C.R., Frank, T.D., and Isbell, J.L. 2008. The late Paleozoic ice age – a review of current understanding and synthesis of global climate patterns. Geological Society of America Special Paper 441. pp. 343-353.

Folk, R. L. 1980. Petrology of sedimentary rocks: Austin, Texas, Hemphill Publishing Co., 182 p.

Frank, T.D., Birgenheier, L.P., Montanez, I.P., Fielding, C.R., and Rygel, M.C. 2008. Late Paleozoic climate dynamics revealed by comparison of ice-proximal stratigraphic and ice-distal isotopic records. Geological Society of America Special Paper 441. pp. 331-342.

Gustafson, L.B. and Williams, N. 1981. Sediment-hosted deposits of copper, lead, and zinc. In: Skinner, B.J. (editor). Seventy-Fifth Anniversary Volume, The Economic Geology Publishing Co., Yale, 139-178.

Gutschick, R. and C. Sandberg. 1983. Mississippian continental margins on the conterminous United States, in D. J. Stanley and G. T. Moore, The shelf break: Critical interface on continental margins. SEPM Special Publication 33. p. 79– 96.

Hass, W. H. 1953. Conodonts of Barnett Formation of Texas: U.S. Geological Survey Professional Paper 243-F, p. 69– 94.

Helz, G.R., Miller, C.V., Charnock, J.M., Mosselmans, J.F.W., Pattrick, R.A.D., Garner, C.D., Vaughan, D.J. 1996. Mechanism of molybdenum removal from the sea and its concentration in black shales: EFAXS evidence. Geochimica et Cosmochimica Acta. 60: 3631–3642.

Henk, F., Breyer, J., and Jarvie, D.M. 2000. Lithofacies, petrology, and geochemistry of the Barnett Shale in conventional core and Barnett Shale outcrop geochemistry (abs.), in L. Brogden, ed., Barnett Shale Symposium, Fort Worth Texas: Oil Information Library of Fort Worth, Texas, p. 7.

Henry, J. D. 1982. Stratigraphy of the Barnett Shale (Mississippian) and associated reefs in the northern Fort Worth Basin, *in* Martin, C. A., ed., Petroleum Geology of the Fort Worth Basin and Bend Arch Area: Dallas Geological Society, p. 157-178.

Hill, R.J., Jarvie, D.M., Zumberge, J., Henry, M., and Pollastro, R.M. 2007. Oil and gas geochemistry and petroleum systems of the Fort Worth Basin. AAPG Bulletin. vol. 91, no. 4. pp. 445–473.

Hughes, E.N., Rowe, H.D., Ruppel, S., and Loucks, R. 2009. Geochemistry of the Barnett Formation from three Texas Hill Country cores (in Geological Society of America, South-Central Section, 43rd annual meeting, Anonymous,) Abstracts with Programs - Geological Society of America (March 2009), 41(2):7

Jarvie, D.M., Hill, R.J., Ruble, T.E., and Pollastro, R.M. 2007. Unconventional shale-gas systems: The Mississippian Barnett Shale of north-central Texas as one model for thermogenic shale-gas assessment. AAPG Bulletin. vol. 91, no. 4. pp. 475–499.

Johnson, K.S., Amsden, T.W., Denison, R.E., Dutton, S.P., Goldstein, A.G., Rascoe Jr B., et al. 1988. Southern midcontinent region. (Chp. 12). In: Sloss LL, editor. Sedimentary Cover—North American Craton. The Geology of North America, vol. D-2. Geological Society of America; p. 307– 59.

Jurdy, D.M., Stefanick, M., and Scotese, C.R. 1995. Paleozoic plate dynamics. Journal of Geophysical Research. 100(B9), 17: 965–975.

Kammer, T.W. and Matchen, D.L. 2008. Evidence for eustasy: Response to late Tournaisian glaciations? Geological Society of America Special Paper 441. pp. 261-273.

Kier, R.S., Brown Jr., L.F., and McBride, E.F. 1979. The Mississippian and Pennsylvanian (Carboniferous) Systems in the United States – Texas. U.S. Geological Survey Professional Paper 1110-S.

Kier, R. S. 1988. Paleozoic strata of the Llano region, Central Texas: Geological Society of America Centennial Field Guide – South – Central Section, v. 6, p. 351-360.

Loucks, R.G. 2008. Unpublished. Project STARR Progress Report, September 2008. Bureau of Economic Geology Publication. Austin, Texas. 95 p.

Loucks, R.G. 2009. Unpublished. General map of study area.

Loucks, R.G. and Ruppel, S.C. 2007. Mississippian Barnett Shale: Lithofacies and depositional setting of a deep-water shale-gas succession in the Fort Worth Basin, Texas. AAPG Bulletin, vol. 91, no. 4; 579-601.

Loucks, R.G. and Ruppel, S.C. 2008. The Barnett Shale of the southern Fort Worth Basin; comparison of depositional setting, lithofacies, and mineralogy with equivalent deposits in the northern basin. Abstracts: Annual Meeting - American Association of Petroleum Geologists.

Lyons, T.W., Werne, J.P., Hollander, D.J., and Murray, R.W. 2003. Contrasting sulfur geochemistry and Fe/Al and Mo/Al ratios across the last oxic-to-anoxic transition in the Cariaco Basin, Venezuela. Chemical Geology. 195: 131–157.

Lyons, T.W. and Severmann, S. 2006. A critical look at iron paleoredox proxies: New insights from modern euxinic marine basins. Geochimica et Cosmochimica Acta. 70: 5698–5722.

Maiz, N. 2007. Geochemical characterization of gases from the Barnett Shale, Fort Worth Basin, Texas. Master's thesis: University of Oklahoma. 123 pp.

Maynard, J.P., Eriksson, K.A., and Law, R.D. 2006. The upper Mississippian Bluefield Formation in the Central Appalachian basin: A hierarchical sequence-stratigraphic record of a greenhouse to icehouse transition. Sedimentary Geology. 192: 99-122.

McManus, J., Berelson, W.M., Severmann, S., Poulson, R.L., Hammond, D.E., Klinkhammer, G.P., and Holm, C. 2006. Molybdenum and uranium geochemistry in continental margin sediments: Paleoproxy potential. Geochimica et Cosmochimica Acta. 70: 4643–4662.

Merrill, G. K., 1980. Preliminary report on the restudy of conodonts from the Barnett Formation, in D. Windle, ed., Geology of the Llano region, central Texas: West Texas Geological Society Publication 80-73, 103– 107.

Meyers, P.A. 1994. Preservation of elemental and isotopic source identification of sedimentary organic matter. Chemical Geology. 114: 289-302.

Meyers, P.A. 1997. Organic geochemical proxies of paleoceanographic, paleolimnologic, and paleoclimatic processes. Organic Geochemistry. Vol. 27, No. 5/6, pp 231-250.

Meyers, P.A., Bernasconi, S.M., and Forster, A. 2006. Origins and accumulation of organic matter in expanded Albian to Santonian black shale sequences on the Demerara Rise, South American margin. Organic Geochemistry. 37: 1816–1830.

Meyers, P.A., Bernasconi, S.M., and Yum, J-G. 2009A. 20 My of nitrogen fixation during deposition of mid-Cretaceous black shales on the Demerara Rise, equatorial Atlantic Ocean. Organic Geochemistry. 40: 158-166.

Meyers, P.A., Yum, J-G., and Wise, S.W. 2009B. Origins and maturity of organic matter in mid-Cretaceous black shales from ODP Site 1138 on the Kerguelen Plateau. Marine and Petroleum Geology. 26: 909-915.

Montgomery, S. L., Jarvie, D.M., Bowker, K.A., and Pollastro, R.M. 2005. Mississippian Barnett Shale, Fort Worth Basin, northcentral Texas: Gas-shale play with multi-trillion cubic foot potential. AAPG Bulletin. vol. 89. p. 155–175.

Morford, J.L. and Emerson, S. 1999. The geochemistry of redox sensitive trace metals in sediments. Geochimica et Cosmochimica Acta. Vol. 63, No. 11/12, pp. 1735–1750.

Morford, J.L., Russell, A.D., Emerson, S. 2001. Trace metal evidence for changes in the redox environment associated with the transition from terrigenous clay to diatomaceous sediment, Saanich Inlet, BC. Marine Geology. 174: 355–369.

Papazis, P.K. 2005. Petrographic characterization of the Barnett Shale, Fort Worth Basin, Texas. Master's thesis: University of Texas at Austin. 142 p.

Piper, D.Z. 1994. Seawater as the source of minor elements in black shales, phosphorites and other sedimentary rocks. Chemical Geology. 114: 95-114.

Piper, D.Z. and Calvert, S.E. 2009. A marine biogeochemical perspective on black shale deposition. Earth-Science Reviews. 95: 63-96.

Plummer, F.B. and Moore, R.C. 1922. Stratigraphy of the Pennsylvanian formations of North-Central Texas: University of Texas, Bulletin, 2, 132.

Pollastro, R.M., Jarvie, D.M., Hill, R.J., Adams, C.W., 2007. Geologic framework of the Mississippian Barnett Shale, Barnett-Paleozoic total petroleum system, Bend arch-Fort Worth Basin, Texas. AAPG Bulletin, vol. 91, no. 4; 405-436.

Posamentier, H.W. and Allen, G.P. 1999. Siliciclastic sequence stratigraphy: concepts and applications. Concepts in Sedimentology and Paleontology, vol. 7. Society of Economic Paleontologists and Mineralogists (SEPM). 210 pp.

Potter, P. E., Maynard, J.B. and Pryor, W.A. 1980. Sedimentology of Shale: New York, Springer Verlag. 306 p.

Potts, Philip J. and Webb, Peter C. 1992. X-ray fluorescence Spectrometry. Journal of Geochemical Exploration. 44: 251-296.

Raiswell, R. and Berner, R.A. 1986. Pyrite and organic matter in Phanerozoic normal marine shales. Geochimica et Cosmochimica Acta. 50: 1967–1976.

Raiswell, R., Buckley, F., Berner, R.A., and Anderson, T.F. 1988. Degree of pyritization of iron as a paleoenvironmental indicator of bottom-wateroxygenation. Journal of Sedimentary Petrology. 58: 812–819.

Rimmer, S.M. 2004. Geochemical paleoredox indicators in Devonian-Mississippian black shales, Central Appalachian Basin (USA). Chemical Geology. 206: 373-391.

Rimmer, S.M., Thompson, J.A., Goodnight, S.A., and Robl, T.L. 2004. Multiple controls on the preservation of organic matter in Devonian–Mississippian marine black shales: geochemical and petrographic evidence. Palaeogeography, Palaeclimatology, Palaeoecology. 215: 125–154.

Rodriguez, R.D. and Philp, R.P. 2010. Geochemical characterization of gases from the Mississippian Barnett Shale, Fort Worth Basin, Texas. AAPG Bulletin. vol 94. no. 11. pp. 1641–1656.

Ross, C. A. and Ross, J.R.P. 1987. Late Paleozoic sea levels and depositional sequences, in C. A. Ross and D. Haman, eds., Timing and deposition of eustatic sequences: Constraints on seismic stratigraphy: Cushman Foundation for Foraminiferal Research Special Publication. 24: 137– 149.

Rousseau, R. M. 2001. Detection limit and estimate of uncertainty of analytical XRF results: The Rigaku Journal. 18: 33-47.

Rowe, H.D., Loucks, R.G., Ruppel, S.C., Rimmer, S.M., 2008. Mississippian Barnett Formation, Fort Worth Basin, Texas: Bulk geochemical inferences and Mo-TOC constraints on the severity of hydrographic restriction. Chemical Geology. 257: 16-25.

Rowe, H. D.; Ruppel, S.; Rimmer, S.; Loucks, R.G. 2009. Core-based chemostratigraphy of the Barnett Shale, Permian Basin, Texas. Gulf Coast Association of Geological Societies Transactions. 59: 675-686.

Rowe, H.D. et al. 2011. In Review.

Sageman, B.B., Hollander, D.J., Lyons, T.W., Murphy, A.E., Ver Straeten, C.A., Werne, J.P. 2003. A tale of shales: the relative roles of production, decomposition, and dilution in the accumulation of organic-rich strata, Middle–Upper Devonian, Appalachian Basin. Chemical Geology. 195: 229–273.

Schieber, J. 1998. Developing a sequence stratigraphic framework for Late Devonian Chattanooga Shale of the Southeastern U.S.A.: Relevance for the Bakken Shale. In J.E.

Christopher, C.F. Gilboy, D.F. Paterson, and S.L. Bend, eds., Eight International Williston Basin Symposium, Saskatchewan Geological Society Special Publication, No. 13, pp 58-68.

Schieber, J., and Zimmerle, W. 1998. Introduction and overview: The history and promise of shale research, in J. Schieber, W. Zimmerle, and P. Sethi, eds., Shales and Mudstones I: Stuttgart, Germany, E. Schweizerhbart'sche Verlagsbuchhandlung, p. 1-10.

Schwarz, M.E. 1975. Cephalopods of the Barnett Formation, central Texas. Master's thesis: The University of Texas at Austin. 74 p.

Scotese, C.R. and McKerrow, W.S. 1990. Revised World maps and introduction. Geological Society, London, Memoirs. vol. 12. p. 1-21.

Scotese, C.R. 2010. Personal Correspondence. PALEOMAP Project. Arlington, Texas.

Singh, M.K. 2007. Correlation and biostratigraphy of surface and shallow subsurface sections of the Barnett Shale, Llano Uplift, south-central, Texas. Master's thesis: Oklahoma State University. 102 p.

Smith Jr., L.B. and Read, J.F. 2000. Rapid onset of late Paleozoic glaciation on Gondwana: Evidence from Upper Mississippian strata of the Midcontinent, United States. Geology. 28: 279-282.

Thompson, D.M. 1982. Atoka Group (Lower to Middle Pennsylvanian), Northern Fort Worth Basin, Texas: Terrigenous depositional systems, diagenesis, and reservoir distribution and quality. Bureau of Economic Geology, The University of Texas at Austin, Report of Investigations No. 125.

Thompson, D.M. 1988. Fort Worth basin. In: Sloss, L.L. (Ed.), The Geology of North America, D-2. Geological Society of America, pp. 346–352.

Tribovillard, N., Riboulleau, A., Lyons, T., and Baudin, F. 2004. Enhanced trapping of molybdenum by sulfurized marine organic matter of marine origin in Mesozoic limestones and shales. Chemical Geology. 213: 385-401.

Tribovillard, N., Algeo, T.J., Lyons, T., and Riboulleau, A. 2006. Trace metals as paleoredox and paleoproductivity indicators: an update. Chemical Geology. 232: 12–32.

Turgeon, S. and Brumsack, H-J. 2006. Anoxic vs dysoxic events reflected in sediment geochemistry during the Cenomanian–Turonian Boundary Event (Cretaceous) in the Umbria–Marche Basin of central Italy. Chemical Geology. Volume 234. Issues 3-4. 15: 321-339.

Twichell, S.C., Meyers, P.A., and Diester-Haass, L. 2002. Significance of high C/N ratios in organic-carbon-rich Neogene sediments under the Benguela Current upwelling system. Organic Geochemistry. 33: 715-722.

Vail, P.R., Mitchum Jr., R.M., Thompson III, S. 1977. Seismic stratigraphy and global changes of sea level, part 3: relative changes of sea level from coastal onlap. In: Payton, C.E. (Ed.), Seismic Stratigraphy — Applications to Hydrocarbon Exploration. Memoir, vol. 26. American Association of Petroleum Geologists. pp. 63–81.

Verardo,D.J., Froelich, P.N., and McIntyre, A. 1990. Determination of organic carbon and nitrogen in marine sediments using the Carlo Erba NA-1500. Deep-Sea Research. 37: 157-165.

Ver Straeten, C.A., Brett, C.E., and Sageman, B.B. 2011. Mudrock sequence stratigraphy: A multi-proxy (sedimentological, paleobiological and geochemical) approach, Devonian Appalachian Basin. Palaeogeography, Palaeoclimatology, Palaeoecology. Volume 304, Issues 1-2. 15: 54-73.

Vine, J.D., and Tourtelot, E.B. 1970. Geochemistry of black shale deposits—A summary report. Economic Geology. 65: 253–272.

Walper, J.L., 1982. Plate tectonic evolution of the FortWorth Basin. In: Martin, C.A. (Ed.), Petroleum Geology of the Fort Worth Basin and Bend Arch Area. Dallas Geological Society, pp. 237–251.

Wardlaw, B.R. and Boardman, D.R. 2007. Conodont biostratigraphy of the Barnett Shale in the Llano Uplift region, Texas (in Geological Society of America, 2007 annual meeting, Anonymous,) Abstracts with Programs - Geological Society of America (October 2007), 39(6):357.

Wedepohl, K.H., 1971. Environmental influences on the chemical composition of shales and clays. In: Ahrens, L.H., Press, F., Runcorn, S.K., Urey, H.C. (Eds.), Physics and Chemistry of the Earth vol. 8, Pergamon, Oxford (1971), pp. 305–333.

Wedepohl, K.H., 1991. The composition of the upper earth's crust and the natural cycles of selected metals. Metals in natural rawmaterials. Natural Resources. In: Merian, E. (Ed.), Metals and Their Compounds in the Environment. VCH, Weinheim, pp. 3–17.

Whiticar, M.J. 1999. Carbon and hydrogen isotope systematics of bacterial formation and oxidation of methane. Chemical Geology. 161: 291-314.

Wilkin, R.T., Barnes, H.L., and Brantley, S.L. 1996. The size distribution of framboidal pyrite in modern sediments: an indicator of redox conditions. Geochimica et Cosmochimica Acta. 60:3897–3912.

Wilkin, R. T., Arthur, M.A., and Dean, W.E. 1997. History of watercolumn anoxia in the Black Sea indicated by pyrite framboids size distributions. Earth and Planetary Science Letters. vol. 148, p. 517– 525.

BIOGRAPHICAL INFORMATION

James Daniel Hoelke was born on January 5, 1980 in Dallas, Texas. James grew up in Arlington, Texas and graduated from Cistercian Preparatory in 1998. He attended the University of Dallas in Irving, Texas where he earned a Bachelor of Arts degree in Politics in May 2002. After graduation, he worked in private industry for five years. Returning to full-time university studies in 2007, James enrolled at the University of Texas at Arlington to pursue a second degree in geology. He graduated with a Bachelor of Science degree in geology in December 2009. Continuing his studies in geology, James entered the Master of Science program at the University of Texas at Arlington under the supervision of Dr. Harry Rowe. He is scheduled to complete his Master's degree in geology in 2011.